

AD 679848

NRL Report 6852

Systematic Errors in Ultrasonic Propagation Parameter Measurements

Part 4 - Effect of Finite Thickness Elastic Solid Tubes Enclosing the Liquid Cylinder of Interest

VINCENT A. DEL GROSSO

*Physical Acoustics Branch
Acoustics Division*

November 15, 1968

DDC
RECEIVED
DEC 9 1968
RECEIVED
E



NAVAL RESEARCH LABORATORY
Washington, D.C.

This document has been approved for public release and sale; its distribution is unlimited.

144

FOREWORD

This report is the reproduction of a dissertation titled "Axial Acoustic Propagation Within Inviscid Liquid Cylinders in Elastic Solid Tubes - Mode Summations for Propagation Parameter Determination" submitted to the Catholic University of America in partial fulfillment of the requirements for the degree Doctor of Philosophy. The dissertation was submitted to be an NRL Report on October 28, 1968, as an interim report on NRL Problem S01-02, Project RF 05-511-401-5251.

ABSTRACT

The exact formulation of the characteristic or frequency equation for an inviscid liquid cylinder radially enclosed within a finite impedance elastic solid of finite wall thickness is solved for the permissible modes, including degenerations to the surrounding medium being of infinite extent and either an elastic solid or another liquid, as well as to the limiting cases of infinite impedance (rigid boundary) and zero impedance (free boundary). These modes are utilized to expand both the potential within the otherwise unterminated cylinder and the source impedance variation with position of an opposing termination. A piston source of appreciable ka ($= 100\pi$) is found to render further source specification indifferent as to uniform pressure or uniform velocity, and a large radial impedance mismatch ($= 28$) is found to permit a simplifying orthogonality assumption. With the inviscid assumption, the formulation indicates that a judicious selection of experimental configuration can limit diffraction propagation uncertainties to a few parts per million. An incidental result is the demonstration that the zero elastic tube mode exists at all frequencies rather than displaying an upper cutoff frequency as was recently reported.

ACKNOWLEDGMENTS

With a deep sense of gratitude, I thank the Acoustics Division and the Training Branch of the Naval Research Laboratory for permitting me the opportunity to pursue courses at the Catholic University of America.

The penetrating dialogues with Professor Albert E. Hudimac were very enlightening, and I take this opportunity to thank him for his guidance. Thanks are also due Professor Martin Greenspan, also of the National Bureau of Standards, and Professor Herbert Überall, who read and approved this manuscript.

Most of the programming was done by Mr. Richard E. McGill with invaluable aid from Miss Dianna Denton.

The outstanding efforts of the Graphic Arts Branch of the Laboratory, particularly the Composition Section and Mrs. Dora Wilbanks, in the preparation of this manuscript in a relatively short time, is sincerely acknowledged.

Lastly, I wish to express my thanks to my wife Faye, and our children, Alfred, Jodi, Nicholas, Teresa, and Regina for their forbearance for many months.

TABLE OF CONTENTS

		Page
	ACKNOWLEDGEMENTS.....	iii
	LIST OF TABLES	vii
	LIST OF ILLUSTRATIONS	x
Section		
I	INTRODUCTION	1
	I.1 Purpose of Investigation.....	1
	I.2 Zero Mode Controversy	2
II	PRELIMINARY	3
	II.1 Use of a Potential	3
	II.2 Misuse of Convention of the Real	6
III	FINITE-SOURCE FREE-FIELD DIFFRACTION	9
IV	GUIDED-MODE DISPERSION	11
	IV.1 Characteristic Function Formulation for Modes.....	11
	IV.2 Plane Wave Synthesis of Modes.....	14
	IV.3 General Characteristics of Modes	16
V	PROPAGATION IN NON-TERMINATED CYLINDER	19
	V.1 Characteristic Function Expansion for Potential	19
	V.2 General Non-Orthogonality of Characteristic Functions	21
	V.3 Piston Excitation of Modes	23
	V.4 Critique of Integrating Only Over Liquid Cylinder	28
	V.5 Critique of Limiting Summation to Propagated Modes	28
VI	PROPAGATION IN TERMINATED CYLINDER	30
	VI.1 Characteristic Function Expansion for Source Impedance.....	30
	VI.2 Plane Wave Degeneration	35
	VI.3 Critique of Limited Integration and Limited Sum	37
VII	RADIALLY SURROUNDING ELASTIC SOLID OF INFINITE EXTENT	
	OUTWARDS	39
	VII.1 Scalar and Vector Displacement Potentials.....	39
	VII.2 Bessel Function Solutions	41

TABLE OF CONTENTS--Continued

Section	Page
VII.3	Alternative Use of a Modified Vector Displacement Potential 44
VII.4	Characteristic Equation for Elm Modes 46
VII.5	Finite Number of Elm Modes, All Propagating. 49
VII.6	Imaginary Characteristic Value for a Propagating E10 Mode. 53
VII.7	Degeneration to Characteristic Equation for Radially Surrounding Liquid or LIm Modes 55
VII.8	Alternative Derivation of Characteristic Equation for LIm Modes . 56
VII.9	Finite Number of L1k1 Modes, All Propagating. 57
VII.10	Degeneration to Characteristic Equations for Absolutely Rigid or Free Radial Boundaries with Infinity of Modes. 58
VIII	RADIALLY SURROUNDING FINITE WALL THICKNESS ELASTIC SOLID TUBE 60
VIII.1	Characteristic Equation for ETm Modes 60
VIII.2	Infinite Number of ETm Modes, Not All Propagating 69
VIII.3	Imaginary Characteristic Value for a Propagating ET0 Mode. 72
VIII.4	Degeneration to Characteristic Equation for Radially Surrounding Elastic Solid of Infinite Extent Outwards or Elm Modes 73
VIII.5	Degeneration to Characteristic Equation for Radially Surrounding Finite Wall Thickness Liquid (Different) Tube or Ltm Modes 76
VIII.6	Alternative Derivation of Characteristic Equation for Ltm Modes 78
VIII.7	Degeneration of Ltm Equation to LIm Equation. 79
IX	RESULTS AND DISCUSSION 80
IX.1	Selection of Parameters to Validate Orthogonality Assumption . . 80
IX.2	Selection of Parameters to Render Piston Assumption Choice Indifferent. 82
IX.3	Satisfaction of Source Boundary Condition with Propagating Modes Only 82
IX.4	Satisfaction of Source Boundary Condition with Existing Finite Number of Modes. 88
IX.5	Satisfaction of " ρc " Loading of Source. 89

TABLE OF CONTENTS—Continued

Section		Page
IX.6	No Untoward Implication for $r > b$ Because of Limiting Integration Limit to $r = b$	89
IX.7	No Untoward Implication for $r > b$ Because of Constant Reflector Impedance Assumption	94
IX.8	Mode Sound Speed Dispersion Plots.....	97
IX.9	Zero Mode Controversy Settled.....	97
IX.10	Relative Pressure and Phase Plots for Non-Terminated Cylinder	100
IX.11	Source Impedance Variation Plots for Terminated Cylinder.....	112
IX.12	Other Sources of Error in Measurement of Propagation Parameters.....	123
X	CONCLUSIONS	125
	REFERENCES.....	127

LIST OF TABLES

Table		Page
1	Reference Conditions of Pertinent Parameters as Used for Calculations When Appropriate	80
2	The Roots X_{Lm} and Orthogonality Checks for Reference Parameters of Table 1 except $k_1 a = 20\pi$ or $\lambda_1 = 0.15$ cm	81
3	Comparison of Coefficients K_{Lm} Obtained by Orthogonality Assumption and by Correct Matrix Inversion for Reference Parameters of Table 1 except $k_1 a = 20\pi$ or $\lambda_1 = 0.15$ cm	83
4	Comparison of Average Relative Pressure Values Obtained by Using Orthogonal Assumption K_{Lm} and Actual K_{Lm} from Table 3	84
5	Comparison of Average Relative Phase-Difference Values Obtained by Using Orthogonal Assumption K_{Lm} and Actual K_{Lm} from Table 3	84
6	Comparison of Results with Uniform Velocity Piston Assumption Versus Uniform Pressure Piston Assumption for Pertinent Parameters of Table 1 for LI Boundary Conditions	85
7a	Relative Particle Velocity at Source Calculated Using Only Propagated Modes X_{Rm} for Pertinent Parameters of Table 1 for $0 \leq r \leq b$ with Uniform Velocity Piston Assumption	86
7b	Relative Particle Velocity at Source Calculated Using an Equal Number of Evanescent Modes in Addition to the 201 Propagated Modes X_{Rm} for Pertinent Parameters of Table 1 for $0 \leq r \leq b$ with Uniform Velocity Piston Assumption.	86
7c	Same as 7b. Except Finer Detail to Show Gibb's-Type Phenomenon about $r/b = 0$. The Same Effect is Noted at $r/b = 0.50$ (or $r = a$). Even Finer Detail Indicates No Smaller Period	87
7d	Comparison of Field Results with and without an Equal Number of Evanescent Modes for Pertinent Parameters of Table 1 for R_m Boundary Conditions	87

LIST OF TABLES (Continued)

Table	Page
<p>8a Relative Particle Velocity at Source Calculated Using All Modes X_{Lm} for Pertinent Parameters of Table 1 for $0 \leq r \leq b$ with Uniform Velocity Piston Assumption.</p>	88
<p>8b Relative Particle Velocity at Source Calculated Using All Modes X_{Lm} for Pertinent Parameters of Table 1 for $r \geq b$ with Uniform Velocity Piston Assumption</p>	93
<p>9a Impedance within Liquid Cylinder at $z = \ell$ with Constant Reflector Impedance Assumption and for LIm Boundary Conditions . . .</p>	96
<p>9b Impedance in Surrounding Liquid Medium II at $z = \ell$ with Constant Reflector Impedance Assumption and for LIm Radial Boundary Conditions</p>	96
<p>10 Apparent Sound Speeds C for Successive Intervals Between Indicated Source-to-Reflector Separations ℓ Corresponding to Half Wavelengths n for the Imposed Characteristics of Zero Phase, Maximum R, and Maximum Z for the Standard Reference Parameters of Table 1 with Absolutely Rigid Boundary Conditions Rm.</p>	118
<p>11 Apparent Sound Speeds C for Successive Intervals Between Indicated Source-to-Reflector Separations ℓ Corresponding to Half Wavelengths n for the Imposed Characteristics of Zero Phase, Maximum R, and Maximum Z for the Standard Reference Parameters of Table 1 with Free Boundary Conditions Fm</p>	119
<p>12 Apparent Sound Speeds C for Successive Intervals Between Indicated Source-to-Reflector Separations ℓ Corresponding to Half Wavelengths n for the Imposed Characteristics of Zero Phase, Maximum R, and Maximum Z for the Standard Reference Parameters of Table 1 with Infinite Liquid Boundary Conditions LIm</p>	120

LIST OF TABLES (Continued)

Table		Page
13	Apparent Sound Speeds C for Successive Intervals Between Indicated Source-to-Reflector Separations l Corresponding to Half Wavelengths n for the Imposed Characteristics of Zero Phase, Maximum R , and Maximum Z for the Standard Reference Parameters of Table 1 with Infinite Elastic Solid Boundary Conditions EIm	121
14	Apparent Sound Speeds C for Successive Intervals Between Indicated Source-to-Reflector Separations l Corresponding to Half Wavelengths n for the Imposed Characteristics of Zero Phase, Maximum R , and Maximum Z for the Standard Reference Parameters of Table 1 with Finite Elastic Solid Tube Boundary Conditions ETm	122

LIST OF ILLUSTRATIONS

Figure		Page
1	Geometry for Liquid Cylinder Which is Modified in Text	12
2	Sound Speed Dispersion Plots C_{0m}/C_1 vs $k_1 b$ for liquid cylinder modes of order m for rigid radial boundary conditions R_m , free radial boundary condition F_m , infinite liquid radial boundary condition L_m , and infinite elastic solid radial boundary condition E_m with appropriate reference conditions in Table 1	98
3	Sound Speed Dispersion Plots C_{0m}/C_1 vs $k_1 b$ for liquid cylinder modes of order m for finite elastic solid tube radial boundary condition E_m with appropriate reference conditions in Table 1	99
4	a & b. $\langle P \rangle_{rel}$ and $\langle \theta \rangle_{rel}$ vs $0 \leq z(\lambda/a^2) \leq 1$ for liquid cylinder with rigid radial boundary condition R_m and uniform velocity source assumption and including all propagated modes for appropriate reference conditions in Table 1. Free Field Diffraction curves are plotted for comparison	102
5	a & b. $\langle P \rangle_{rel}$ and $\langle \theta \rangle_{rel}$ vs $0 \leq z(\lambda/a^2) \leq 1$ for liquid cylinder with free radial boundary condition F_m and uniform velocity source assumption and including all propagated modes for appropriate reference conditions in Table 1. Free Field Diffraction Curves are plotted for Comparison	104
6	a & b. $\langle P \rangle_{rel}$ and $\langle \theta \rangle_{rel}$ vs $0 \leq z(\lambda/a^2) \leq 1$ for liquid cylinder with infinite liquid radial boundary condition L_m and uniform velocity source assumption using orthogonal characteristic function assumption and including all propagated modes for appropriate reference conditions in Table 1. Free Field Diffraction curves are plotted for comparison	106

LIST OF ILLUSTRATIONS (Continued)

Figure		Page
7	<p>a & b. $\langle P \rangle_{rel}$ and $\langle \theta \rangle_{rel}$ vs $0 \leq z(\lambda/a^2) \leq 1$ for liquid cylinder with infinite elastic solid radial boundary condition Elm and uniform velocity source assumption using orthogonal characteristic function assumption and including all propagated modes for appropriate reference conditions in Table 1. Free Field Diffraction curves are plotted for comparison</p>	108
8	<p>a & b. $\langle P \rangle_{rel}$ and $\langle \theta \rangle_{rel}$ vs $0 \leq z(\lambda/a^2) \leq 1$ for liquid cylinder with finite elastic solid tube radial boundary condition ETm and uniform velocity source assumption using orthogonal characteristic function assumption and including all propagated modes for appropriate reference conditions in Table 1. Free Field Diffraction curves are plotted for comparison</p>	110
9	<p>R vs X Circle Diagram for terminated liquid cylinder with rigid radial boundary condition Rm and uniform velocity source assumption and including all propagated modes for appropriate reference conditions in Table 1. The points are separated by $\Delta \ell = 0.2$ micrometers and the circled numerals refer to the value of n where $\ell = n(\lambda_1/2)$</p>	113
10	<p>R vs X Circle Diagram for terminated liquid cylinder with free radial boundary condition Fm and uniform velocity source assumption and including all propagated modes for appropriate reference conditions in Table 1. The points are separated by $\Delta \ell = 0.2$ micrometers and the circled numerals refer to the value of n where $\ell = n(\lambda_1/2)$</p>	114

LIST OF ILLUSTRATIONS (Continued)

Figure		Page
11	<p>R vs X Circle Diagram for terminated liquid cylinder with infinite liquid radial boundary condition LIm and uniform velocity source assumption and including all propagated modes for appropriate reference conditions in Table 1. The points are separated by $\Delta\ell = 0.2$ micrometers and the circled numerals refer to the value of n where $\ell = n(\lambda_1/2)$</p>	115
12	<p>R vs X Circle Diagram for terminated liquid cylinder with infinite elastic solid radial boundary condition EIm and uniform velocity source assumption and including all propagated modes for appropriate reference conditions in Table 1. The points are separated by $\Delta\ell = 0.2$ micrometers and the circled numerals refer to the value of n where $\ell = n(\lambda_1/2)$</p>	116
13	<p>R vs X Circle Diagram for terminated liquid cylinder with finite elastic solid tube boundary condition ETm and uniform velocity source assumption and including all propagated modes for appropriate reference conditions in Table 1. The points are separated by $\Delta\ell = 0.2$ micrometers and the circled numerals refer to the value of n where $\ell = n(\lambda_1/2)$</p>	117

Section I

INTRODUCTION

1.1 Purpose of Investigation

The experimental configuration most usually employed for laboratory investigations of ultrasonic propagation parameters in liquids is a liquid cylinder contained within metal walls. This small finite sample size is dictated by considerations of relative scarcity of test liquid, requirement for homogeneity and uniformity of physical parameters, and desire to extend the pressure parameter to 1000 atmospheres.

The purpose of this present investigation is to describe the axial propagation of acoustic energy down such a liquid cylinder in terms of the permitted modes, and thus predict aberrations in behavior and define optimum geometric configurations for enhanced accuracy of measurement of the acoustic propagation parameters.

Earlier investigations along this line were hampered and limited by the assumption that the metal enclosure could be adequately represented by an absolutely rigid or, in some instances, free boundary. A consequence of the erroneous assumption of absolute rigidity is the existence of a plane wave mode of propagation among the family of permissible axial modes, with the further indication that a piston source completely filling the cross section of the liquid cylinder excites only this plane wave mode.

This report presents the expected behavior predicted by a more realistic theoretical treatment of the experimental configuration than has been done previously.

In particular, the oversimplification to walls of absolute rigidity is removed, and instead the radial boundary conditions considered have been extended to include both a radially surrounding elastic solid of infinite extent and the most realistic laboratory situation of a surrounding elastic solid tube of finite wall thickness. In the former situation, the equations pertinent to the case of an infinite surrounding liquid as well as the limiting cases of absolutely rigid and free boundaries are obtained as degenerations.

The characteristic or frequency equations obtained for these realistic boundary conditions are solved for the characteristic values relating to the mode propagation constants. These are then utilized in characteristic function expansions which have been obtained

for both the nonterminated liquid cylinder and the situation wherein a reflector is used for termination. In this latter interferometer case, indicated accuracies have been calculated.

1.2 Zero Mode Controversy

Apart from the major purpose of this investigation, a recent controversy concerning the phase velocity versus frequency plot for the "0" mode for the finite tube case is resolved. Kumar (1) gives results of his study using exact equations with approximations: (a) to a very small thickness shell so that the ratio of outer-to-inner shell radius is very close to unity ($=1 + \delta$) and (b) that the ratio of the bulk modulus of the liquid to the second Lamé constant for the shell material can be represented by a constant times δ . The significance of this latter approximation is not clear, but while he finds the 1st mode that was missed by Thomson (2) but described by Lin and Morgan (3) and confirms its existence at all frequencies, Kumar states that the "0" mode does not exist at all frequencies, a finding in direct disagreement with the conclusions of Thomson and of Lin and Morgan. The three papers quoted above all agree that the higher order axially symmetric modes display minimum cutoff frequencies. Investigations both by Thomson and by Lin and Morgan employed approximate equations for the motion of the cylindrical tube, Lin and Morgan including the effects of transverse shear and rotatory inertia. The latter state that the neglect of transverse shear and rotatory inertia changes the "0" mode only slightly, with rotatory inertia relatively unimportant there and both effects unimportant for the higher modes. It is interesting that Jacobi (4) following Fay, Brown, and Fortier (5), states that the "0" mode obtained from their approximate equation does exist at all frequencies and also that this single purely imaginary root displays the character later found by Kumar if the flexural (shear) forces in the wall are completely neglected.

Section II

PRELIMINARY

II.1 Use of a Potential

The general wave equation satisfied by a potential analogous to the wave function in quantum mechanics is

$$\nabla^2 \psi + g^2(q) \psi = A \frac{\partial \psi}{\partial t} + B \frac{\partial^2 \psi}{\partial t^2}$$

where g^2 is real and independent of the coordinates q for homogeneous media or for harmonic waves, and the ψ represents a stationary wave function, e.g., one for which the time dependence can be factored out as

$$\psi = \phi T.$$

Using a separation constant $-K^2$ leads to the simultaneous equations

$$\nabla^2 \phi + g^2 \phi = -K^2 \phi$$

and

$$B \frac{\partial^2 T}{\partial t^2} + A \frac{\partial T}{\partial t} = -K^2 T.$$

When the harmonic solutions, so chosen to satisfy the radiation condition,

$$\phi = \phi_0 e^{ikq}$$

and

$$T = e^{-i\omega t}$$

are substituted back, two equations are obtained

$$-k^2 + g^2 = -K^2$$

$$-\omega^2 B - iA\omega = -K^2$$

with the simultaneous solution

$$\mathbf{k}^2 = \mathbf{g}^2 + \omega^2 \mathbf{B} + i\mathbf{A}\omega$$

indicating dispersion for

$$c^2 = \frac{\mathbf{k}^2}{\omega^2} = c^2(\omega).$$

For the usual acoustics case

$$\mathbf{g}^2 = 0$$

which does not eliminate the dispersion but also

$$\mathbf{A} = 0$$

which does remove it. In any event, by the imposition of appropriate boundary conditions, the solution is quantized, validating the expansion

$$\psi = \sum_{n=-\infty}^{\infty} c_n \phi_n T_n.$$

Separating out the time dependence in the usual acoustics case yields the time independent homogeneous Helmholtz equation

$$\nabla^2 \phi + \mathbf{k}^2 \phi = 0.$$

The general solution of the ordinary wave equation in free space is, in terms of this potential, which we will now refer to as a velocity potential (but later as a displacement potential)

$$\phi = \phi_0 e^{-i\omega t}.$$

Continuing the analogy to wave mechanics, we note that the logarithmic derivative is widely used to fit different solutions to the time independent general quantum mechanical wave equation called the Schrodinger Equation. The logarithmic derivative

$$\frac{1}{\psi} \frac{\partial \psi(z)}{\partial z}$$

is precisely that with its utility following from

$$\frac{d}{dz} (\ln az) = \frac{d}{dz} (\ln z) = \frac{1}{z}.$$

The logarithmic derivative is related to the specific acoustic impedance Z_s which is defined as the quotient between pressure p and particle velocity u . Of the several operator notations which could be written for p and u we select

$$p = -\rho \frac{\partial \phi}{\partial t}$$

$$u = \nabla \phi$$

and obtain

$$Z_s = \frac{i\omega\rho\phi}{\nabla\phi}$$

where $\nabla\phi/\phi$ is the logarithmic derivative related to impedance (actually susceptance) by $i\omega\rho$ where ρ is density. We note that even the factor $i\omega$ cancels when equating this expression on both sides of a boundary so that the logarithmic derivative equality is modified in the acoustics case only by the inclusion of respective densities or density ratio. For a plane wave moving in the positive z direction

$$\nabla \rightarrow \frac{\partial}{\partial z} = \frac{d}{dz} \quad \text{and} \quad Z_s = \rho c.$$

If instead of a velocity potential ϕ (so $u = \nabla\phi$) we use a scalar displacement potential Φ (so $\vec{S} = \nabla\Phi$) we then require

$$p = -\rho\ddot{\Phi}$$

$$u = \nabla\dot{\Phi}$$

with

$$Z = \frac{p}{u} = -\frac{\rho\ddot{\Phi}}{\nabla\dot{\Phi}}$$

and again for a plane wave moving in the positive z direction or

$$\Phi = \Phi_0 e^{-i\omega t} e^{ikz}$$

we have with

$$\begin{aligned} u(z) &= \frac{\partial}{\partial z} \dot{\Phi} \\ &= \omega k \Phi \end{aligned}$$

and

$$p = \rho \omega^2 \Phi$$

that

$$Z(z) = \rho c$$

which is the same as obtained with a velocity potential.

II.2 Misuse of Convention of the Real

Another point to be made now concerns a valid but nonetheless misleading convention usually employed in acoustics, by which only the real part (or only the imaginary part) of a complex quantity represents the physical parameter in question. This convention of the real is most likely responsible for the startling omission of relative phase information in the acoustics literature while relative amplitudes were and are commonly employed. To illustrate this, for a simple undamped homogeneous harmonic oscillator we have

$$m \frac{d^2 z}{dt^2} + Kz = 0$$

written most simply in terms of displacement z since no propagation is involved. The general solution is

$$z = z_0 e^{-i\omega t}$$

where

$$\omega^2 = \frac{K}{m}$$

and the convention of the real, permissible with linear equations, represents the displacement by

$$z = a_1 \cos \omega t + a_2 \sin \omega t$$

where we note

$$z_0 = a_1 + i a_2.$$

Since this can be written

$$z_0 = R e^{i\theta}$$

we may also represent the displacement by

$$\begin{aligned} z_0 &= \Re_e [\Re e^{-i(\omega t - \theta)}] \\ &= R \cos (\omega t - \theta) \end{aligned}$$

where there is no great loss in setting the initial phase angle θ to zero. For example, the average value of the square of this quantity would be

$$\begin{aligned}\langle z^2 \rangle &= \frac{1}{2} R^2 \\ &= \frac{1}{2} (a_1^2 + a_2^2) \\ &= \frac{1}{2} |z_0|^2.\end{aligned}$$

While absolutely correct, the application of this convention to acoustics has resulted in the loss of information carried by the wave function or potential. Specifically, all phase information is lost. Of course, phase information is obtained simply if there is a driving force in the simple harmonic oscillator equation, but is not for a homogeneous acoustic wave equation.

Carrying the development along, postulating a wave function or velocity potential ψ , a simple example of a wave travelling with constant velocity and unchanging shape through a medium is a harmonic wave

$$\psi = \psi_0 e^{ikz} e^{-i\omega t}.$$

The amplitude ψ_0 is in general complex

$$\psi_0 = |\psi_0| e^{-i\beta}$$

so that

$$\psi = |\psi_0| \exp [i(kz - \beta - \omega t)]$$

but there is again no particular loss in setting $\beta = 0$. We also note that the average value of the real part of an exponential time dependence is $1/\sqrt{2}$ times the magnitude.

Using q for the generalized wave number (reserving k for the plane wave value of q)

$$\psi = |\psi_0| \exp [i(qz - \omega t)]$$

and applying the convention of the real

$$\psi = |\psi_0| \cos (qz - \omega t).$$

However, we are dealing with stationary states and so are not concerned with the average value of the real part of an exponential time dependence. It is easily seen that using

$$\psi_{\text{rel}} = \frac{\psi_{\text{diffracted}}}{\psi_{\text{plane wave}}}$$

we may write

$$|\psi_{\text{rel}}| = \sqrt{(\mathcal{R}e \psi_{\text{rel}})^2 + (\mathcal{I}m \psi_{\text{rel}})^2}$$

and

$$|\psi_{\text{rel}}| = P_{\text{rel}}$$

But the important point is that it readily follows that

$$\begin{aligned} \theta_{\text{rel}} &\equiv \theta_{\text{diffracted}} - \theta_{\text{plane wave}} \\ &= \tan^{-1} \frac{\mathcal{I}m \psi_{\text{rel}}}{\mathcal{R}e \psi_{\text{rel}}} \end{aligned}$$

an immensely useful albeit simple step which has apparently not been previously used in the literature by others. Actually, the work reported here utilizes cylindrical coordinates and the average over a circle of radius a or

$$\langle \psi \rangle = \frac{1}{\pi a^2} \int_0^a \psi(r, z) 2\pi r dr$$

and thence $\langle \psi \rangle_{\text{rel}}$, $\langle p \rangle_{\text{rel}}$, and $\langle \theta \rangle_{\text{rel}}$.

Section III

FINITE-SOURCE FREE-FIELD DIFFRACTION

This investigator's interest in acoustic propagation measurements in the laboratory dates back to the early NRL Sea Water Sound Speed results (6) and the later investigations of accuracy (7) wherein diffraction was stated to be the principal remaining source of error. In the latter reference, use was made of King's expression (8) for velocity potential in cylindrical coordinates in order to map the radiation field of a 1 MHz, 1 inch dia. acoustic source. King's expression for a source in an infinite baffle.

$$\phi = v_0 a \int_0^a \mu^{-1} e^{-\mu z} J_0(\alpha r) J_1(\alpha a) d\alpha$$

with v_0 the velocity of the disc of radius a and

$$\mu = (\alpha^2 - k^2)^{1/2}$$

is not affected by his later error. Following Williams' method (9) we obtained

$$\Re \langle \phi \rangle_{rel} = 1 - B \cos A - C \sin A$$

$$\Im \langle \phi \rangle_{rel} = B \sin A - C \cos A$$

where

$$A = M + N$$

$$M = \frac{ka^2}{z} - \frac{ka^4}{z^3}$$

$$N = \frac{ka^4}{4z^3}$$

$$B = J_0 - \frac{N^2}{4} J_0 - \frac{N}{2} J_1 + \frac{N}{2} J_3 - \frac{N^2}{4} J_4$$

$$C = J_1 - \frac{N^2}{4} J_1 - N J_2 + \frac{N^2}{8} J_3 - \frac{N^2}{8} J_5$$

and the J 's are Bessel functions of the first kind of indicated order and argument M , z is the axial cylindrical coordinate, a the acoustic source radius and k the ordinary wave number.

Although the amplitude variations detailed by these expressions were missed by Williams, they were pointed out by Seki, Granato, and Truell (10) and by Bass (11) who recalculated the average pressure by a more valid approximation. In (12) a higher-order approximation was shown to be not appreciably better. However, for reasons possibly following those indicated in the previous section no investigator calculated the indicated average phase relative to plane wave value prior to that. In that report the second-order approximation obtained following Bass' method is

$$\Re_e \langle \phi \rangle_{rel} = 1 - D [J_0 \cos x + J_1 \sin x] - E J_1 \frac{\sin x}{x}$$

$$\Im_m \langle \phi \rangle_{rel} = D [J_0 \sin x - J_1 \cos x] - E J_1 \frac{\cos x}{x}$$

where

$$D = 1 - \frac{1}{2} \left(\frac{x}{ka} \right)^2 - \frac{1}{8} \left(\frac{x}{ka} \right)^4$$

$$E = \left(\frac{x}{ka} \right)^2 + \frac{1}{4} \left(\frac{x}{ka} \right)^4$$

and the argument of the Bessel functions is

$$x = \frac{k}{2} [(z^2 + 4a^2)^{1/2} - z].$$

It was noted that although the $\langle p \rangle_{rel}$ calculated by the first-order approximation in (11) differ from the above by less than 1 percent at the closest calculated point ($z = 0.075$ cm) the calculations for $\langle \theta \rangle_{rel}$ disagree by over 30 percent at this same point. Of course, none of the earlier authors calculated $\langle \theta \rangle_{rel}$, nor is Williams' approximation valid at such small z .

Section IV

GUIDED-MODE DISPERSION

IV.1 Characteristic Function Formulation for Modes

As indicated in an earlier section, and as is usually the case, a velocity potential $\phi(r, \theta, z, t)$ is assumed throughout the liquid cylinder of interest (Fig. 1) which satisfies the scalar wave equation

$$\nabla^2 \phi = \frac{1}{c^2} \frac{\partial^2 \phi}{\partial t^2}.$$

Separating out a harmonic time dependence

$$e^{\pm i\omega t}$$

yields the homogeneous time-independent wave equation called the Helmholtz equation

$$\nabla^2 \phi + k^2 \phi = 0.$$

This is accomplished by writing

$$\phi = \phi(r, \theta, z) T(t)$$

and utilizing a separation constant $-k^2$ as

$$\frac{\nabla^2 \phi}{\phi} = \frac{1}{C^2 T} \frac{\partial^2 T}{\partial t^2} = -k^2.$$

The Helmholtz equation is written in cylindrical coordinates as

$$\frac{\partial^2 \phi}{\partial r^2} + \frac{1}{r} \frac{\partial \phi}{\partial r} + \frac{1}{r^2} \frac{\partial^2 \phi}{\partial \theta^2} + \frac{\partial^2 \phi}{\partial z^2} + k^2 \phi = 0$$

and separating the variables as

$$\phi = R(r) \Theta(\theta) Z(z)$$

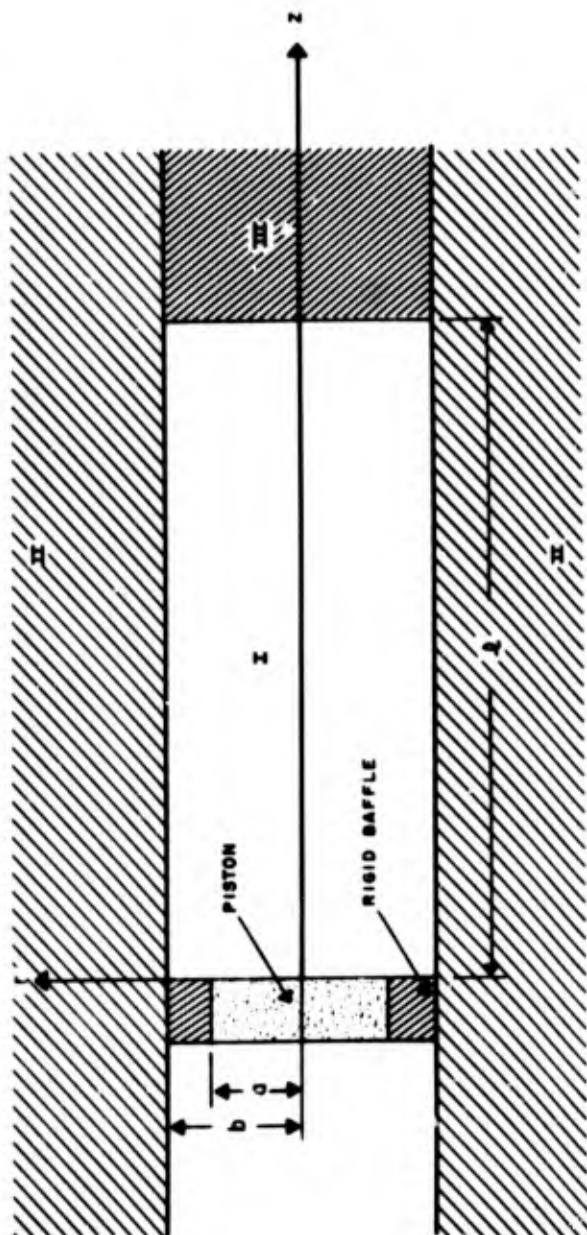


Fig. 1—Geometry for liquid cylinder which is modified in text.

the differential equations

$$\frac{d^2 \Theta}{d\theta^2} + n^2 \Theta = 0$$

$$\frac{d^2 Z}{dz^2} + q^2 Z = 0$$

and

$$\frac{d^2 R}{dr^2} + \frac{1}{r} \frac{dR}{dr} + R \left[k^2 - q^2 - \frac{n^2}{r^2} \right] = 0$$

are obtained using the separation constants $-n^2$ and $-q^2$. The corresponding solutions are

$$\Theta = C \cos n\theta + D \sin n\theta$$

where for single-valuedness of Θ we note that n must be an integer,

$$Z = E e^{iqz} + F e^{-iqz}$$

and

$$R = G J_n(r\sqrt{k^2 - q^2}).$$

The general solution to the time-independent part of the wave equation is then written as a mode of order (nm) as

$$\phi_{nm} = (K_{nm} \cos n\theta + L_{nm} \sin n\theta) e^{\pm iq_{nm}z} J_n(r\sqrt{k^2 - q_{nm}^2}).$$

Limiting consideration only to those modes with axial (circular) symmetry, n is restricted to zero whereby the θ dependence of ϕ is eliminated; thus

$$\phi_{0m} = \phi_{0m}(r, z) = K_{0m} J_0(r\sqrt{k^2 - q_{0m}^2}) e^{\pm iq_{0m}z}.$$

And finally considering only outgoing waves for a harmonic time dependence $e^{-i\omega t}$, we have

$$\phi_{0m} = K_{0m} J_0(r\sqrt{k^2 - q_{0m}^2}) e^{iq_{0m}z}.$$

We express the argument of the characteristic function for the radial dependence as

$$r \frac{X_{0m}}{b}$$

by defining a characteristic value X_{0m} as

$$X_{0m} \equiv b \sqrt{k^2 - q_{0m}^2}$$

where b is the liquid cylinder radius. The specification of the characteristic values X_{0m} involves radial boundary conditions equivalent to equating impedances. The impedance in the radial direction from the liquid cylinder side at the boundary $r = b$ is determined by evaluating

$$\left. \frac{p}{u(r)} \right|_{r=b}$$

where

$$p = -\rho \frac{\partial \phi}{\partial t}$$

$$u(r) = \frac{\partial \phi}{\partial r}$$

and ϕ with the time dependence restored is for each mode m

$$\phi_{0m} = M_{0m} J_0 \left(r \frac{X_{0m}}{b} \right) e^{i(q_{0m}z - \omega t)}$$

whereby the impedance in the radial direction from the liquid side evaluated at $r = b$ is

$$Z^L(r) \Big|_{r=b} = \frac{-i\omega\rho b J_0(X_{0m})}{X_{0m} J_1(X_{0m})}$$

IV.2 Plane Wave Synthesis of Mode

The form of the individual natural modes ϕ_{0m} is an expression of the fact that the total field within the liquid cylinder can be considered as the summation of an "infinite" sum of "plane waves" each making a different angle with the z axis of the cylinder. The words "infinite" and "plane waves" are written with quotation marks because it will be shown that the required sum in practice is indeed finite and the plane waves are of the type usually referred to as inhomogeneous, that is, with amplitude decreasing in a

direction normal to the direction of propagation. The plane wave synthesis of a waveguide mode is demonstrated by one of the many integral representations of the Bessel function $J_n(X)$ as

$$J_n(X) = \frac{i^{-n}}{2\pi} \int_0^{2\pi} e^{(iX \cos \alpha + in\alpha)} d\alpha$$

which becomes in our symmetrical case

$$J_0(X) = \frac{1}{2\pi} \int_0^{2\pi} e^{iX \cos \alpha} d\alpha.$$

Considering a plane wave travelling at an angle β to the x -axis in the xz plane as

$$Ae^{ik(x \cos \beta + z \sin \beta)} e^{-i\omega t}$$

we sum an infinite number of such waves all making the same angle $(\pi/2 - \beta)$ with the z -axis so that the loci of their wave normals is a cone about the z -axis with apex at the origin. These waves then make a variable angle $(\theta - \alpha)$ with the x -axis in the xy plane so that reverting to cylindrical coordinates we have $x = r \cos(\theta - \alpha)$ where without loss of generality we set $\theta = 0$ so $x = r \cos \alpha$. We then have for the infinite sum

$$\int_0^{2\pi} Ae^{ik(r \cos \alpha \cos \beta + z \sin \beta)} e^{-i\omega t} d\alpha.$$

Applying the integral representation this becomes

$$2\pi A J_0(kr \cos \beta) e^{ikz \sin \beta} e^{-i\omega t}$$

which can be written

$$C_m J_0\left(r \frac{X_{0m}}{b}\right) e^{iq_{0m} z - i\omega t}$$

where

$$\frac{X_{0m}}{b} = k \cos \beta$$

and

$$q_{0m} = k \sin \beta$$

whereby we note that the sum of the squares yield

$$\left(\frac{X_{0m}}{b}\right)^2 + q_{0m}^2 = k^2 \cos^2 \beta + k^2 \sin^2 \beta = k^2$$

or

$$X_{0m} = b \sqrt{k^2 - q_{0m}^2}$$

which was previously defined. Thus the modes we shall use for expansion are inhomogeneous plane waves or plane waves modified in the r direction normal to the propagation direction z by a Bessel function dependence.

IV.3 General Mode Characteristics

Those radial characteristic functions representing propagation are a finite subset of the usually infinite set which could be used for expansion of the velocity potential within the liquid cylinder. For such an expansion to be permissible the set of functions must be complete, but if the expansion degenerates to a finite series the question of completeness may no longer be germane. Such an expansion is easily carried out if the characteristic functions are mutually orthogonal, but such a requirement is not necessary. From the defined characteristic value X_{0m} we obtain for the waveguide mode propagation constant

$$q_{0m} = \frac{1}{b} \sqrt{(kb)^2 - (X_{0m})^2}$$

and for propagation we require q_{0m} to be real so the individual modes designated by the integer m are summed at most to describe propagation over

$$0 \leq X_{0m} \leq kb.$$

We note that imaginary X_{0m} ($= i \bar{X}_{0m}$) is admissible for propagation since even in this case q_{0m} remains real. The relative phase velocity of the m th mode with respect to the intrinsic sound speed of the liquid constituting the cylinder is also obtained from the defined characteristic value X_{0m} as

$$\frac{C_{0m}}{C} = \frac{1}{\sqrt{1 - \left(\frac{X_{0m}}{kb}\right)^2}}.$$

The relative group velocity is then obtained as

$$\frac{v_{0m}}{c} = \sqrt{1 - \left(\frac{x_{0m}}{kb}\right)^2}$$

directly from the definition

$$v_{0m} = \frac{d\omega}{dq_{0m}}$$

so that the relationship between group velocity, phase velocity, and intrinsic velocity is

$$c^2 = c_{0m} v_{0m}$$

The following conclusions are obvious from the relative phase velocity relation: For real x_{0m} and $x_{0m} < kb$,

$$\frac{c_{0m}}{c} > 1.$$

For real x_{0m} and $x_{0m} = kb$,

$$\frac{c_{0m}}{c} = \infty.$$

For $x_{0m} = 0$,

$$q_{0m} = k,$$

$$\frac{c_{0m}}{c} = 1.$$

For $kb = \infty$,

$$\frac{c_{0m}}{c} = 1.$$

For $x_{0m} = i\bar{x}_{0m}$,

$$\frac{c_{0m}}{c} < 1.$$

For $kb \leq x_{0m} \leq \infty$, q_{0m} is imaginary.

In this last case the mode is nonpropagating or evanescent with an imaginary wavelength and as previously stated this leads directly to the expansion over propagated

modes being a finite rather than an infinite series. When C_{0m}/C is identically unity the propagation is in a plane wave mode.

The possible imaginary characteristic value

$$X_{0m} = i\bar{X}_{0m}$$

is interesting also since then

$$\frac{C_{0m}}{C} = \frac{1}{\sqrt{1 + \left(\frac{\bar{X}_{0m}}{kb}\right)^2}}$$

and, unlike the modes with a real characteristic value, no lower cutoff frequency is predicted and the mode extends down to zero frequency or $kb = 0$. The situations wherein such a mode is permitted will be indicated in Section 7.

Section V

PROPAGATION IN NONTERMINATED CYLINDER

V.1 Characteristic Function Expansion for Potential

Without detailing as yet the characteristic or frequency equations which determine the characteristic values X_{0m} , and which are themselves determined by radial boundary conditions, we expand the velocity potential ϕ within the liquid cylinder in terms of the natural modes ϕ_{0m} as

$$\phi(r, z) = \sum_m K_{0m} J_0\left(r \frac{X_{0m}}{b}\right) e^{iq_{0m} z}$$

where as previously noted we have assumed radial symmetry for no θ dependence in cylindrical coordinates. The expansion coefficients as usual depend upon the type of excitation of the liquid cylinder and indicate the relative amplitudes of the various modes. Concerning ourselves only with axial propagation within the liquid cylinder and invoking radial symmetry we have obviously restricted ourselves to a form of excitation which is not only axial but axially-symmetric. Such an exciter is a piston source centrally located on the axis and at the origin of the cylindrical coordinate system. The piston source radius is taken as a and the liquid cylinder radius is again b . The geometry, with the inclusion of an outer medium about which nothing is now said, is shown in Fig. 1 where we disregard for now the reflector medium III. We need not yet specify the nature of the axial boundary condition at $z = 0$ to develop the formulation for the evaluation of the expansion coefficients. Indeed we note at $z = 0$

$$\phi(r, 0) = \sum_m K_{0m} R_{0m}$$

where, to simplify the notation we have defined

$$R_{0m} = J_0\left(r \frac{X_{0m}}{b}\right).$$

The expansion coefficients are obtained by the Fourier method by multiplying both sides of the equation for velocity potential at the origin by $r R_{0\ell}$ and integrating with respect to r over the limits 0 to b to obtain

$$\int_0^b \phi(r, 0) R_{0\ell} r dr = \int_0^b \sum_m K_{0m} R_{0m} R_{0\ell} r dr$$

which represents a set of simultaneous equations as follows:

$\ell = 0$:

$$\begin{aligned} \int_0^b \phi(r, 0) R_{00} r dr &= \int_0^b K_{00} R_{00}^2 r dr + \int_0^b K_{01} R_{01} R_{00} r dr \\ &+ \int_0^b K_{02} R_{02} R_{00} r dr + \int_0^b K_{03} R_{03} R_{00} r dr + \dots \end{aligned}$$

$\ell = 1$:

$$\begin{aligned} \int_0^b \phi(r, 0) R_{01} r dr &= \int_0^b K_{00} R_{00} R_{01} r dr + \int_0^b K_{01} R_{01}^2 r dr \\ &+ \int_0^b K_{02} R_{02} R_{01} r dr + \int_0^b K_{03} R_{03} R_{01} r dr + \dots \end{aligned}$$

$\ell = 2$:

$$\begin{aligned} \int_0^b \phi(r, 0) R_{02} r dr &= \int_0^b K_{00} R_{00} R_{02} r dr + \int_0^b K_{01} R_{01} R_{02} r dr \\ &+ \int_0^b K_{02} R_{02}^2 r dr + \int_0^b K_{03} R_{03} R_{02} r dr + \dots \text{etc.} \end{aligned}$$

This finite set of simultaneous equations can be written in matrix form as

$$\begin{pmatrix} \int_0^b \phi(r,0) R_{00} r dr \\ \int_0^b \phi(r,0) R_{01} r dr \\ \vdots \\ \int_0^b \phi(r,0) R_{0m} r dr \end{pmatrix} = \begin{pmatrix} \int_0^b R_{00}^2 r dr & \int_0^b R_{01} R_{00} r dr & \cdots & \int_0^b R_{0m} R_{00} r dr \\ \int_0^b R_{00} R_{01} r dr & \int_0^b R_{01}^2 r dr & \cdots & \int_0^b R_{0m} R_{01} r dr \\ \vdots & \vdots & \ddots & \vdots \\ \int_0^b R_{00} R_{0m} r dr & \int_0^b R_{01} R_{0m} r dr & \cdots & \int_0^b R_{0m}^2 r dr \end{pmatrix} \begin{pmatrix} K_{00} \\ K_{01} \\ \vdots \\ K_{0m} \end{pmatrix}$$

V.2 General Nonorthogonality of Characteristic Functions

As previously stated, if the characteristic functions R_{0m} are orthogonal the expansion is most easily carried out. The orthogonality criterion is

$$\int_0^b R_{0m} R_{0\ell} r dr = 0, \quad m \neq \ell$$

$$\neq 0, \quad m = \ell$$

It is easily shown (13) that

$$\int_0^b R_{0m}^2 r dr = \frac{b^2}{2} [J_0^2(X_{0m}) + J_1^2(X_{0m})]$$

and

$$\int_0^b R_{0m} R_{0\ell} r dr = \frac{b^2}{X_{0m}^2 - X_{0\ell}^2} [X_{0m} J_0(X_{0\ell}) J_1(X_{0m}) - X_{0\ell} J_0(X_{0m}) J_1(X_{0\ell})]$$

so that the orthogonality criterion is

$$X_{0m} J_0(X_{0\ell}) J_1(X_{0m}) - X_{0\ell} J_0(X_{0m}) J_1(X_{0\ell}) = 0 \quad \text{for } \ell \neq m.$$

Obviously the functions utilized for expansion are orthogonal only if the characteristic values are zeroes of J_0 , or zeroes of J_1 , or in the rather unlikely event that the orthogonality criterion is otherwise satisfied, that is,

$$X_{0m} J_0(X_{0\ell}) J_1(X_{0m}) = X_{0\ell} J_0(X_{0m}) J_1(X_{0\ell})$$

or

$$\frac{J_0(X_{0l})}{X_{0l} J_1(X_{0l})} = \frac{J_0(X_{0m})}{X_{0m} J_1(X_{0m})} \quad \text{for } l \neq m.$$

This is otherwise stated by requiring that the logarithmic derivative evaluated at the end points is not a function of the argument of the characteristic function or characteristic value or

$$\frac{1}{R_{0m}} \frac{d}{dr} (R_{0m}) \Big|_0^b \neq F(X_{0m}).$$

Indeed, the left-hand side is just the Wronskian. It is shown later that the characteristic functions chosen for expansion are orthogonal only for rather trivial and physically unrealizable boundary conditions. The simple situation of the characteristic values being either zeroes of J_0 or zeroes of J_1 is tantamount to invoking homogeneous boundary conditions, that is, requiring that either the function or its derivative vanish at the boundary.

For orthogonal characteristic functions then the matrix of the coefficients is diagonalized, that is, indicating orthogonal R_{0m} as R_{0m}^N

$$\begin{pmatrix} \int_0^b \phi(r, 0) R_{00}^N r dr \\ \int_0^b \phi(r, 0) R_{01}^N r dr \\ \vdots \\ \int_0^b \phi(r, 0) R_{0m}^N r dr \end{pmatrix} = \begin{pmatrix} \int_0^b (R_{00}^N)^2 r dr & 0 & \dots & 0 \\ 0 & \int_0^b (R_{01}^N)^2 r dr & \dots & 0 \\ \vdots & \vdots & \ddots & \vdots \\ 0 & 0 & \dots & \int_0^b (R_{0m}^N)^2 r dr \end{pmatrix} \begin{pmatrix} K_{00}^N \\ K_{01}^N \\ \vdots \\ K_{0m}^N \end{pmatrix}$$

$$= \begin{pmatrix} K_{00}^N \int_0^b (R_{00}^N)^2 r dr \\ K_{01}^N \int_0^b (R_{01}^N)^2 r dr \\ \vdots \\ K_{0m}^N \int_0^b (R_{0m}^N)^2 r dr \end{pmatrix}$$

which are separate equations

$$\int_0^b \phi(r, 0) R_{0m}^N r dr = K_{0m}^N \int_0^b (R_{0m}^N)^2 r dr$$

solved directly for K_{0m}^N .

The intent in this nonreflection situation in this Section is to obtain the velocity potential within the liquid cylinder averaged over a fiducial receiver centrally located on the axis and with the same radius as and concentric with the source or

$$\langle \phi \rangle = \frac{1}{\pi a^2} \int_0^a \phi(r, z) 2\pi r dr$$

assuming a response proportional to the average excess pressure over the receiver. Then the average velocity potential above is expressed relative to a plane wave as

$$\langle \phi \rangle_{rel} = \frac{\langle \phi \rangle}{\phi_0 e^{ikz}}$$

V.3 Piston Excitation of Modes

At this point we must specify the form of the excitation at $z = 0$. Considering only circular disc excitation in the axial direction or piston-like sources in infinite baffles we could have (a) a rigid piston in a rigid baffle so

$$\frac{\partial \phi(r, z)}{\partial z} = U_0$$

over the source

$$\frac{\partial \phi(r, z)}{\partial z} = 0$$

on the baffle

or (b) a rigid piston in an infinitely flexible baffle so

$$\frac{\partial \phi(r, z)}{\partial z} = U_0$$

over the source

$$\phi(r, z) = 0$$

on the baffle

or (c) a source with uniform pressure distribution in an infinitely flexible baffle so

$$\phi(r, z) = \phi_0$$

over the source

$$\phi(r, z) = 0$$

on the baffle

or (d) a source with uniform pressure distribution in a rigid baffle so

$$\phi(r, z) = \phi_0$$

over the source

$$\frac{\partial \phi(r, z)}{\partial z} = 0$$

on the baffle.

Condition (a) is the most easily physically realizable one and is the usual connotation of a piston source. Condition (d) is similar to the diffraction of a plane wave by a circular aperture (14) and has been used by Mangulis (15). It leads to the prediction for example, that for $ka \ll 1$, the velocity of the disc becomes infinite at the edge of the disc (16). Though condition (a) will be principally used in this report, the relatively unphysical condition (c) will now be invoked as a simple illustration of further development as it involves only the velocity potential. With this unphysical condition we then have

$$\begin{aligned} \int_0^b \phi(r, 0) R_{0\ell} r dr &= \phi_0 \int_0^a R_{0\ell} r dr \\ &= \phi_0 \int_0^a J_0\left(r \frac{X_{0\ell}}{b}\right) r dr \\ &= \phi_0 \frac{ab}{X_{0\ell}} J_1\left(X_{0\ell} \frac{a}{b}\right) \end{aligned}$$

with the result

$$\phi_0 \frac{ab}{X_{0l}} J_1 \left(X_{0l} \frac{a}{b} \right) = \int_0^b \sum_m K_{0m} R_{0m} R_{0l} r dr$$

as the set of simultaneous equations or matrix formulation with the elements on the left side evaluated. The matrix solution must then be obtained for the coefficients, but if the characteristic functions were orthogonal the above would then lead to individual equations for the expansion coefficients K_{0m}^N as

$$\begin{aligned} K_{0m}^N &= \phi_0 \frac{ab J_1 \left(X_{0m} \frac{a}{b} \right)}{X_{0m} \int_0^b (R_{0m}^N)^2 r dr} \\ &= \phi_0 \frac{2a J_1 \left(X_{0m} \frac{a}{b} \right)}{b X_{0m} [J_0^2(X_{0m}) + J_1^2(X_{0m})]} \end{aligned}$$

Without invoking orthogonality but utilizing the source boundary condition (c) we have

$$\begin{aligned} \langle \phi \rangle \phi_0 &= \frac{1}{\pi a^2} \sum_m 2\pi \int_0^a K_{0m} J_0 \left(r \frac{X_{0m}}{b} \right) e^{iq_{0m} z} r dr \\ &= \sum_m \frac{2b}{a} K_{0m} e^{iq_{0m} z} \frac{1}{X_{0m}} J_1 \left(X_{0m} \frac{a}{b} \right) \end{aligned}$$

and

$$\langle \phi \rangle_{rel} \phi_0 = \sum_m \frac{2b}{a \phi_0} K_{0m} e^{-i(k-q_{0m})z} \frac{J_1 \left(X_{0m} \frac{a}{b} \right)}{X_{0m}}$$

which becomes for orthogonal characteristic functions ($K_{0m} \rightarrow K_{0m}^N$)

$$\langle \phi \rangle_{rel} \phi_0 = \sum_m \frac{4 J_1^2 \left(X_{0m} \frac{a}{b} \right) e^{-i(k-q_{0m})z}}{X_{0m}^2 [J_0^2(X_{0m}) + J_1^2(X_{0m})]}$$

We now go back and utilize the more appropriate source boundary condition (a) instead of the source boundary condition (c) for which the development was just done.

From

$$u_z(r, z) = \frac{\partial \phi(r, z)}{\partial z}$$

we obtain

$$u_z = i \sum_m q_{0m} J_0\left(r \frac{X_{0m}}{b}\right) e^{iq_{0m} z} K_{0m}$$

so that

$$u_z(r, 0) = i \sum_m q_{0m} J_0\left(r \frac{X_{0m}}{b}\right) K_{0m}$$

and the determination of the coefficients is obtained by

$$\int_0^b u_z(r, 0) J_0\left(r \frac{X_{0l}}{b}\right) r dr = i \int_0^b \sum_m K_{0m} q_{0m} J_0\left(r \frac{X_{0m}}{b}\right) J_0\left(r \frac{X_{0l}}{b}\right) r dr$$

and applying the source boundary condition (c) the left side is

$$U_0 \int_0^a J_0\left(r \frac{X_{0l}}{b}\right) r dr = U_0 \frac{ab}{X_{0l}} J_1\left(X_{0l} \frac{a}{b}\right)$$

so that

$$U_0 \frac{ab}{X_{0l}} J_1\left(X_{0l} \frac{a}{b}\right) = i \int_0^b \sum_m K_{0m} q_{0m} J_0\left(r \frac{X_{0m}}{b}\right) J_0\left(r \frac{X_{0l}}{b}\right) r dr$$

which is again a set of simultaneous equations which can be cast in matrix formulation and be solved for the K_{0m} . If we now simplify the formulation by assuming the characteristic functions are orthogonal, the matrix is again diagonalized and separate equations for the K_{0m}^N are obtained as

$$K_{0m}^N = \frac{2U_0 a J_1\left(X_{0m} \frac{a}{b}\right)}{iq_{0m} b X_{0m} [J_0^2(X_{0m}) + J_1^2(X_{0m})]}$$

In obtaining $\langle \phi \rangle_{rel}$ we divided $\langle \phi \rangle$ by a plane wave representation

$$\phi_{\text{plane wave}} = \phi_0 e^{ikz}.$$

For a plane wave simple relations hold as

$$\begin{aligned} u_z &:: \frac{\partial \phi}{\partial z} = ik\phi_0 e^{ikz} \\ &= U_0 e^{ikz} \end{aligned}$$

so that

$$U_0 = ik\phi_0$$

and

$$K_{0m}^N = \frac{2ak\phi_0}{q_{0m}b} \frac{J_1\left(X_{0m} \frac{a}{b}\right)}{X_{0m} [J_0^2(X_{0m}) + J_1^2(X_{0m})]}$$

whereby it is obvious that K_{0m}^N for a uniform velocity source designated $(K_{0m}^N)^{U_0}$ is related to K_{0m}^N for a uniform pressure source designated $(K_{0m}^N)^{\phi_0}$ by the factor k/q_{0m} as

$$(K_{0m}^N)^{U_0} = \frac{k}{q_{0m}} (K_{0m}^N)^{\phi_0}.$$

We recall that for a plane wave, $q_{00} = k$, so that the factor disappears for a plane wave. Also with $m = 0$ we have

$$\phi_{00} = K_{00} J_0\left(r \frac{X_{00}}{b}\right) e^{ikz} e^{-i\omega t}$$

and

$$X_{00} = b \sqrt{k^2 - q_{00}^2} = 0$$

so that

$$\phi_{00} = K_{00} e^{ikz} e^{-i\omega t}$$

where we used $J_0(0) = 1$.

For the orthogonal assumption characteristic functions then we have for a uniform velocity source

$$\langle \phi \rangle_{\text{rel}}^{U_0} = \sum_m \frac{4kJ_1^2\left(X_{0m} \frac{a}{b}\right) e^{-i(k-q_{0m})z}}{q_{0m} X_{0m}^2 [J_0^2(X_{0m}) + J_1^2(X_{0m})]}$$

V.4 Critique of Integrating Only Over Liquid Cylinder

It should be noted that we have chosen to expand the velocity potential within the liquid cylinder in terms of axially symmetric characteristic functions which were obtained without consideration of the impedance of the radially surrounding medium, and indeed are an orthogonal set of functions only for the limiting cases of the surrounding medium having an impedance either infinite (absolutely rigid boundary) or zero (free boundary). In these trivial cases no penetration of acoustic energy into the wall material can occur, and no fault is found with our integration only over the liquid cylinder or $0 \leq r \leq b$.

But the use of this same source boundary condition when the liquid cylinder is enclosed by a finite impedance medium of infinite extent, or more, by a finite impedance tube, is admittedly insufficiently investigated at this point. In particular, it is as yet unproved that carrying out the integration only over the liquid cylinder to evaluate the expansion coefficients does not imply any untoward assumptions as to the nature of the source boundary condition at $z = 0$ for $r > b$. This point will be dealt with in detail after the appropriate mathematical formulation of specific modes for specified radial boundary conditions is obtained. It will be shown then that no difficulty results from restricting the integration to the liquid cylinder, or alternatively, that no different result incurs if the integral is expressed over all space, at least for the parameters deliberately selected and specified later in Table 1.

V.5 Critique of Limiting Summation to Propagated Modes

It could be successfully argued that only the propagated modes do in fact propagate down the liquid cylinder and affect $\langle p \rangle_{rel}$ and $\langle \theta \rangle_{rel}$ at some few wavelengths from the source. But it will be shown in a later section that consideration of only the propagated modes does in fact more than adequately specify the source boundary condition at $z = 0$. Indeed for the orthogonal characteristic functions resulting for the trivial cases of absolutely rigid or free radial boundaries, the coefficient determining equations are distinct and separate, and no earlier coefficients are changed by the later inclusion of more modes, evanescent or otherwise. This is related to the concept of finality which essentially indicates that after inclusion of a certain number of terms, the earlier coefficients are no longer changed by including more.

Actually it will be seen in Section 7, for the more realistic situations of a radially surrounding medium of finite impedance but infinite extent, that there are no evanescent modes and in fact there are only a finite number of propagating modes. That is, modal solutions or roots to the characteristic or frequency equation cease to exist before they

would have become nonpropagating. It will be shown that this finite smaller number of modes is still more than adequate to describe the source boundary condition at $z = 0$.

Before the proofs of the foregoing are presented, which must await the more detailed specification of modes, we will give further consideration to the deliberate omission of the evanescent modes when they occur (and to the effect of having only a smaller finite number of propagating modes for the infinite extent but finite impedance surrounding media) in the next section, where our concern, rather than being with the evaluation of $\langle p \rangle_{rel}$ and $\langle \theta \rangle_{rel}$ at some distance from the source is instead with the impedance of the source itself. A saving feature, however, is that we are interested only in the changes of source impedance with reflector-to-source distance variation.

Section VI

PROPAGATION IN TERMINATED CYLINDER

VI.1 Characteristic Function Expansion for Source Impedance

Again the configuration assumed is a right circular cylinder of liquid of radius b terminated at one end by a circular disc source of radius a but now also closed at the other end by a plane parallel reflector of radius b situated at $z = l$ and extending infinitely outward for $z > l$. Both source and reflector are centered on and normal to the cylinder axis as shown in Fig. 1. Again we do not yet say anything specific about the medium which radially surrounds the liquid cylinder.

We again separate a harmonic time dependence from the ordinary wave equation and obtain the time independent Helmholtz equation

$$\nabla^2 \phi + k^2 \phi = 0$$

with solution

$$\begin{aligned} \phi_{nm}(r, \theta, z) = & (C_{nm} \cos n\theta + D_{nm} \sin n\theta)(E_{nm} e^{iq_{nm}z} + F_{nm} e^{-iq_{nm}z}) \\ & \times \left(G_{nm} J_n \left(r \frac{X_{nm}}{b} \right) \right) \end{aligned}$$

where

$$X_{nm} = b \sqrt{k^2 - q_{nm}^2}.$$

Again invoking axial (circular) symmetry restricts n to zero, so

$$\phi_{0m}(r, z) = J_0 \left(r \frac{X_{0m}}{b} \right) [K_{0m} e^{iq_{0m}z} + L_{0m} e^{-iq_{0m}z}]$$

and

$$X_{0m} = b \sqrt{k^2 - q_{0m}^2}.$$

The velocity potential field within the liquid cylinder is again expanded in terms of these natural modes ϕ_{0m} as

$$\phi(r, z) = \sum_m J_0\left(r \frac{X_{0m}}{b}\right) [K_{0m} e^{iq_{0m}z} + L_{0m} e^{-iq_{0m}z}].$$

If we were to assume a uniform pressure source we would then write for $z = 0$

$$\phi(r, 0) = \sum_m J_0\left(r \frac{X_{0m}}{b}\right) [K_{0m} + L_{0m}]$$

and proceed as previously, but we will detail here only the most realistic case, that of a uniform velocity piston where

$$\left. \frac{\partial \phi(r, z)}{\partial z} \right|_{z=0} = U_0$$

over the source

$$\left. \frac{\partial \phi(r, z)}{\partial z} \right|_{z=l} = 0$$

over the baffle.

Applying this to $\phi(r, z)$, multiplying by

$$r J_0\left(r \frac{X_{0l}}{b}\right)$$

and integrating with respect to r over the limits 0 to b yields

$$U_0 \frac{ab}{X_{0l}} J_1\left(X_{0l} \frac{a}{b}\right) = \int_0^b \sum_m iq_{0m} (K_{0m} - L_{0m}) R_{0m} R_{0l} r dr$$

where we again used

$$R_{0m} = J_0\left(r \frac{X_{0m}}{b}\right).$$

Again these are a set of simultaneous equations which can be cast in matrix formulation and solved for $K_{0m} - L_{0m}$. We note that, for example,

$$K_{01} - L_{01} = N_1 U_0$$

$$K_{02} - L_{02} = N_2 U_0$$

etc., and

$$\frac{K_{0m} - L_{0m}}{N_m} = U_0$$

where the N_m are numerical constants. As before we solve for

$$\langle \phi \rangle = \frac{1}{\pi a^2} \int_0^a \phi(r, z) 2\pi r dr$$

and obtain, after some manipulation,

$$\langle \phi \rangle = \sum_m (K_{0m} e^{iq_{0m}z} + L_{0m} e^{-iq_{0m}z}) \frac{2J_1\left(X_{0m} \frac{a}{b}\right)}{\left(X_{0m} \frac{a}{b}\right)}$$

Then, utilizing

$$p = -\rho \frac{\partial \phi}{\partial t} = i\rho\omega\phi$$

we obtain

$$\langle p \rangle_0 = i\rho\omega \sum_m (K_{0m} + L_{0m}) \frac{2J_1\left(X_{0m} \frac{a}{b}\right)}{\left(X_{0m} \frac{a}{b}\right)}$$

where $\langle p \rangle_0$ is the pressure averaged over the source at $z = 0$. Then Z_0 , the radiation impedance of the source, is obtained as

$$Z_0 = \frac{\langle p \rangle_0}{U_0}$$

which leads to

$$Z_0 = i\omega\rho \sum_m \frac{(K_{0m} + L_{0m})}{U_0} \frac{2J_1\left(X_{0m} \frac{a}{b}\right)}{\left(X_{0m} \frac{a}{b}\right)}$$

where we recall that the N_m are obtained as solutions to the simultaneous equations. At this point it might be well to indicate the simplification brought about if the characteristic functions were orthogonal. Applying the source boundary conditions to $\phi(r, z)$ but invoking orthogonality leads to

$$(K_{0m} - L_{0m})^N = \frac{-2i U_0 a J_1 \left(X_{0m} \frac{a}{b} \right)}{b q_{0m} X_{0m} [J_0^2(X_{0m}) + J_1^2(X_{0m})]}$$

where, as used previously, the superscript N denotes orthogonality, and

$$N_m^N = \frac{-2i a J_1 \left(X_{0m} \frac{a}{b} \right)}{b q_{0m} X_{0m} [J_0^2(X_{0m}) + J_1^2(X_{0m})]}$$

Having calculated impedance at the source $z = 0$ we now calculate the impedance in the liquid cylinder at the reflector end $z = \ell$ by

$$Z^L(z) \Big|_{z=\ell} = \frac{P}{u(z)} \Big|_{z=\ell}$$

where

$$P = -\rho \frac{\partial \phi}{\partial t} \quad u(z) = \frac{\partial \phi}{\partial z}$$

so that

$$P_{0m}(z) = P (K_{0m} e^{iq_{0m}z} + L_{0m} e^{-iq_{0m}z})$$

and

$$u_{0m}(z) = \frac{P q_{0m}}{\omega \rho_1} (K_{0m} e^{iq_{0m}z} - L_{0m} e^{-iq_{0m}z})$$

where

$$P = i\omega \rho_1 J_0 \left(r \frac{X_{0m}}{b} \right) e^{-i\omega t}$$

and ρ_1 is the cylinder liquid medium density. We now denote the impedance of the reflector material as $\rho_3 C_3$ where ρ_3 is the density of the reflector material and C_3 is its wave velocity. Then, equating impedances at $z = \ell$, with the above assumption that the reflector impedance is independent of ℓ and r , (the effect of this assumption is detailed in IX.7)

$$Z^L(z)|_{z=l} = \rho_3 C_3$$

yields

$$\rho_3 C_3 = \frac{\sum_m \omega \rho_1 (K_{0m} e^{iq_{0m}l} + L_{0m} e^{-iq_{0m}l}) J_0\left(r \frac{X_{0m}}{b}\right)}{\sum_m i_{0m} (K_{0m} e^{iq_{0m}l} - L_{0m} e^{-iq_{0m}l}) J_0\left(r \frac{X_{0m}}{b}\right)}$$

which, in order to hold independently of l and r , implies

$$K_{0m} \left(1 + \frac{q_{0m} \rho_3 C_3}{k_1 \rho_1 C_1}\right) e^{iq_{0m}l} + L_{0m} \left(1 - \frac{q_{0m} \rho_3 C_3}{k_1 \rho_1 C_1}\right) e^{-iq_{0m}l} = 0.$$

By defining

$$A_{0m} = \frac{q_{0m} \rho_3 C_3}{k_1 \rho_1 C_1}$$

we may write

$$K_{0m} = \frac{(A_{0m} - 1) e^{-iq_{0m}l}}{(A_{0m} + 1) e^{-iq_{0m}l}} L_{0m}$$

and

$$\frac{K_{0m} + L_{0m}}{K_{0m} - L_{0m}} = \frac{e^{-iq_{0m}l} - \left(\frac{1 + A_{0m}}{1 - A_{0m}}\right) e^{iq_{0m}l}}{e^{-iq_{0m}l} + \left(\frac{1 + A_{0m}}{1 - A_{0m}}\right) e^{iq_{0m}l}}.$$

By further defining

$$\frac{1 + A_{0m}}{1 - A_{0m}} = S_{0m}$$

we obtain

$$Z_0 = -\rho_1 \omega \sum_m \frac{4 J_1^2\left(X_{0m} \frac{a}{b}\right)}{q_{0m} X_{0m}^2 [J_0^2(X_{0m}) + J_1^2(X_{0m})]} \left[\frac{e^{-iq_{0m}l} - S_{0m} e^{iq_{0m}l}}{e^{-iq_{0m}l} + S_{0m} e^{iq_{0m}l}} \right].$$

Now

$$\sum_{m=0}^{\infty} \frac{4J_1^2\left(X_{0m} \frac{a}{b}\right)}{X_{0m}^2 [J_0^2(X_{0m}) + J_1^2(X_{0m})]} = 1$$

but m is summed at most only to $X_{0m} \leq kb$.

If we finally define

$$\theta_{0m} = \coth^{-1} A_{0m}$$

we find

$$S_{0m} = \frac{1 + \coth \theta_{0m}}{1 - \coth \theta_{0m}} = -e^{2\theta_{0m}}$$

so that

$$Z_0 = \sum_m Z_{0m} \coth(iq_{0m} \ell + \theta_{0m})$$

where

$$Z_{0m} = \frac{\rho_1 C_1 k_1 4J_1^2\left(X_{0m} \frac{a}{b}\right)}{q_{0m} X_{0m}^2 [J_0^2(X_{0m}) + J_1^2(X_{0m})]}$$

and

$$\theta_{0m} = \coth^{-1} \frac{\rho_3 C_3 q_{0m}}{\rho_1 C_1 k_1}.$$

VI.2 Plane Wave Degeneration

If plane waves only are considered, $q_{0m} \rightarrow k_{00}$ and $X_{0m} \rightarrow 0$ so

$$Z_{0P} = \rho_1 C_1 \coth(ik\ell + \theta')$$

where the subscript **P** denotes plane wave conditions and

$$\theta' = \coth^{-1} \frac{\rho_3 C_3}{\rho_1 C_1}.$$

Then, we could write

$$\frac{Z_{0P}}{\rho_1 C_1} = \frac{\sinh 2\theta' - i \sin 2k\ell}{\cosh 2\theta' - \cos 2k\ell}$$

for plane waves in a dissipationless medium. This indicates that $Z_{0P}/\rho_1 C_1$ is real when either

$$2k\ell = (2n - 1)\pi$$

or

$$k\ell = n\pi.$$

The first case corresponds to minimum resistance R since then

$$\frac{Z_{0P}}{\rho_1 C_1} \rightarrow \frac{R_{0P}}{\rho_1 C_1}$$

for

$$\ell = \left(n - \frac{1}{2}\right) \frac{\lambda_1}{2}$$

and

$$\frac{R_{0P}}{\rho_1 C_1} = \frac{\sinh 2\theta'}{\cosh 2\theta' + 1} = \tanh \theta' = \frac{\rho_1 C_1}{\rho_3 C_3}.$$

The second case corresponds to maximum resistance R since then

$$\frac{Z_{0P}}{\rho_1 C_1} \rightarrow \frac{R_{0P}}{\rho_1 C_1}$$

for

$$\ell = n \frac{\lambda_1}{2}$$

and

$$\frac{R_{0P}}{\rho_1 C_1} = \coth \theta' = \frac{\rho_3 C_3}{\rho_1 C_1}.$$

It is noted that for plane waves in a dissipationless medium that both maximum R and minimum R coincide with zero reactance and are thus also points of zero phase.

VI.3 Critique of Limited Integration and Limited Sum

Addressing again the effect of including only the propagating modes in the potential expansion within the liquid cylinder, we cannot now argue that we are interested in the mode summation only at some distance from the source and that only propagated modes arrive there. Indeed we are now interested in the impedance of the source itself and all the modes contribute. In the cases of a radially surrounding medium of finite impedance but infinite extent we have indicated (and will demonstrate in Section 7) that there are no nonpropagating modes. That is, the solutions to the characteristic equation end before the resulting modes become evanescent. Thus the summation is carried out over all the existing modes with no approximations.

When the radially surrounding medium is considered absolutely rigid or free, the appropriate characteristic functions are orthogonal, and the property of finality ensures that the calculation of coefficients does not result in new values for the propagating mode coefficients when a finite number of evanescent modes is considered in addition to the propagating ones. Indeed, since the coefficient determining equations are individual for each mode, none depend on any other.

In the case of a radially surrounding finite thickness tube of finite impedance, however, the family of modes again consists of a finite number of propagating ones and an infinite number of evanescent ones, and in this case, unlike for the trivial limiting conditions, the characteristic functions are not orthogonal. But here we do make use of the fact that we are considering a source of appreciable $k_1 a = 2\pi a / \lambda_1$ where λ_1 is the intrinsic wavelength of the liquid cylinder medium and a is the radius of the source. Indeed, in the configuration used for calculation in Section 9 we have $k_1 a = 100\pi$. For a radiator this large in comparison to a wavelength the real part of the radiation impedance or the resistance has settled down to $\rho_1 C_1$ ("p C" loading) and the imaginary part or the reactance has essentially vanished. But, even stronger, we are concerned only with the variation in the impedance of the source as modified by the reflector located at some distance l from the source. Thus again we can successfully argue that the variation in impedance is caused only by the modes which propagate out to the reflector and back to the source and whose resultant phase and amplitude are varied with reflector position. Obviously this process is iterative and many successive reflections ensue (though we have not invoked a simple iterative summation to describe the effect). This process of iterative reflection however, operates in the fashion of a Fabry-Perot optical interferometer to preferentially accentuate those modes which are most plane-wavelike. Another way, the process discriminates against the higher order modes, with increasing discrimination as the complexity of the mode or its order increases. For these several reasons set forth

above the effect of not including propagated modes is nil, or, more positively, a summation over all the propagated modes is sufficient. And, we recall that only in the most realistic case of a finite thickness tube of finite impedance is a discourse such as the above at all required.

Another point in analogy to the previous discussion is that the attribution of an impedance $\rho_3 C_3$ to the reflector (whose "ka" equals 200π) again is tantamount to invoking " ρC " loading.

But the identical discussion alluded to in the previous section and made later which indicates no unusual implied assumption for $r > b$ at the plane $z = 0$ will also hold for this case.

And in addition, results of calculations over only the propagated modes or even less if the modes are indeed finite in number will demonstrate the degree of validity of the assumption of " ρC " loading.

Section VII

RADIALLY SURROUNDING ELASTIC SOLID OF INFINITE EXTENT OUTWARDS

VII.1 Scalar and Vector Displacement Potentials

For the first time now we discuss the medium which radially surrounds the liquid cylinder. For the most general case we consider an elastic solid and in this section we allow it to extend radially outward from $r = b$ to ∞ . As is usual with solids, we use a displacement vector \vec{S} which is related to a scalar displacement potential Φ and a vector displacement potential $\vec{\Psi}$ as

$$\vec{S} = \nabla \Phi + \nabla \times \vec{\Psi}.$$

This is consistent with ordinary wave equations in Φ and $\vec{\Psi}$

$$\nabla^2 \Phi = \frac{1}{C_c^2} \frac{\partial^2 \Phi}{\partial t^2}$$

and

$$\nabla^2 \vec{\Psi} = \frac{1}{C_s^2} \frac{\partial^2 \vec{\Psi}}{\partial t^2}$$

and with the vector form of the linear elastic equations of motion for an isotropic homogeneous material obeying Hooke's law

$$\rho_2 \frac{\partial^2 \vec{S}}{\partial t^2} = (\mathbf{L} + 2\mu) \text{grad } \Delta - 2\mu \text{curl } \vec{\omega}$$

where \mathbf{L} (usually denoted by λ) and μ are Lamé's constants and the rotation $\vec{\omega} = 1/2 \text{curl } \vec{S}$ and the dilatation $\Delta = \text{div } \vec{S}$.

We note that in general, in cylindrical coordinates

$$\nabla \Phi = \frac{\partial \Phi}{\partial r} \hat{i}_r + \frac{1}{r} \frac{\partial \Phi}{\partial \theta} \hat{i}_\theta + \frac{\partial \Phi}{\partial z} \hat{i}_z$$

and

$$\begin{aligned}\nabla \times \vec{\Psi} &= \left[\frac{1}{r} \frac{\partial}{\partial \theta} \Psi_z - \frac{\partial}{\partial z} \Psi_\theta \right] \hat{i}_r \\ &+ \left[\frac{\partial}{\partial z} \Psi_r - \frac{\partial}{\partial r} \Psi_z \right] \hat{i}_\theta \\ &+ \frac{1}{r} \left[\frac{\partial}{\partial r} (r \Psi_\theta) - \frac{\partial}{\partial \theta} \Psi_r \right] \hat{i}_z\end{aligned}$$

so, in general, writing $\vec{S} = S_r \hat{i}_r + S_\theta \hat{i}_\theta + S_z \hat{i}_z$

$$S_r = \frac{\partial \Phi}{\partial r} + \frac{1}{r} \frac{\partial}{\partial \theta} \Psi_z - \frac{\partial}{\partial z} \Psi_\theta$$

$$S_\theta = \frac{1}{r} \frac{\partial \Phi}{\partial \theta} + \frac{\partial}{\partial z} \Psi_r - \frac{\partial}{\partial r} \Psi_z$$

$$S_z = \frac{\partial \Phi}{\partial z} + \frac{1}{r} \left[\frac{\partial}{\partial r} (r \Psi_\theta) - \frac{\partial}{\partial \theta} \Psi_r \right]$$

but in our case of assumed axial (radial) symmetry where

$$S_\theta = 0$$

and

$$\frac{\partial}{\partial \theta} = 0$$

we have only

$$S_r = \frac{\partial \Phi}{\partial r} - \frac{\partial}{\partial z} \Psi_\theta$$

and

$$S_z = \frac{\partial \Phi}{\partial z} + \frac{1}{r} \frac{\partial}{\partial r} (r \Psi_\theta)$$

and we note that only the single θ component of $\vec{\Psi}$ remains. We shall henceforth designate Ψ_θ simply as Ψ .

The wave equations then become "wave" equations

$$\nabla^2 \Phi - \frac{1}{C_c^2} \frac{\partial^2 \Phi}{\partial t^2} = 0$$

and

$$\nabla^2 \Psi - \frac{\Psi}{r^2} - \frac{1}{C_s^2} \frac{\partial^2 \Psi}{\partial t^2} = 0$$

where the quotation marks refer to the extraneous term in the Ψ equation. We repeat that Ψ is an abbreviation for Ψ_θ which is the sole remaining component of $\vec{\Psi}$.

VII.2 Bessel Function Solutions

Removing the harmonic time dependence $e^{-i\omega t}$ and the consequent axial dependence $e^{iq_{0m}z}$ leave radial equations as

$$\frac{\partial^2 \Phi}{\partial r^2} + \frac{1}{r} \frac{\partial \Phi}{\partial r} + \left[(k_c^2 - q_{0m}^2) - \frac{0^2}{r^2} \right] \Phi = 0$$

and

$$\frac{\partial^2 \Psi}{\partial r^2} + \frac{1}{r} \frac{\partial \Psi}{\partial r} - \left[(k_s^2 - q_{0m}^2) + \frac{1^2}{r^2} \right] \Psi = 0$$

which are respectively a Bessel equation with parameter

$$\beta_1 = \sqrt{k_c^2 - q_{0m}^2}$$

and order zero and a modified Bessel equation with parameter

$$\beta_2 = \sqrt{k_s^2 - q_{0m}^2}$$

and order unity. The rather unusual display of 0^2 and 1^2 is done deliberately to help indicate the order of the respective Bessel function solutions.

The solution of the scalar potential equation is

$$\Phi = C_1 J_0(\beta_1 r) + C_2 N_0(\beta_1 r)$$

and the solution of the original vector potential equation is

$$\Psi = C_3 I_1(\beta_2 r) + C_4 K_1(\beta_2 r).$$

For the liquid cylinder, then, to which only a scalar potential is applicable, we require necessarily that $C_2 = 0$ since N_0 is undefined at the origin. For the radially surrounding medium to which we attribute in general both a scalar and vector potential, we note

that $r = 0$ is not included so we retain both solutions for Φ and further note that if $r = \infty$ is included we must necessarily set $C_3 = 0$. To reemphasize, for the liquid cylinder we retain only the solution J_0 , while for the elastic solid radially surrounding medium extending from $b \leq r \leq \infty$ we retain both J_0 and N_0 for Φ and only K_1 for Ψ . In particular, we may choose for the outside region

$$C_1 = 1 \quad \text{and} \quad C_2 = i$$

so that we consider only outgoing waves and

$$\begin{aligned} \Phi &= J_0(\beta_1 r) + i N_0(\beta_1 r) \\ &= H_0^{(1)}(\beta_1 r) \end{aligned}$$

and, defining

$$\beta_1 = i \gamma_1$$

we may write

$$\Phi = \frac{2}{\pi i} K_0(\gamma_1 r).$$

Thus, for the liquid cylinder we utilize a solution J_0 and for the radially surrounding medium we select solutions K_0 (or $H_0^{(1)}$) for the scalar potential solution and K_1 for the vector potential where it exists.

For the general case then, we write for the infinite radially surrounding medium

$$\Phi = \Phi_0 K_0(r \sqrt{q_{0m}^2 - k_c^2}) e^{-i(\omega t - q_{0m} z)}$$

and

$$\Psi = \Psi_0 K_1(r \sqrt{q_{0m}^2 - k_s^2}) e^{-i(\omega t - q_{0m} z)}$$

where the argument of the Bessel function indicates the appropriate wave number, i.e., k_s or k_c .

For guided waves within the liquid cylinder we write

$$\phi = \phi_0 J_0(r \sqrt{k_1^2 - q_{0m}^2}) e^{-i(\omega t - q_{0m} z)}$$

for $k_1^2 > q_{0m}^2$. If $q_{0m}^2 > k_1^2$ we write

$$\phi = \phi_0 I_0(r \sqrt{q_{0m}^2 - k_1^2}) e^{-i(\omega t - q_{0m} z)}$$

where $J_0(ix) = I_0(x)$.

Emphasizing that ϕ is a scalar displacement potential now rather than the velocity potential discussed in detail in an earlier section, we now have the pressure

$$p = -\rho_1 \ddot{\phi}$$

and the particle velocity

$$U_r^L = \frac{\partial}{\partial r} \dot{\phi}$$

where the subscript r refers to the radial component and the superscript L refers to the liquid cylinder medium.

Instead of using pressure and particle velocity boundary conditions or their quotient as impedance which was expedient with a velocity potential, we now find it desirable to use pressure and displacement boundary conditions or the combined condition of their quotient when a displacement potential is utilized. Thus, for the liquid cylinder we find, for $C_{0m} > C$,

$$p = \phi_0 \rho_1 \omega^2 J_0(r \sqrt{k_1^2 - q_{0m}^2}) e^{-i(\omega t - q_{0m} z)}$$

and, for the particle displacement

$$S_r^L = \frac{\partial}{\partial r} \phi = -\phi_0 \sqrt{k_1^2 - q_{0m}^2} J_1(r \sqrt{k_1^2 - q_{0m}^2}) e^{-i(\omega t - q_{0m} z)}$$

where we used $J_1(X) = -J_0'(X)$. Thus,

$$\left. \frac{p}{S_r^L} \right|_{r=b} = \frac{-\rho_1 \omega^2 J_0(b \sqrt{k_1^2 - q_{0m}^2})}{\sqrt{k_1^2 - q_{0m}^2} J_1(b \sqrt{k_1^2 - q_{0m}^2})}$$

or, using the previous definition $X_{0m} \equiv b \sqrt{k_1^2 - q_{0m}^2}$

$$\left. \frac{p}{S_r^L} \right|_{r=b} = \frac{-\rho_1 \omega^2 b J_0(X_{0m})}{X_{0m} J_1(X_{0m})}$$

We note that this is just a disguised form of the logarithmic derivative.

Now, returning to the radially surrounding medium, we note the stress components for this general elastic case are

$$\sigma_{rr} = 2\mu \frac{\partial S_r}{\partial r} + L \left(\frac{\partial S_r}{\partial r} + \frac{S_r}{r} + \frac{\partial S_z}{\partial z} \right)$$

and

$$\sigma_{rz} = \mu \left(\frac{\partial S_r}{\partial z} + \frac{\partial S_z}{\partial r} \right)$$

where, incidentally, the shear modulus is

$$\mu = \rho_2 C_s^2$$

and the other Lamé constant usually denoted λ is

$$L = 2\rho_2 C_s^2 \left(\frac{\nu}{1-2\nu} \right).$$

In terms of the potentials Φ and Ψ then the stress components are

$$\sigma_{rr} = 2\mu \left(\frac{\partial^2 \Phi}{\partial r^2} - \frac{\partial^2 \Psi}{\partial r \partial z} \right) + \rho_2 \left(\frac{\nu}{1-\nu} \right) \frac{\partial^2 \Phi}{\partial t^2}$$

$$\sigma_{rz} = 2\mu \left(\frac{\partial^2 \Phi}{\partial r \partial z} - \frac{\partial^2 \Psi}{\partial z^2} \right) + \rho_2 \frac{\partial^2 \Psi}{\partial t^2}$$

where we also used the relationship between C_c and C_s .

VII.3 Alternative Use of a Modified Vector Displacement Potential

If the use of a pseudowave equation in Ψ is disturbing, rectification may be accomplished by defining another potential $\bar{\Psi}$ as

$$\Psi = - \frac{\partial \bar{\Psi}}{\partial r}$$

where now $\bar{\Psi}$ is a solution to an ordinary wave equation

$$\nabla^2 \bar{\Psi} = \frac{1}{C_s^2} \frac{\partial^2 \bar{\Psi}}{\partial t^2}.$$

This is seen immediately by differentiating the latter re r . Writing out the wave equation in $\bar{\Psi}$ we have

$$\frac{\partial^2 \bar{\Psi}}{\partial r^2} + \frac{1}{r} \frac{\partial \bar{\Psi}}{\partial r} + \frac{\partial^2 \bar{\Psi}}{\partial z^2} = \frac{1}{C_s^2} \frac{\partial^2 \bar{\Psi}}{\partial t^2}$$

and differentiating re r gives

$$\frac{\partial^2}{\partial r^2} \left(\frac{\partial \bar{\Psi}}{\partial r} \right) + \frac{\partial \bar{\Psi}}{\partial r} \frac{\partial}{\partial r} \left(\frac{1}{r} \right) + \frac{1}{r} \frac{\partial}{\partial r} \left(\frac{\partial \bar{\Psi}}{\partial r} \right) + \frac{\partial^2}{\partial z^2} \left(\frac{\partial \bar{\Psi}}{\partial r} \right) = \frac{1}{C_s^2} \frac{\partial^2}{\partial t^2} \left(\frac{\partial \bar{\Psi}}{\partial r} \right)$$

or

$$\frac{\partial^2}{\partial r^2} \left(\frac{\partial \bar{\Psi}}{\partial r} \right) - \frac{1}{r^2} \left(\frac{\partial \bar{\Psi}}{\partial r} \right) + \frac{1}{r} \frac{\partial}{\partial r} \left(\frac{\partial \bar{\Psi}}{\partial r} \right) + \frac{\partial^2}{\partial z^2} \left(\frac{\partial \bar{\Psi}}{\partial r} \right) = \frac{1}{C_s^2} \frac{\partial^2}{\partial t^2} \left(\frac{\partial \bar{\Psi}}{\partial r} \right)$$

which, on substitution of the definition, becomes

$$\nabla^2 \Psi - \frac{\Psi}{r^2} = \frac{1}{C_s^2} \frac{\partial^2 \Psi}{\partial t^2}$$

or the "wave" equation previously used. The negative sign in the definition is apparently immaterial here, but, continuing further, the displacement components become

$$S_r = \frac{\partial \Phi}{\partial r} + \frac{\partial}{\partial z} \left(\frac{\partial \bar{\Psi}}{\partial r} \right)$$

$$S_z = \frac{\partial \Phi}{\partial z} - \frac{1}{r} \frac{\partial}{\partial r} \left(r \frac{\partial \bar{\Psi}}{\partial r} \right)$$

and the stresses, in terms of the redefined potentials become

$$\sigma_{rr} = 2\mu \left[\frac{\partial^2 \Phi}{\partial r^2} - \frac{\partial^2}{\partial r \partial z} \left(- \frac{\partial \bar{\Psi}}{\partial r} \right) \right] + \rho_2 \left(\frac{\nu}{1-\nu} \right) \frac{\partial^2 \Phi}{\partial t^2}$$

$$\sigma_{rz} = 2\mu \left[\frac{\partial^2 \Phi}{\partial r \partial z} - \frac{\partial^2}{\partial z^2} \left(- \frac{\partial \bar{\Psi}}{\partial r} \right) \right] + \rho_2 \frac{\partial^2}{\partial t^2} \left(- \frac{\partial \bar{\Psi}}{\partial r} \right).$$

But we note that whereas solutions \mathbf{K}_0 for Φ and \mathbf{K}_1 for Ψ were utilized with the pseudowave equation, for the modified potentials Φ and $\bar{\Psi}$ with ordinary wave equations we select solutions \mathbf{K}_0 for both Φ and $\bar{\Psi}$. Then, noting further

$$\mathbf{K}'_0(x) = -\mathbf{K}_1(x)$$

we see that identical Bessel function dependences are obtained using either proper formulation.

VII.4 Characteristic Equation for Elm Modes

Boundary conditions appropriate to this problem are continuity of tangential stress, continuity of normal (radial) stress, and continuity of radial displacement, all at the boundary $r = b$. Since the liquid has been assumed dissipationless or without shear the tangential stress in the surrounding elastic solid must vanish at the boundary, or

$$\sigma_{rz}|_{r=b} = 0.$$

The normal stress in the elastic solid is equal to the negative fluid pressure at the boundary or

$$p|_{r=b} = -\sigma_{rr}|_{r=b}$$

and the continuity of displacement is written

$$S_r^L|_{r=b} = S_r|_{r=b}$$

where the superscript L again refers to the liquid cylinder medium. These latter two conditions can be combined as a form of the logarithmic derivative

$$\frac{p}{S_r^L}|_{r=b} = \frac{-\sigma_{rr}}{S_r}|_{r=b}.$$

From the vanishing of tangential stress we obtain

$$\frac{\Phi_0}{\Psi_0} = \frac{i(2q_{0m}^2 - k_s^2) K_1(b\sqrt{q_{0m}^2 - k_s^2})}{2q_{0m}\sqrt{q_{0m}^2 - k_c^2} K_0'(b\sqrt{q_{0m}^2 - k_c^2})}$$

where the prime refers, as usual, to differentiation with respect to the entire argument.

Now, solving for $\sigma_{rr}|_{r=b}$ we find

$$\begin{aligned} \sigma_{rr}|_{r=b} e^{i(\omega t - q_{0m} z)} &= 2 \rho_2 C_s^2 (q_{0m}^2 - k_c^2) \Phi_0 K_0' (b \sqrt{q_{0m}^2 - k_c^2}) \\ &\quad - 2i \rho_2 C_s^2 q_{0m} \sqrt{q_{0m}^2 - k_s^2} \Psi_0 K_1' (b \sqrt{q_{0m}^2 - k_s^2}) \\ &\quad - \rho_2 \omega^2 \left(\frac{\nu}{1-\nu} \right) \Phi_0 K_0 (b \sqrt{q_{0m}^2 - k_c^2}). \end{aligned}$$

Solving for $S_r|_{r=b}$ we find, eliminating Φ_0 by the previous equation,

$$S_r|_{r=b} e^{i(\omega t - q_{0m} z)} = \frac{-i k_s^2}{2 q_{0m}} \Psi_0 K_1 (b \sqrt{q_{0m}^2 - k_s^2})$$

so that

$$\begin{aligned} \frac{\sigma_{rr}}{S_r}|_{r=b} &= \frac{i 4 \rho_2 C_s^2}{k_s^2} q_{0m} (q_{0m}^2 - k_c^2) \frac{\Phi_0 K_0' (b \sqrt{q_{0m}^2 - k_c^2})}{\Psi_0 K_1 (b \sqrt{q_{0m}^2 - k_s^2})} \\ &\quad + \frac{4 \rho_2 C_s^2}{k_s^2} q_{0m}^2 \sqrt{q_{0m}^2 - k_s^2} \frac{K_1' (b \sqrt{q_{0m}^2 - k_s^2})}{K_1 (b \sqrt{q_{0m}^2 - k_s^2})} \\ &\quad - i 2 \rho_2 C_s^2 q_{0m} \left(\frac{\nu}{1-\nu} \right) \frac{\Phi_0 K_0 (b \sqrt{q_{0m}^2 - k_c^2})}{\Psi_0 K_1 (b \sqrt{q_{0m}^2 - k_s^2})} \end{aligned}$$

Replacing the ratio Φ_0/Ψ_0 this becomes

$$\begin{aligned} \frac{\sigma_{rr}}{S_r}|_{r=b} &= - \frac{2 \rho_2 C_s^2}{k_s^2} \sqrt{q_{0m}^2 - k_c^2} (2 q_{0m}^2 - k_s^2) \frac{K_0' (b \sqrt{q_{0m}^2 - k_c^2})}{K_0' (b \sqrt{q_{0m}^2 - k_c^2})} \\ &\quad + \frac{4 \rho_2 C_s^2}{k_s^2} q_{0m}^2 \sqrt{q_{0m}^2 - k_s^2} \frac{K_1' (b \sqrt{q_{0m}^2 - k_s^2})}{K_1 (b \sqrt{q_{0m}^2 - k_s^2})} \\ &\quad + \rho_2 C_s^2 (2 q_{0m}^2 - k_s^2) \left(\frac{\nu}{1-\nu} \right) \frac{K_0 (b \sqrt{q_{0m}^2 - k_c^2})}{\sqrt{q_{0m}^2 - k_c^2} K_0' (b \sqrt{q_{0m}^2 - k_c^2})} \end{aligned}$$

Using the identities

$$K_0'(x) = -K_1(x) \quad K_1'(x) = -K_0(x) - \frac{K_1(x)}{x}$$

$$K_0''(x) = -K_1'(x) = K_0(x) + \frac{K_1(x)}{x}$$

and the relationship

$$\frac{\nu}{1-\nu} = 1 - 2 \frac{k_c^2}{k_s^2}$$

we obtain

$$\begin{aligned} \left. \frac{\sigma_{rr}}{S_r} \right|_{r=b} &= - \frac{2\rho_2 \omega^2}{bk_s^2} - \frac{4\rho_2 \omega^2 q_{0m}^2}{k_s^4} \frac{\sqrt{q_{0m}^2 - k_s^2}}{K_1(b\sqrt{q_{0m}^2 - k_s^2})} \frac{K_0(b\sqrt{q_{0m}^2 - k_s^2})}{K_1(b\sqrt{q_{0m}^2 - k_s^2})} \\ &+ \frac{\rho_2 \omega^2 (2q_{0m}^2 - k_s^2)^2}{k_s^4 \sqrt{q_{0m}^2 - k_c^2}} \frac{K_0(b\sqrt{q_{0m}^2 - k_c^2})}{K_1(b\sqrt{q_{0m}^2 - k_c^2})} \end{aligned}$$

Using the second boundary condition we have

$$\begin{aligned} \frac{J_0(X_{0m})}{X_{0m} J_1(X_{0m})} \frac{\rho_1}{\rho_2} &= - \frac{2}{b^2 k_s^2} - \frac{4q_{0m}^2}{bk_s^4} \frac{\sqrt{q_{0m}^2 - k_s^2}}{K_1(b\sqrt{q_{0m}^2 - k_s^2})} \frac{K_0(b\sqrt{q_{0m}^2 - k_s^2})}{K_1(b\sqrt{q_{0m}^2 - k_s^2})} \\ &+ \frac{(2q_{0m}^2 - k_s^2)^2}{bk_s^4 \sqrt{q_{0m}^2 - k_c^2}} \frac{K_0(b\sqrt{q_{0m}^2 - k_c^2})}{K_1(b\sqrt{q_{0m}^2 - k_c^2})} \end{aligned}$$

Finally, using the previous

$$X_{0m} = b \sqrt{k_1^2 - q_{0m}^2}$$

and defining in analogy

$$Y_s = b \sqrt{k_1^2 - k_s^2}$$

$$Y_c = b \sqrt{k_1^2 - k_c^2}$$

we obtain

$$\frac{J_0(X_{Em})}{X_{Em} J_1(X_{Em})} \frac{\rho_1}{\rho_2} = - \frac{2}{b^2 k_s^2} - \frac{4}{(bk_s)^4} [(bk_1)^2 - X_{Em}^2] \sqrt{Y_s^2 - X_{Em}^2} \frac{K_0(\sqrt{Y_s^2 - X_{Em}^2})}{K_1(\sqrt{Y_s^2 - X_{Em}^2})} + \left\{ \frac{2}{(bk_s)^2} [(bk_1)^2 - X_{Em}^2] - 1 \right\}^2 \frac{K_0(\sqrt{Y_c^2 - X_{Em}^2})}{\sqrt{Y_c^2 - X_{Em}^2} K_1(\sqrt{Y_c^2 - X_{Em}^2})}$$

The characteristic values for this surrounding elastic medium of infinite extent have been written X_{Em} where the original subscript zero referring to the invoked cylindrical symmetry has been replaced by E for elastic. The individual modes will be designated EIm , representing the m th elastic infinite surrounding medium mode.

VII.5 Finite Number of EIm Modes, All Propagating

As previously stated, for the propagating modes, m usually runs from 0 to some finite number where $X_{Em} \leq k_1 b$. Actually we shall see that even fewer modes exist and that

$$0 \leq X_{Em} \leq Y_s \leq Y_c \leq k_1 b \leq \infty.$$

Considering the EI equation, we note that the left-hand side or

$$\frac{J_0(X_{Em})}{X_{Em} J_1(X_{Em})}$$

is real, while the right-hand side involves possibly imaginary functions which may be abbreviated as

$$A = \frac{K_0(\sqrt{Y_c^2 - X_{Em}^2})}{\sqrt{Y_c^2 - X_{Em}^2} K_1(\sqrt{Y_c^2 - X_{Em}^2})}$$

$$B = \sqrt{Y_s^2 - X_{Em}^2} \frac{K_0(\sqrt{Y_s^2 - X_{Em}^2})}{K_1(\sqrt{Y_s^2 - X_{Em}^2})}$$

for which we know there are roots $X_{Em} \leq Y_B \leq Y_C$. If we look for roots $Y_B < X_{Em} < Y_C$ then we would have

$$\sqrt{Y_B^2 - X_{Em}^2} = i \sqrt{X_{Em}^2 - Y_B^2} = iy_B = z_B$$

$$\sqrt{Y_C^2 - X_{Em}^2} = y_A \text{ is real}$$

so A is real but B has an imaginary part. From

$$K_0(iy_B) = \frac{\pi i}{2} [J_0(-y_B) + iN_0(-y_B)]$$

$$= \frac{\pi i}{2} [J_0(y_B) + iN_0(y_B)]$$

$$K_1(iy_B) = \frac{-\pi}{2} [J_1(-y_B) + iN_1(-y_B)]$$

$$= \frac{\pi}{2} [J_1(y_B) + iN_1(y_B)]$$

we have on the right-hand side

$$\begin{aligned} B &= iy_B \frac{\pi i/2 [J_0(y_B) + iN_0(y_B)]}{\pi/2 [J_1(y_B) + iN_1(y_B)]} \\ &= \frac{-y_B}{J_1^2(y_B) + N_1^2(y_B)} [J_0(y_B)J_1(y_B) + N_0(y_B)N_1(y_B)] \\ &\quad + \frac{-iy_B}{J_1^2(y_B) + N_1^2(y_B)} [J_1(y_B)N_0(y_B) - J_0(y_B)N_1(y_B)]. \end{aligned}$$

So equating the imaginary implies $J_1N_0 - J_0N_1 = 0$ which is a "nonsequitur" since

$$J_1N_0 - J_0N_1 = -\frac{2}{\pi y_B}.$$

Thus there can be no imaginary part to B or there can be no roots X_{Em} such that

$$Y_B < X_{Em} < Y_C.$$

If we search for roots X_{Em} such that

$$Y_s < Y_c < X_{Em}$$

then

$$\sqrt{Y_s^2 - X_{Em}^2} = i \sqrt{X_{Em}^2 - Y_s^2} = iy_B$$

$$\sqrt{Y_c^2 - X_{Em}^2} = i \sqrt{X_{Em}^2 - Y_c^2} = iy_A$$

and both A and B are complex.

In this case we must include the factors in front of A and B since we are dealing with the sum of the terms rather than a single one so, setting the imaginary to zero implies

$$\begin{aligned} & -y_B \frac{4}{(bk_s)^4} [(bk_1)^2 - X_{Em}^2] \left[\frac{J_1(y_B) N_0(y_B) - J_0(y_B) N_1(y_B)}{J_1^2(y_B) + N_1^2(y_B)} \right] \\ & = \left\{ \frac{2}{(bk_s)^2} [(bk_1)^2 - X_{Em}^2] - i \right\}^2 \frac{1}{y_A} \left[\frac{J_1(y_A) N_0(y_A) - J_0(y_A) N_1(y_A)}{J_1^2(y_A) + N_1^2(y_A)} \right] \end{aligned}$$

which becomes

$$\frac{-4q_{Em}^2}{b^2 k_s^4 [J_1^2(y_B) + N_1^2(y_B)]} = \frac{(2q_{Em}^2 - k_s^2)^2}{k_s^4 y_A^2 [J_1^2(y_A) + N_1^2(y_A)]}$$

The left-hand side is always negative (or zero) and the right-hand side is always positive (or zero) so the result is inadmissible unless both sides are zero. But then the left-hand side zero implies $q_{Em} = 0$ and the right-hand side for $q_{Em} = 0$ becomes

$$\frac{1}{y_A^2 [J_1^2(y_A) + N_1^2(y_A)]} \neq 0$$

so there are no roots for $X > Y_c$.

Actually, this above result was foreordained by the selection of the characteristic functions representing the potentials, as will be now shown. For real X_{Em} and propagating modes or $X_{Em} \leq k, b$ so that q_{Em} is real the displacement potentials are

$$\Phi = \Phi_0 K_0(r \sqrt{q_{Em}^2 - k_c^2}) e^{-i(\omega t - q_{Em} z)}$$

and

$$\Psi = \Psi_0 K_1(r \sqrt{q_{Em}^2 - k_c^2}) e^{-i(\omega t - q_{Em} z)}$$

with pressure obtained from the scalar displacement potential as

$$p = -\rho \ddot{\Phi}$$

so that

$$p = \rho_2 \omega^2 \Phi_0 K_0(r \sqrt{q_{Em}^2 - k_c^2}) e^{-i(\omega t - q_{Em} z)}$$

and the intensity I is

$$I = \frac{\rho_2 \omega^2}{2\rho_2 C_2} \Phi_0 \left| [K_0(r \sqrt{q_{Em}^2 - k_c^2})]^2 e^{i2q_{Em} z} \right|$$

which may be written

$$I = \frac{\omega^2}{2C_2} \Phi_0 \left| \frac{\pi^2}{4} [H_0^{(1)}(r \sqrt{k_c^2 - q_{Em}^2})]^2 e^{i2q_{Em} z} \right|.$$

Since

$$H_0^{(1)}(x) = \sqrt{\frac{2}{\pi x}} e^{i(x - \pi/4)}$$

we have

$$I = \frac{\omega^2 \Phi_0 \pi}{4C_2 r \sqrt{k_c^2 - q_{Em}^2}} \left| e^{i(2r \sqrt{k_c^2 - q_{Em}^2} + 2q_{Em} z)} \right| = \frac{\omega^2 \Phi_0 \pi}{4C_2 r \sqrt{k_c^2 - q_{Em}^2}}.$$

The energy radiated through an area ds normal to the direction of propagation is given by

$$\int_0^\infty \int_0^{2\pi} I R d\theta dz$$

which yields

$$\frac{\pi^2 \omega^2 \Phi_0}{2C_2 \sqrt{k_c^2 - q_{Em}^2}} \int_0^\infty dz = \infty.$$

This is not permissible and thus there must be a restriction

$$q_{Em} \geq k_c.$$

It may be shown in a similar manner that finiteness at infinity also implies

$$q_{Em} \geq k_s \geq k_c$$

so that a requirement for the propagating modes with real X_{Em} is

$$\infty \geq k_1 \geq q_{Em} \geq k_s \geq k_c \geq 0$$

or

$$0 \leq X_{Em} \leq Y_s \leq Y_c \leq k_1 b \leq \infty.$$

We note that any $X_{Em} > k_1 b$ would result in a positive imaginary q_{Em} and so represent evanescent modes. While such X_{Em} would obviously satisfy the radiation condition, we have seen there are no $X_{Em} > Y_s$. We also note the possibility of imaginary X_{Em} or $X_{Em} = i\bar{X}_{Em}$ so that

$$q_{Em} = \frac{1}{b} \sqrt{(k_1 b)^2 + \bar{X}_{Em}^2}$$

gives q_{Em} real and

$$q_{Em} \geq k_1$$

which obviously would be a propagating mode (see next section).

VII.6 Imaginary Characteristic Value for a Propagating E10 Mode

There also is a zero mode, so-called in analogy with the plane wave mode, for which there is an imaginary characteristic value $i\bar{X}_{E0} = X_{E0}$. This mode is designated E10 and applies to the boundary wave for which

$$C_{E0} < C$$

rather than to the reflected waves for which $C_{Em} > C$ for $m > 0$.

The elastic boundary equation is modified for this E10 mode simply by writing $i\bar{X}_{E0}$ for the X_{E0} and noting

$$J_0(ix) = I_0(x) \quad J_1(ix) = iI_1(x)$$

whereby

$$\frac{I_0(\bar{X}_{E0})}{\bar{X}_{E0} I_1(\bar{X}_{E0})} \frac{\rho_1}{\rho_2} = + \frac{2}{b^2 k_s^2} + \frac{4}{(bk_s)^4} [(bk_1)^2 + (\bar{X}_{E0})^2] \frac{\sqrt{Y_s^2 + \bar{X}_{E0}^2} K_0(\sqrt{Y_s^2 + \bar{X}_{E0}^2})}{K_1(\sqrt{Y_s^2 + \bar{X}_{E0}^2})} - \left\{ \frac{2}{(bk_s)^2} [(bk_1)^2 + (\bar{X}_{E0})^2] - 1 \right\}^2 \frac{K_0(\sqrt{Y_c^2 + \bar{X}_{E0}^2})}{\sqrt{Y_c^2 + \bar{X}_{E0}^2} K_1(\sqrt{Y_c^2 + \bar{X}_{E0}^2})}$$

It should be noted that there is no need to search for an infinite number of complex roots such as is required for handling an arbitrary body force with the Pochhammer - Chree equations for an elastic solid cylinder. Rather there exists in this liquid cylinder case, besides a finite number of real roots, only the above one pure imaginary root for an elastic solid boundary of infinite extent radially outward. This mode is a degeneration of the plane wave mode existing for absolutely rigid walls and results from the interaction of the media in contact, bearing no resemblance to the waves that occur independently in either medium. Such a wave has been called a Stoneley wave by analogy to an interface wave, but the appellation may be incorrect. We note a Rayleigh wave is a surface wave in an elastic half space with trajectories ellipses with principal axes parallel and perpendicular to the boundary; it has components of vibration both normal to the surface and along the direction of propagation, that is, restricted to a plane perpendicular to the surface and containing the direction of propagation. A Love wave is restricted to vibrations parallel to the surface and only perpendicular to the direction of propagation and may therefore be compared to shear waves with particle motion parallel to the surface (horizontally polarized transverse waves). Rayleigh waves cannot exist if the solid thickness is less than the Rayleigh wavelength. However, besides the Love waves still possible in such a case, there are two modified Rayleigh or Lamb waves which can exist—one with both surfaces executing vibrations in phase (anti-symmetrical or bending) and one with both surfaces vibrating out of phase (symmetrical or extensional). Between the surfaces, the particles oscillate longitudinally for the extensional Lamb waves and oscillate wholly transversely for the bending Lamb waves. When Love investigated the effect of a surface layer of liquid on the propagation of Rayleigh waves, he found the Rayleigh wave highly attenuated and, besides another wave existing with velocity determined by properties of the surface layer, a modified Rayleigh wave for wavelength much

less than the layer thickness whose velocity of propagation depended on the properties of both media—this wave is now called a Stoneley wave. This Stoneley wave is subject to the severe restriction that the shear wave velocities in both media be approximately equal. However, a generalized Rayleigh wave (with speed less than a regular Rayleigh wave) is always possible at the interface of a fluid and an elastic solid. This generalized Rayleigh wave which has also been referred to as a Stoneley wave is the type corresponding to the imaginary root for the elastic boundary.

VII.7 Degeneration to Characteristic Equation for Radially Surrounding Liquid or LIm Modes

A particularly pleasing circumstance is that unlike some others (18) this Elm equation leads directly to the correct formulation for a degenerate situation where the radially surrounding elastic solid is simplified to another liquid. This is seen most simply by letting $C_s = 0$ or $k_s = \infty$ which corresponds to the absence of shear and results in $Y_s = i\infty$ and the equation for liquid modes as

$$\frac{J_0(X_{Lm})}{X_{Lm} J_1(X_{Lm})} = \frac{\rho_2}{\rho_1} \frac{K_0(\sqrt{Y_c^2 - X_{Lm}^2})}{\sqrt{Y_c^2 - X_{Lm}^2} K_1(\sqrt{Y_c^2 - X_{Lm}^2})}$$

which, using

$$H_0^{(1)}(ix) = \frac{2}{\pi i} K_0(x) \quad H_1^{(1)}(ix) = \frac{-2}{\pi} K_1(x)$$

may be also written

$$\frac{J_0(X_{Lm})}{X_{Lm} J_1(X_{Lm})} = \frac{\rho_2}{\rho_1} \frac{H_0^{(1)}(i\sqrt{Y^2 - X_{Lm}^2})}{i\sqrt{Y^2 - X_{Lm}^2} H_1^{(1)}(i\sqrt{Y^2 - X_{Lm}^2})}$$

where we have also deleted the subscript c since Y_c becomes Y with no need to differentiate between shear and compressional velocities in a liquid.

The first term on the right side of the Elm equation disappears obviously upon going to the LIm equation just detailed ($k_s \rightarrow \infty$). The middle term requires a little more care before it is summarily eliminated. Under the given conditions it becomes

$$\frac{4q_{0m}^2}{b^2 \infty^4} (i\infty) \frac{K_0(i\infty)}{K_1(i\infty)}$$

which can also be written

$$\frac{4q_{0m}^2 H_0^{(1)}(-\infty)}{b^2 \omega^3 H_1^{(1)}(-\infty)}$$

Asymptotic representations of the Hankel functions, valid for

$$-\pi < \arg z < 2\pi$$

which conditions are met here, are

$$H_0^{(1)}(z) \sim \sqrt{\frac{2}{\pi z}} e^{i(z - \pi/4)} \quad H_1^{(1)}(z) \sim \sqrt{\frac{2}{\pi z}} e^{i(z - 3\pi/4)}$$

becoming for $Z = -\infty$

$$H_0^{(1)}(-\infty) = \sqrt{\frac{2}{-\pi \infty}} e^{-i\infty} \quad H_1^{(1)}(-\infty) = \sqrt{\frac{2}{-\pi \infty}} e^{-i\infty}$$

Thus their ratio is unity and this middle term disappears with ∞^3 in the denominator.

VII.8 Alternative Derivation of Characteristic Equation for Llm Modes

This liquid boundary characteristic equation is also simply obtained by writing velocity potentials for the liquid cylinder medium I

$$\phi_{0m}^I = K_{0m}^I J_0(r \sqrt{k_1^2 - q_{0m}^2}) e^{i q_{0m} z}$$

and the radially surrounding liquid medium II

$$\phi_{0m}^{II} = K_{0m}^{II} [L_{0m} J_0(r \sqrt{k_2^2 - q_{0m}^2}) + M_{0m} N_0(r \sqrt{k_2^2 - q_{0m}^2})] e^{i q_{0m} z}$$

the second equation is simplified by defining (to satisfy the radiation condition)

$$L_{0m} = 1 \text{ and } M_{0m} = i$$

to obtain two unknown coefficients consistent with the two boundary conditions of continuity of pressure and continuity of normal velocity. Thus

$$\phi_{0m}^{II} = K_{0m}^{II} H_0^{(1)}(r \sqrt{k_2^2 - q_{0m}^2}) e^{i q_{0m} z}$$

Again the two boundary conditions may be combined in logarithmic derivative form as a condition of continuity of impedance as

$$\rho_1 \left. \frac{\phi^I}{\partial \phi^I} \right|_{r=b} = \rho_2 \left. \frac{\phi^{II}}{\partial \phi^{II}} \right|_{r=b}$$

which directly yields

$$\frac{J_0(X_{Lm})}{X_{Lm} J_1(X_{Lm})} = \frac{\rho_2}{\rho_1} \frac{H_0^{(1)}(i\sqrt{Y^2 - X_{Lm}^2})}{i\sqrt{Y^2 - X_{Lm}^2} H_1^{(1)}(i\sqrt{Y^2 - X_{Lm}^2})}$$

where as usual we defined

$$X_{Lm} = b \sqrt{k_1^2 - q_{Lm}^2}$$

$$Y = b \sqrt{k_1^2 - k_2^2}.$$

VII.9 Finite Number of LIm Modes, All Propagating

It is easily seen that no roots exist for $X_{Lm} > Y$. If we write

$$i\sqrt{Y^2 - X_{Lm}^2} = \sqrt{X_{Lm}^2 - Y^2} = z$$

we note again the left hand side is real but the right hand side becomes

$$\frac{J_0(z) J_1(z) + N_0(z) N_1(z) + i[N_0(z) J_1(z) - N_1(z) J_0(z)]}{z[J_1^2(z) + N_1^2(z)]}$$

and equating the imaginary parts on both sides implies

$$N_0(z) J_1(z) - N_1(z) J_0(z) = 0$$

which again is not true, so there can be no roots $X_{Lm} > Y$. For real Y we then require $C_2 > C_1$ or $k_1 > k_2$.

VII.10 Degeneration to Characteristic Equations for Absolutely Rigid or Free Radial Boundaries, With Infinity of Modes

We recall that these characteristic equations for the modes are a statement of equality of impedance across the boundary $r = b$ with the left hand side representing the liquid

cylinder side. Even simpler degenerate cases are obtained if the surrounding medium is assumed to be either absolutely rigid or free. In either of these limiting cases no penetration by acoustic energy of the surrounding medium occurs. For an absolutely rigid boundary the impedance is infinite or

$$\frac{J_0(X_{Rm})}{X_{Rm} J_1(X_{Rm})} = \infty$$

so that the characteristic equation is simply

$$J_1(X_{Rm}) = 0$$

where also $X_{R0} = 0$ or $m = 0$ is one of the allowed roots. This is the only situation so far, and indeed the only one in this report, for which a plane wave mode is one of the family of permissible modes and applies to an unrealistic case.

For a free boundary then, the impedance is zero and the characteristic equation is simply

$$J_0(X_{Fm}) = 0.$$

These latter two cases are the trivial ones found throughout the literature. Just as we let the subscript E represent an elastic boundary with modes Elm, so we let the subscript L represent a liquid boundary with modes Llm and the subscripts R and F represent absolutely rigid and free boundaries with corresponding modes Rm and Fm.

Obviously no F0 mode exists. There is also no L10 mode for which either $X_{L0} = 0$ or $X_{L0} = i\bar{X}_{L0}$ with equations

$$\frac{J_0(0)}{0J_1(0)} = \frac{\rho_2}{\rho_1} \frac{H_0^{(1)}(iY)}{iYH_1^{(1)}(iY)}$$

or

$$\frac{J_0(i\bar{X}_{L0})}{i\bar{X}_{L0}J_1(i\bar{X}_{L0})} = \frac{\rho_2}{\rho_1} \frac{H_0^{(1)}(i\sqrt{Y^2 + \bar{X}_{L0}^2})}{i\sqrt{Y^2 + \bar{X}_{L0}^2} H_1^{(1)}(i\sqrt{Y^2 + \bar{X}_{L0}^2})}$$

In the first equation, the left hand side is infinite while the right hand side is always finite imaginary so no solutions exist. In the second equation the left hand side is equal to

$$\frac{-I_0(\bar{X}_{L0})}{\bar{X}_{L0} I_1(\bar{X}_{L0})} \text{ which is real}$$

while the right hand side is still always finite imaginary.

Unlike the Elm and LIm equations for the roots X_{Em} and X_{Lm} we find now there exist an infinity of roots X_{Rm} and X_{Fm} , but the propagating ones extend only to $X_{0m} \leq k_1 b$. Since in these limiting cases the characteristic functions using either the X_{Rm} or the X_{Fm} are orthogonal, the property of finality holds and the inclusion of the nonpropagating modes in a summation over the characteristic functions would not change the values of the respective coefficients in the expansion from what they were in an expansion limited to the propagating modes. We note also the property that each higher order mode enters the sum with a smaller coefficient.

Section VIII

RADIALLY SURROUNDING FINITE WALL THICKNESS ELASTIC SOLID TUBE

VIII.1 Characteristic Equation for ETm Modes

We now consider our most general case of a finite elastic solid tube of outer radius d surrounding the liquid cylinder of radius b , and we slightly simplify the formulation by considering the elastic tube to be surrounded by empty space.

As in the infinite radially surrounding elastic solid case we again use a displacement vector \vec{S} expressed in terms of a scalar displacement potential Φ and a vector displacement potential $\vec{\Psi}$ as

$$\vec{S} = \nabla \Phi + \nabla \times \vec{\Psi}$$

which led for axially symmetric motion to a radial displacement S_r and an axial displacement S_z as

$$S_r = \frac{\partial \Phi}{\partial r} - \frac{\partial \Psi}{\partial z}$$

$$S_z = \frac{\partial \Phi}{\partial z} + \frac{1}{r} \frac{\partial}{\partial r} (r \Psi)$$

with appropriate stress components as before

$$\sigma_{rr} = L \left[\frac{1}{r} \frac{\partial}{\partial r} (r S_r) + \frac{\partial S_z}{\partial z} \right] + 2\mu \frac{\partial S_r}{\partial r}$$

$$\sigma_{rz} = \mu \left[\frac{\partial S_r}{\partial z} + \frac{\partial S_z}{\partial r} \right]$$

where again

$$\mu = \rho_2 c_s^2$$

$$L = \frac{2\nu}{1-2\nu} \rho_2 c_b^2.$$

For the infinite case with the boundary conditions

$$\sigma_{rz}|_{r=b} = 0$$

and

$$\left. \frac{-\sigma_{rr}}{S_r} \right|_{r=b} = \left. \frac{p(r)}{S_r L} \right|_{r=b}$$

the appropriate solutions were

$$\Phi = \Phi_0 K_0(r \sqrt{q_{Em}^2 - k_c^2}) e^{-i(\omega t - q_{Em} z)}$$

$$\Psi = \Psi_0 K_1(r \sqrt{q_{Em}^2 - k_s^2}) e^{-i(\omega t - q_{Em} z)}$$

but for this case of a surrounding elastic solid tube we have four boundary conditions to satisfy, specifically

$$\sigma_{rz}|_{r=b} = 0 \quad \sigma_{rr}|_{r=d} = 0$$

$$\sigma_{rz}|_{r=d} = 0 \quad \left. \frac{-\sigma_{rr}}{S_r} \right|_{r=b} = \left. \frac{p(r)}{S_r L} \right|_{r=b}$$

We note that if we were considering a solid elastic cylinder rather than a tube we would use as solutions

$$\Phi = \Phi_0 J_0(r \sqrt{k_c^2 - q_{0m}^2}) e^{-i(\omega t - q_{0m} z)}$$

$$\Psi = \Psi_0 J_1(r \sqrt{k_s^2 - q_{0m}^2}) e^{-i(\omega t - q_{0m} z)}$$

but our tube does not include the origin so we must retain both solutions to the Bessel equations or

$$\Phi = [A J_0(P_m r) + B N_0(P_m r)] e^{-i(\omega t - q_{Tm} z)}$$

$$\Psi = [C J_1(T_m r) + D N_1(T_m r)] e^{-i(\omega t - q_{Tm} z)}$$

where we used

$$P_m = \sqrt{k_c^2 - q_{Tm}^2} = \frac{1}{b} \sqrt{X_{Tm}^2 - Y_c^2}$$

$$T_m = \sqrt{k_s^2 - q_{Tm}^2} = \frac{1}{b} \sqrt{X_{Tm}^2 - Y_s^2}$$

and we do not use the combination $H_n^{(1)}$ or K_n as was done previously so that we retain four arbitrary constants for the four boundary conditions.

Thus the displacements are written

$$S_r = \left\{ \frac{\partial}{\partial r} [A J_0(r P_m) + B N_0(r P_m)] - \frac{\partial}{\partial z} [C J_1(r T_m) + D N_1(r T_m)] \right\} e^{-i(\omega t - q_{Tm} z)}$$

$$S_z = \left\{ \frac{\partial}{\partial z} [A J_0(r P_m) + B N_0(r P_m)] + \frac{1}{r} \frac{\partial}{\partial r} [C r J_1(r T_m) + D r N_1(r T_m)] \right\} e^{-i(\omega t - q_{Tm} z)}$$

which become

$$S_r = \left\{ -P_m [A J_1(r P_m) + B N_1(r P_m)] - i q_{Tm} [C J_1(r T_m) + D N_1(r T_m)] \right\} e^{-i(\omega t - q_{Tm} z)}$$

$$S_z = \left\{ i q_{Tm} [A J_0(r P_m) + B N_0(r P_m)] + T_m [C J_0(r T_m) + D N_0(r T_m)] \right\} e^{-i(\omega t - q_{Tm} z)}$$

From the boundary condition

$$\sigma_{rr}|_{r=d} = 0$$

we find

$$\begin{aligned} & A \left[-P_m^2 J_0(d P_m) - (P_m^2 + q_{Tm}^2) \left(\frac{\nu}{1-2\nu} \right) J_0(d P_m) + \frac{P_m}{d} J_1(d P_m) \right] \\ & + B \left[-P_m^2 N_0(d P_m) - (P_m^2 + q_{Tm}^2) \left(\frac{\nu}{1-2\nu} \right) N_0(d P_m) + \frac{P_m}{d} N_1(d P_m) \right] \\ & + C \left[-i q_{Tm} T_m J_0(d T_m) + \frac{i q_{Tm}}{d} J_1(d T_m) \right] \\ & + D \left[-i q_{Tm} T_m N_0(d T_m) + \frac{i q_{Tm}}{d} N_1(d T_m) \right] = 0 \end{aligned}$$

Similarly from

$$\sigma_{rz}|_{r=d} = 0$$

we have

$$A [2iq_{T_m} P_m J_1(dP_m)] + B [2iq_{T_m} P_m N_1(dP_m)] \\ + C [(T_m^2 - q_{T_m}^2) J_1(dT_m)] + D [(T_m^2 - q_{T_m}^2) N_1(dT_m)] = 0$$

and from

$$\sigma_{rz}|_{r=b} = 0$$

we obtain

$$A [2iq_{T_m} P_m J_1(bP_m)] + B [2iq_{T_m} P_m N_1(bP_m)] \\ + C [(T_m^2 - q_{T_m}^2) J_1(bT_m)] + D [(T_m^2 - q_{T_m}^2) N_1(bT_m)] = 0.$$

By defining

$$E_m = - \left[P_m^2 + (P_m^2 + q_{T_m}^2) \frac{\nu}{1-2\nu} \right] = q_{T_m}^2 - \frac{k_s^2}{2}$$

and noting that

$$T_m^2 - q_{T_m}^2 = k_s^2 - 2q_{T_m}^2 = -2E_m$$

we may simplify these equations to, for the first

$$A \left[E_m J_0(dP_m) + \frac{P_m}{d} J_1(dP_m) \right] \\ + B \left[E_m N_0(dP_m) + \frac{P_m}{d} N_1(dP_m) \right] \\ + C \left[-iq_{T_m} T_m J_0(dT_m) + i \frac{q_{T_m}}{d} J_1(dT_m) \right] \\ + D \left[-iq_{T_m} T_m N_0(dT_m) + i \frac{q_{T_m}}{d} N_1(dT_m) \right] = 0$$

for the second,

$$A [2iq_{Tm} P_m J_1(dP_m)] + B [2iq_{Tm} P_m N_1(dP_m)] \\ + C [-2E_m J_1(dT_m)] + D [-2E_m N_1(dT_m)] = 0$$

and the third,

$$A [2iq_{Tm} P_m J_1(bP_m)] + B [2iq_{Tm} P_m N_1(bP_m)] \\ + C [-2E_m J_1(bT_m)] + D [-2E_m N_1(bT_m)] = 0.$$

The fourth boundary condition yields

$$\left. \begin{aligned} & A \left[E_m J_0(bP_m) + \frac{P_m}{b} J_1(bP_m) \right] \\ & + B \left[E_m N_0(bP_m) + \frac{P_m}{b} N_1(bP_m) \right] \\ & + C \left[-iq_{Tm} T_m J_0(bT_m) + i \frac{q_{Tm}}{b} J_1(bT_m) \right] \\ & + D \left[-iq_{Tm} T_m N_0(bT_m) + i \frac{q_{Tm}}{b} N_1(bT_m) \right] \\ & \frac{A [-P_m J_1(bP_m)] + B [-P_m N_1(bP_m)]}{+ C [-iq_{Tm} J_1(bT_m)] + D [-iq_{Tm} N_1(bT_m)]} \end{aligned} \right\} = \rho_1 \omega^2 b \frac{J_0(X_{Tm})}{X_{Tm} J_1(X_{Tm})}$$

which, by defining

$$Q_m = \frac{\rho_1 \omega^2 b}{2\rho_2 c_s^2} \frac{J_0(X_{Tm})}{X_{Tm} J_1(X_{Tm})}$$

may be written

$$A \left[E_m J_0(bP_m) + P_m \frac{(1 + Q_m b)}{b} J_1(bP_m) \right] \\ + B \left[E_m N_0(bP_m) + P_m \frac{(1 + Q_m b)}{b} N_1(bP_m) \right]$$

$$\begin{aligned}
& + C \left[-i q_{T_m} T_m J_0(b T_m) + \frac{i q_{T_m}}{b} (1 + Q_m b) J_1(b T_m) \right] \\
& + D \left[-i q_{T_m} T_m N_0(b T_m) + \frac{i q_{T_m}}{b} (1 + Q_m b) N_1(b T_m) \right] = 0.
\end{aligned}$$

These four simultaneous equations in the unknowns A, B, C, D are solved by equating the determinant of the coefficients (of the unknown constants) to zero which results in 80 terms of which 8 cancel directly and 8 combine as follows

$$\begin{aligned}
& -4q_{T_m}^2 E_m^2 P_m T_m \left[\begin{array}{l} - J_1(b T_m) N_0(b T_m) J_1(d P_m) N_0(d P_m) \\ + N_1(b T_m) J_0(b T_m) J_1(d P_m) N_0(d P_m) \\ + J_1(b P_m) N_0(b P_m) N_1(d T_m) J_0(d T_m) \\ - N_1(b P_m) J_0(b P_m) N_1(d T_m) J_0(d T_m) \\ - J_1(b P_m) N_0(b P_m) J_1(d T_m) N_0(d T_m) \\ + N_1(b P_m) J_0(b P_m) J_1(d T_m) N_0(d T_m) \\ + J_1(b T_m) N_0(b T_m) N_1(d P_m) J_0(d P_m) \\ - N_1(b T_m) J_0(b T_m) N_1(d P_m) J_0(d P_m) \end{array} \right] \\
& = -4q_{T_m}^2 E_m^2 P_m T_m \left\{ \begin{array}{l} [J_1(b T_m) N_0(b T_m) - J_0(b T_m) N_1(b T_m)] \times \\ [J_0(d P_m) N_1(d P_m) - J_1(d P_m) N_0(d P_m)] \\ + [J_1(b P_m) N_0(b P_m) - J_0(b P_m) N_1(b P_m)] \times \\ [J_0(d T_m) N_1(d T_m) - J_1(d T_m) N_0(d T_m)] \end{array} \right\} \\
& = -4q_{T_m}^2 E_m^2 P_m T_m \left[\left(\frac{2}{\pi b T_m} \right) \left(-\frac{2}{\pi d P_m} \right) + \left(\frac{2}{\pi b P_m} \right) \left(-\frac{2}{\pi d T_m} \right) \right] \\
& = \frac{32 q_{T_m}^2 E_m^2}{\pi^2 b d}
\end{aligned}$$

where we used the identity

$$J_0(x) N_0'(x) - N_0(x) J_0'(x) = N_0(x) J_1(x) - J_0(x) N_1(x) = \frac{2}{\pi x}$$

so that, using for brevity (in the first four symbols only)

$$\begin{aligned}
J_0(bT_m) &= A & J_1(bT_m) &= I \\
J_0(bP_m) &= B & J_1(bP_m) &= J \\
J_0(dT_m) &= C & J_1(dT_m) &= K \\
J_0(dP_m) &= D & J_1(dP_m) &= L \\
N_0(bT_m) &= E & N_1(bT_m) &= M \\
N_0(bP_m) &= F & N_1(bP_m) &= N \\
N_0(dT_m) &= G & N_1(dT_m) &= O \\
N_0(dP_m) &= H & N_1(dP_m) &= P
\end{aligned}$$

the expression is reduced to 37 combined terms as follows:

$$\begin{aligned}
& \text{NALO} \left(4q_{Tm}^4 \frac{P_m^2 T_m}{d} - 4q_{Tm}^2 \frac{P_m^2 T_m E_m}{d} \right) \\
& + \text{JAOP} \left(-4q_{Tm}^4 \frac{P_m^2 T_m}{d} + 4q_{Tm}^2 \frac{P_m^2 T_m E_m}{d} \right) \\
& + \text{NEKL} \left(-4q_{Tm}^4 \frac{P_m^2 T_m}{d} + 4q_{Tm}^2 \frac{P_m^2 T_m E_m}{d} \right) \\
& + \text{JEKP} \left(4q_{Tm}^4 \frac{P_m^2 T_m}{d} - 4q_{Tm}^2 \frac{P_m^2 T_m E_m}{d} \right) \\
& + \text{NILG} \left(4q_{Tm}^4 P_m^2 T_m \frac{(1+Q_m b)}{b} - 4q_{Tm}^2 P_m^2 T_m E_m \frac{(1+Q_m b)}{b} \right) \\
& + \text{JIPG} \left(-4q_{Tm}^4 P_m^2 T_m \frac{(1+Q_m b)}{b} + 4q_{Tm}^2 P_m^2 T_m E_m \frac{(1+Q_m b)}{b} \right) \\
& + \text{NNLC} \left(-4q_{Tm}^4 P_m^2 T_m \frac{(1+Q_m b)}{b} + 4q_{Tm}^2 P_m^2 T_m E_m \frac{(1+Q_m b)}{b} \right) \\
& + \text{MJPC} \left(+4q_{Tm}^4 P_m^2 T_m \frac{(1+Q_m b)}{b} - 4q_{Tm}^2 P_m^2 T_m E_m \frac{(1+Q_m b)}{b} \right) \\
& + \text{NEKD} (4q_{Tm}^2 E_m^2 P_m T_m)
\end{aligned}$$

$$+ \text{NAOD} (-4q_{T_m}^2 E_m^2 P_m T_m)$$

$$+ \text{JEKH} (-4q_{T_m}^2 E_m^2 P_m T_m)$$

$$+ \text{JAOH} (4q_{T_m}^2 E_m^2 P_m T_m)$$

$$+ \text{MFKD} (4E_m^4)$$

$$+ \text{IFOD} (-4E_m^4)$$

$$+ \text{MBKH} (-4E_m^4)$$

$$+ \text{IBOH} (4E_m^4)$$

$$+ \text{NILO} \left(-4q_{T_m}^4 \frac{P_m^2 (1 + Q_m b)}{d} \frac{1}{b} + 8q_{T_m}^2 \frac{P_m^2 E_m (1 + Q_m b)}{d} \frac{1}{b} - 4 \frac{E_m^2 P_m^2 (1 + Q_m b)}{d} \frac{1}{b} \right)$$

$$+ \text{JIOP} \left(4q_{T_m}^4 \frac{P_m^2 (1 + Q_m b)}{d} \frac{1}{b} - 8q_{T_m}^2 \frac{P_m^2 E_m (1 + Q_m b)}{d} \frac{1}{b} + 4 \frac{E_m^2 P_m^2 (1 + Q_m b)}{d} \frac{1}{b} \right)$$

$$+ \text{MNKL} \left(4q_{T_m}^4 \frac{P_m^2 (1 + Q_m b)}{d} \frac{1}{b} - 8q_{T_m}^2 \frac{P_m^2 E_m (1 + Q_m b)}{d} \frac{1}{b} + 4 \frac{E_m^2 P_m^2 (1 + Q_m b)}{d} \frac{1}{b} \right)$$

$$+ \text{JMKP} \left(-4q_{T_m}^4 \frac{P_m^2 (1 + Q_m b)}{d} \frac{1}{b} + 8q_{T_m}^2 \frac{P_m^2 E_m (1 + Q_m b)}{d} \frac{1}{b} - 4 \frac{E_m^2 P_m^2 (1 + Q_m b)}{d} \frac{1}{b} \right)$$

$$+ \text{NALG} (-4q_{T_m}^4 P_m^2 T_m^2)$$

$$+ \text{JAPG} (4q_{T_m}^4 P_m^2 T_m^2)$$

$$+ \text{NELC} (4q_{T_m}^4 P_m^2 T_m^2)$$

$$+ \text{JEPC} (-4q_{T_m}^4 P_m^2 T_m^2)$$

$$+ \text{MFLC} (4q_{T_m}^2 E_m^2 P_m T_m)$$

$$+ \text{MBPC} (-4q_{T_m}^2 E_m^2 P_m T_m)$$

$$\begin{aligned}
& + \text{IBPG} (4q_{Tm}^2 E_m^2 P_m T_m) \\
& + \text{IFLG} (-4q_{Tm}^2 E_m^2 P_m T_m) \\
& + \text{MNKD} \left(4E_m^3 P_m \frac{(1+Q_m b)}{b} - 4q_{Tm}^2 E_m^2 P_m \frac{(1+Q_m b)}{b} \right) \\
& + \text{NIOD} \left(-4E_m^3 P_m \frac{(1+Q_m b)}{b} + 4q_{Tm}^2 E_m^2 P_m \frac{(1+Q_m b)}{b} \right) \\
& + \text{JMKH} \left(-4E_m^3 P_m \frac{(1+Q_m b)}{b} + 4q_{Tm}^2 E_m^2 P_m \frac{(1+Q_m b)}{b} \right) \\
& + \text{JIOH} \left(4E_m^3 P_m \frac{(1+Q_m b)}{b} - 4q_{Tm}^2 E_m^2 P_m \frac{(1+Q_m b)}{b} \right) \\
& + \text{IFLO} \left(4q_{Tm}^2 E_m^2 \frac{P_m}{d} - 4E_m^3 \frac{P_m}{d} \right) \\
& + \text{IBPO} \left(-4q_{Tm}^2 E_m \frac{P_m}{d} + 4E_m^3 \frac{P_m}{d} \right) \\
& + \text{MFKL} \left(-4q_{Tm}^2 E_m \frac{P_m}{d} + 4E_m^3 \frac{P_m}{d} \right) \\
& + \text{MBKP} \left(4q_{Tm}^2 E_m \frac{P_m}{d} - 4E_m^3 \frac{P_m}{d} \right) \\
& + \frac{32q_{Tm}^2 E_m^2}{\pi^2 b d} = 0.
\end{aligned}$$

Using the same Wronskian or logarithmic derivative type combination used to collect terms previously, we write

$$L_{mn}(y) = J_m(dy) N_n(by) - J_n(by) N_m(dy)$$

which differs from the previous only in the arguments, and combine the terms further to

$$\begin{aligned}
& 1 + [L_{11}(P_m) L_{00}(T_m)] \left[\frac{\pi^2 q_{T_m}^2 b d P_m^2 T_m^2}{8 E_m^2} \right] \\
& + [L_{11}(T_m) L_{00}(P_m)] \left[\frac{\pi^2 b d E_m^2}{8 q_{T_m}^2} \right] \\
& + [L_{10}(P_m) L_{01}(T_m) + L_{01}(P_m) L_{10}(T_m)] \left[\frac{\pi^2 b d P_m T_m}{8} \right] \\
& + [b L_{11}(P_m) L_{10}(T_m) + d(1 + Q_m b) L_{11}(P_m) L_{01}(T_m)] \left[\frac{\pi^2 P_m^2 T_m}{8 E_m} - \frac{\pi^2 P_m^2 q_{T_m}^2 T_m}{8 E_m^2} \right] \\
& + [b L_{11}(T_m) L_{10}(P_m) + d(1 + Q_m b) L_{11}(T_m) L_{01}(P_m)] \left[\frac{\pi^2 P_m E_m}{8 q_{T_m}^2} - \frac{\pi^2 P_m}{8} \right] \\
& + [(1 + Q_m b) L_{11}(T_m) L_{11}(P_m)] \left[\frac{\pi^2 P_m^2}{8 q_{T_m}^2} + \frac{\pi^2 P_m^2 q_{T_m}^2}{8 E_m^2} - \frac{\pi^2 P_m^2}{4 E_m} \right] = 0.
\end{aligned}$$

This equation holds for

$$q_{T_m} \geq k_s$$

or

$$X_{T_m} \geq Y_s.$$

VIII.2 Infinite Number of ET_m Modes, Not All Propagating

We recall that in the EI formulation the surrounding medium extended radially outward to infinity while for this ET case it is limited to $r = d$. In the EI case there was an exclusion for the propagated modes and for real characteristic functions

$$0 \leq X_{EIm} \leq Y_s \leq Y_c \leq k_1 b \leq \infty.$$

In this ET case, however, the radially surrounding second medium being finite results in no such exclusion and we must consider three separate cases for the real characteristic values:

$$(1) \quad 0 \leq X_{Tm} \leq Y_s \leq Y_c \leq k_1 b \leq \infty$$

or

$$0 \leq C_1 \leq C_{Tm} \leq C_s \leq C_c \leq \infty$$

or

$$\infty \geq k_1 \geq q_{Tm} \geq k_s \geq k_c \geq 0$$

$$(2) \quad 0 \leq Y_s \leq Y_c \leq X_{Tm} \leq k_1 b \leq \infty$$

or

$$0 \leq C_1 \leq C_s \leq C_c \leq C_{Tm} \leq \infty$$

or

$$\infty \geq k_1 \geq k_s \geq k_c \geq q_{Tm} \geq 0$$

$$(3) \quad 0 \leq Y_s \leq X_{Tm} \leq Y_c \leq k_1 b \leq \infty$$

or

$$0 \leq C_1 \leq C_s \leq C_{Tm} \leq C_c \leq \infty$$

or

$$\infty \geq k_1 \geq k_s \geq q_{Tm} \geq k_c \geq 0.$$

For case (1) both P_m and T_m are imaginary. We recall that this is the only case we had for the infinite elastic surrounding medium. Thus we regard this as the most basic case, and in order to simplify calculation we write the previous as

$$L_{mn}(ix) = J_m(idx) N_n(ibx) - J_n(ibx) N_m(idx).$$

Using

$$N_p(ix) = iJ_p(ix) - iH_p^{(1)}(ix)$$

we obtain

$$L_{mn}(ix) = -iJ_m(idx) H_n^{(1)}(ibx) + iJ_n(ibx) H_m^{(1)}(idx)$$

which by

$$I_p(x) = i^{-P} J_p(ix)$$

becomes

$$L_{mn}(ix) = i^{m-1} I_m(dx) H_n^{(1)}(ibx) + i^{n+1} I_n(bx) H_m^{(1)}(idx).$$

Using

$$K_p(x) = \frac{\pi}{2} i^{P+1} H_p^{(1)}(ix)$$

we obtain

$$\frac{\pi}{2} (i)^{-m-m} (-1)^{-m} L_{mn}(ix) = I_n(bx) K_m(dx) - (-1)^{n-m} I_m(dx) K_n(bx) \equiv M_{mn}(ix).$$

We also use

$$P_m = i\bar{P}_m$$

$$T_m = i\bar{T}_m.$$

Thus the complete characteristic equation for case (1) is

$$\begin{aligned} & 1 + [M_{11}(i\bar{P}_m) M_{00}(i\bar{T}_m)] \left[\frac{q_{Tm}^2 b d \bar{P}_m^2 \bar{T}_m^2}{2E_m^2} \right] \\ & + [M_{11}(i\bar{T}_m) M_{00}(i\bar{P}_m)] \left[\frac{b d E_m^2}{2q_{Tm}^2} \right] \\ & + \begin{bmatrix} M_{10}(i\bar{P}_m) M_{01}(i\bar{T}_m) \\ +M_{01}(i\bar{P}_m) M_{10}(i\bar{T}_m) \end{bmatrix} \left[-\frac{b d \bar{P}_m \bar{T}_m}{2} \right] \\ & + \begin{bmatrix} -bM_{11}(i\bar{P}_m) M_{10}(i\bar{T}_m) \\ +d(1 + Q_m b) M_{11}(i\bar{P}_m) M_{01}(i\bar{T}_m) \end{bmatrix} \left[\frac{\bar{P}_m^2 \bar{T}_m}{2E_m} - \frac{\bar{P}_m^2 \bar{T}_m q_{Tm}^2}{2E_m^2} \right] \\ & + \begin{bmatrix} bM_{11}(i\bar{T}_m) M_{10}(i\bar{P}_m) \\ -d(1 + Q_m b) M_{11}(i\bar{T}_m) M_{01}(i\bar{P}_m) \end{bmatrix} \left[\frac{\bar{P}_m E_m}{2q_{Tm}^2} - \frac{\bar{P}_m}{2} \right] \end{aligned}$$

$$+ [(1 + Q_m b) M_{11}(i\bar{T}_m) M_{11}(i\bar{P}_m)] \left[\frac{\bar{P}_m^2}{2q_{Tm}^2} - \frac{\bar{P}_m^2 q_{Tm}^2}{2E_m^2} + \frac{\bar{P}_m^2}{E_m} \right] = 0.$$

For case (2) both P_m and T_m are real and the original formulation using L_{mn} is used.

For case (3) P_m is imaginary and T_m is real so a combined notation is used as

$$\begin{aligned} & 1 + [M_{11}(i\bar{P}_m) L_{00}(T_m)] \left[-\frac{\pi q_{Tm}^2 b d \bar{P}_m^2 T_m^2}{4E_m^2} \right] \\ & + [L_{11}(T_m) M_{00}(i\bar{P}_m)] \left[\frac{\pi b d E_m^2}{4q_{Tm}^2} \right] \\ & + \begin{bmatrix} M_{10}(i\bar{P}_m) L_{01}(T_m) \\ -M_{01}(i\bar{P}_m) L_{10}(T_m) \end{bmatrix} \left[\frac{\pi b d \bar{P}_m T_m}{4} \right] \\ & + \begin{bmatrix} b M_{11}(i\bar{P}_m) L_{10}(T_m) \\ +d(1 + Q_m b) M_{11}(i\bar{P}_m) L_{01}(T_m) \end{bmatrix} \left[-\frac{\pi \bar{P}_m^2 T_m}{4E_m} + \frac{\pi \bar{P}_m^2 T_m q_{Tm}^2}{4E_m^2} \right] \\ & + \begin{bmatrix} b L_{11}(T_m) M_{10}(i\bar{P}_m) \\ -d(1 + Q_m b) L_{11}(T_m) M_{01}(i\bar{P}_m) \end{bmatrix} \left[\frac{\pi \bar{P}_m E_m}{4q_{Tm}^2} - \frac{\pi \bar{P}_m}{4} \right] \\ & + [(1 + Q_m b) L_{11}(T_m) M_{11}(i\bar{P}_m)] \left[-\frac{\pi \bar{P}_m^2}{4q_{Tm}^2} - \frac{\pi \bar{P}_m^2 q_{Tm}^2}{4E_m^2} + \frac{\pi \bar{P}_m^2}{2E_m} \right] = 0. \end{aligned}$$

VIII.3 Imaginary Characteristic Value for a Propagating ET0 Mode

Considering the expected imaginary root

$$X_{T0} = i\bar{X}_{T0}$$

where

$$q_{T0} = \frac{1}{b} \sqrt{k_1^2 b^2 + \bar{X}_{T0}^2}$$

so

$$q_{T0} > k_1$$

and

$$\infty > q_{T0} > k_1 > k_s > k_c > 0$$

so both P_m and T_m are imaginary, implies case (1) where

$$\bar{P}_m = \frac{1}{b} \sqrt{Y_c^2 + \bar{X}_{T0}^2}$$

$$\bar{T}_m = \frac{1}{b} \sqrt{Y_s^2 + \bar{X}_{T0}^2}$$

$$Q_m = \frac{-\rho_1 k_s^2 b I_0(\bar{X}_{T0})}{2\rho_2 \bar{X}_{T0} I_1(\bar{X}_{T0})}$$

Again we note that $q_{T0} > k_1$ implies $C_{T0} < C_1$.

VIII.4 Degeneration to Characteristic Equation for Radially Surrounding Elastic Solid of Infinite Extent Outwards or Elm Modes

The ETm characteristic equation can be converted to the Elm characteristic equation by letting the wall thickness T or the outer radius d go to infinity. The form before the L_{mn} combination is most convenient to use and, with due caution for possible indeterminates, all terms containing d in the denominator are deleted. Dividing the remaining terms by the shorthand LG or $J_1(dP_m)N_0(dT_m)$ we have, noting

$$\frac{N_0(z)}{J_0(z)} \xrightarrow{z \rightarrow i\infty} i$$

$$\frac{N_1(z)}{J_1(z)} \xrightarrow{z \rightarrow i\infty} i$$

that

$$\left[\frac{1 + Qb}{b} \right] [W_1] \begin{bmatrix} + N_1(bP_m) J_1(bT_m) - i J_1(bP_m) J_1(bT_m) \\ + i N_1(bP_m) N_1(bT_m) + N_1(bT_m) J_1(bP_m) \end{bmatrix}$$

$$\begin{aligned}
& + [W_2] \begin{bmatrix} + i N_1(b T_m) N_1(b P_m) + N_1(b P_m) J_1(b T_m) \\ + J_1(b P_m) N_1(b T_m) - i J_1(b P_m) J_1(b T_m) \end{bmatrix} \\
& + [W_3] \begin{bmatrix} + N_1(b P_m) J_0(b T_m) - i J_1(b P_m) J_0(b T_m) \\ + i N_1(b P_m) N_0(b T_m) + J_1(b P_m) N_0(b T_m) \end{bmatrix} \\
& + [W_4] \begin{bmatrix} - i N_1(b T_m) N_0(b P_m) + N_1(b T_m) J_0(b P_m) \\ + i J_1(b T_m) J_0(b P_m) + J_1(b T_m) N_0(b P_m) \\ + i N_1(b P_m) N_0(b T_m) + N_1(b P_m) J_0(b T_m) \\ + J_1(b P_m) N_0(b T_m) - i J_1(b P_m) J_0(b T_m) \end{bmatrix} \\
& + [W_5] \begin{bmatrix} + i N_1(b T_m) N_0(b P_m) + J_1(b T_m) N_0(b P_m) \\ + N_1(b T_m) J_0(b P_m) - i J_1(b T_m) J_0(b P_m) \end{bmatrix} = 0
\end{aligned}$$

where

$$W_1 = 4q_{Tm}^4 P_m^2 T_m - 4q_{Tm}^2 P_m^2 T_m E_m$$

$$W_2 = 4q_{Tm}^2 E_m^2 P_m - 4E_m^3 P_m$$

$$W_3 = -4q_{Tm}^4 P_m^2 T_m^2$$

$$W_4 = -4q_{Tm}^2 E_m^2 P_m T_m$$

$$W_5 = -4E_m^4.$$

Factoring out

$$Q = \frac{\rho_1}{\rho_2} \frac{J_0(X)}{X J_1(X)} \frac{k_s^2 b}{2}$$

yields

$$-Q = 1 + \frac{b W_3}{W_6} \begin{bmatrix} + N_1(b P_m) J_0(b T_m) - i J_1(b P_m) J_0(b T_m) \\ + i N_1(b P_m) N_0(b T_m) + J_1(b P_m) N_0(b T_m) \end{bmatrix}$$

$$\begin{aligned}
& + \frac{b \mathbb{W}_4}{\mathbb{W}_6} \left[\begin{array}{l} + i N_1(b T_m) N_0(b P_m) + N_1(b T_m) J_0(b P_m) \\ - i J_1(b T_m) J_0(b P_m) + J_1(b T_m) N_0(b P_m) \end{array} \right] \\
& + \frac{b \mathbb{W}_4}{\mathbb{W}_6} \left[\begin{array}{l} + i N_1(b P_m) N_0(b T_m) + N_1(b P_m) J_0(b T_m) \\ + J_1(b P_m) N_0(b T_m) - i J_1(b P_m) J_0(b T_m) \end{array} \right] \\
& + \frac{b \mathbb{W}_5}{\mathbb{W}_6} \left[\begin{array}{l} + i N_1(b T_m) N_0(b P_m) + J_1(b T_m) N_0(b P_m) \\ + N_1(b T_m) J_0(b P_m) - i J_1(b T_m) J_0(b P_m) \end{array} \right]
\end{aligned}$$

where the denominator \mathbb{W}_6 is

$$\begin{aligned}
& \mathbb{W}_1 \left[\begin{array}{l} + N_1(b P_m) J_1(b T_m) - i J_1(b P_m) J_1(b T_m) \\ + i N_1(b P_m) N_1(b T_m) + N_1(b T_m) J_1(b P_m) \end{array} \right] \\
& + \mathbb{W}_2 \left[\begin{array}{l} + i N_1(b T_m) N_1(b P_m) + N_1(b P_m) J_1(b T_m) \\ + J_1(b P_m) N_1(b T_m) - i J_1(b P_m) J_1(b T_m) \end{array} \right] = \mathbb{W}_6
\end{aligned}$$

which may be written

$$\begin{aligned}
\mathbb{W}_6 &= -i \mathbb{W}_1 \{ [J_1(b P_m) + i N_1(b P_m)] [J_1(b T_m) + i N_1(b T_m)] \} \\
&\quad - i \mathbb{W}_2 \{ [J_1(b T_m) + i N_1(b T_m)] [J_1(b P_m) + i N_1(b P_m)] \} \\
&= -i [\mathbb{W}_1 + \mathbb{W}_2] H_1^{(1)}(b T_m) H_1^{(1)}(b P_m)
\end{aligned}$$

The numerators are handled in similar fashion to obtain for the entire expression

$$\begin{aligned}
\frac{J_0(X)}{X J_1(X)} \frac{\rho_1 k_s^2 b^2}{\rho_2 2} &= -1 + \frac{H_0^{(1)}(b P_m) [-b \mathbb{W}_5 - b \mathbb{W}_4]}{H_1^{(1)}(b P_m) [\mathbb{W}_1 + \mathbb{W}_2]} \\
&\quad + \frac{H_0^{(1)}(b T_m) [-b \mathbb{W}_3 - b \mathbb{W}_4]}{H_1^{(1)}(b T_m) [\mathbb{W}_1 + \mathbb{W}_2]}
\end{aligned}$$

which straightforwardly becomes

$$\frac{J_0(X_{Em})}{X_{Em} J_1(X_{Em})} \frac{\rho_1}{\rho_2} = - \frac{2}{k_s^2 b^2} + \frac{K_0(\sqrt{Y_c^2 - X_{Em}^2}) (2q_{Em}^2 - k_s^2)^2}{K_1(\sqrt{Y_c^2 - X_{Em}^2}) \sqrt{Y_c^2 - X_{Em}^2} k_s^4} - \frac{K_0(\sqrt{Y_s^2 - X_{Em}^2}) \sqrt{Y_s^2 - X_{Em}^2} 4q_{Em}^2}{K_1(\sqrt{Y_s^2 - X_{Em}^2}) b^2 k_s^4}$$

which is identically the Elm characteristic equation. We recall that the LIm equation is desirable from this Elm equation by allowing the shear sound speed C_s to vanish, and of course the limiting characteristic equations Rm and Fm are simple degenerations of the LIm formulation.

VIII.5 Degeneration to Characteristic Equation for Radially Surrounding Finite Wall Thickness Liquid (Different) Tube or Ltm modes

Just as the ETm characteristic equation was degenerated to the Elm equation by letting the tube thickness T become infinite, so may the ETm equation be degenerated to that for a radially surrounding finite thickness liquid tube by imposing the vanishing of shear sound speed ($k_s \rightarrow \infty$) as was done in transforming the Elm equation to the LIm equation. Again the separate terms before the L_{mn} combination are used, and each is divided by $T_m^2 E_m^3$ where as before

$$T_m^2 = k_s^2 - q_{Tm}^2$$

$$E_m = q_{Tm}^2 - \frac{k_s^2}{2}$$

and eventually $k_s \rightarrow \infty$. With sufficient awareness, the terms which will obviously become zero when the limit is applied may be deleted. The terms remaining for consideration then are

$$\begin{aligned}
 & [\text{MFKD} - \text{IFOD} - \text{MBKH} + \text{IBOH}] \left[\frac{4E_m}{T_m^2} \right] \\
 & + [\text{MNKD} - \text{NIOD} - \text{JMKH} + \text{JIOH}] \left[\frac{4P_m(1 + Q_m b)}{T_m^2 b} \right] = 0.
 \end{aligned}$$

The second factors are evaluated by direct substitution (no k_s remain) and the entire expression, upon replacing the shorthand notation, becomes

$$\begin{aligned}
 & [N_0(bP_m) J_0(dP_m) - J_0(bP_m) N_0(dP_m)] \\
 & \times [N_1(bT_m) J_1(dT_m) - J_1(bT_m) N_1(dT_m)] = \frac{bP_m J_0(X)}{X J_1(X)} \frac{\rho_1}{\rho_2} \\
 & \quad [N_1(bP_m) J_0(dP_m) - j_1(bP_m) N_0(dP_m)] \\
 & \quad \times [N_1(bT_m) J_1(dT_m) - J_1(bT_m) N_1(dT_m)]
 \end{aligned}$$

where the seemingly troublesome second brackets containing T_m cancel on both sides to yield

$$\frac{J_0(X_{tm})}{X_{tm} J_1(X_{tm})} \frac{\rho_1}{\rho_2} = \left(\frac{1}{bP_m} \right) \left[\frac{N_0(bP_m) J_0(dP_m) - J_0(bP_m) N_0(dP_m)}{N_1(bP_m) J_0(dP_m) - J_1(bP_m) N_0(dP_m)} \right]$$

where now

$$bP_m = b\sqrt{k_2^2 - q_{tm}^2} = \sqrt{X_{tm}^2 - Y^2}$$

and the subscript two refers to the tube (not cylinder) liquid where $k_c \rightarrow k_2$.

This L_{tm} equation readily becomes the F_m characteristic equation when the tube thickness T vanishes or $b = d$. In that case the right hand side becomes identically

$$\frac{0}{2/\pi b P_m}$$

and the equation degenerates to

$$J_0(X_{Fm}) = 0.$$

VIII.6 Alternative Derivation of Characteristic Equation for Ltm Modes

The characteristic equation for a liquid (different) tube radially surrounding the liquid cylinder may also be obtained directly from the boundary conditions in the usual way. The velocity potential in the liquid cylinder may be written as

$$\phi_1 = A_1 J_0(k_I r) e^{-i(\omega t - q_{0m} z)}$$

and for the liquid tube as

$$\phi_2 = [B_1 J_0(k_{II} r) + B_2 N_0(k_{II} r)] e^{-i(\omega t - q_{0m} z)}$$

where

$$k_I = \sqrt{k_1^2 - q_{0m}^2} = \frac{X_{0m}}{b}$$

$$k_{II} = \sqrt{k_2^2 - q_{0m}^2} = \frac{\sqrt{X_{0m}^2 - Y^2}}{b} = P_m$$

and where

$$Y = b \sqrt{k_1^2 - k_2^2}$$

and three arbitrary constants are retained for the three boundary conditions:

- (a) continuity of pressure at $r = b$
- (b) continuity of radial particle velocity at $r = b$ and
- (c) vanishing of pressure at $r = d$.

The first two boundary conditions are combined as a statement of continuity of impedance to yield

$$\frac{J_0(k_I b)}{k_I b J_1(k_I b)} \frac{\rho_1}{\rho_2} = \left(\frac{1}{k_{II} b} \right) \left[\frac{B_1 J_0(k_{II} b) + B_2 N_0(k_{II} b)}{B_1 J_1(k_{II} b) + B_2 N_1(k_{II} b)} \right]$$

The third boundary condition yields

$$B_1 J_0(k_{II} d) + B_2 N_0(k_{II} d) = 0$$

and the equations combine to

$$\frac{J_0(k_I b)}{k_I b J_1(k_I b)} \frac{\rho_1}{\rho_2} = \left(\frac{1}{k_{II} b} \right) \left[\frac{J_0(k_{II} b) N_0(k_{II} d) - N_0(k_{II} b) J_0(k_{II} d)}{J_1(k_{II} b) N_0(k_{II} d) - N_1(k_{II} b) J_0(k_{II} d)} \right]$$

which is just the Ltm equation previously obtained.

VIII.7 Degeneration of Ltm Equation to Llm Equation

When the tube wall thickness T becomes infinite ($d \rightarrow \infty$) the Llm equation is obtained from the Ltm equation. The latter can be factored as

$$\frac{J_0(X_{tm})}{X_{tm} J_1(X_{tm})} \frac{\rho_1}{\rho_2} bP_m \left[N_1(bP_m) \frac{J_0(dP_m)}{N_0(dP_m)} - J_1(bP_m) \right] - N_0(bP_m) \frac{J_0(dP_m)}{N_0(dP_m)} + J_0(bP_m) = 0$$

where we also divided by $N_0(dP_m)$. Writing

$$P_m = i \bar{P}_m$$

and again using

$$\frac{J_0(z)}{N_0(z)} \xrightarrow{z \rightarrow i\infty} -i$$

we obtain, allowing $d \rightarrow \infty$, the equation

$$\begin{aligned} \frac{J_0(X_{tm})}{X_{tm} J_1(X_{tm})} \frac{\rho_1}{\rho_2} &= \left(\frac{1}{i b \bar{P}_m} \right) \left[\frac{J_0(i b \bar{P}_m) + i N_0(i b \bar{P}_m)}{J_1(i b \bar{P}_m) + i N_1(i b \bar{P}_m)} \right] \\ &= \frac{1}{i b \bar{P}_m} \frac{H_0^{(1)}(i b \bar{P}_m)}{H_1^{(1)}(i b \bar{P}_m)} \\ &= \frac{1}{b \bar{P}_m} \frac{K_0(b \bar{P}_m)}{K_1(b \bar{P}_m)} \end{aligned}$$

or

$$\frac{J_0(X_{Lm})}{X_{Lm} J_1(X_{Lm})} \frac{\rho_1}{\rho_2} = \frac{1}{\sqrt{Y^2 - X_{Lm}^2}} \frac{K_0(\sqrt{Y^2 - X_{Lm}^2})}{K_1(\sqrt{Y^2 - X_{Lm}^2})}$$

which is the Llm characteristic equation. Obviously this degenerates to the Fm equation

$$J_0(X_{Fm}) = 0$$

when ρ_2 vanishes.

Section IX

RESULTS AND DISCUSSION

IX.1 Selection of Parameters to Validate Orthogonality Assumption

It has been alluded to a number of times that the characteristic functions X_{0m} are orthogonal only for the limiting cases X_{Rm} and X_{Fm} . But, as is the intelligent aim of any real experiment, the pertinent parameters (see Table 1) have been selected to make the characteristic functions almost orthogonal. In (13) and (17) it was shown that for $k_1 a = 100\pi$ the results for $\langle P \rangle_{rel}$, $\langle \theta \rangle_{rel}$ and Z_0 when orthogonal assumption coefficients were used were indistinguishable from the comparable results obtained when the actual coefficients determined by matrix inversion were used even for as small a b/a ratio as $b/a = 1.1$. The value used herein is $b/a = 2.0$, and the comparison of results for this case is even better. For $k_1 b = 200\pi$ there exist a total of 173 roots X_{Em} which are almost orthogonal and, as indicated, when excited by a source of $k_1 a = 100\pi$ give actual results indistinguishable from those calculated using an orthogonality assumption. For brevity, although the indicated results are not as good as those for the parameters selected herein, we show in Table 2 the total number of roots X_{Lm} for $k_1 b = 40\pi$ as well as the orthogonality criterion evaluation for successive roots which would equal zero for truly orthogonal functions. Obviously even for this less-than-optimum case the

TABLE 1
Reference Conditions of Pertinent Parameters
as Used for Calculations When Appropriate.

$\lambda_1 = 0.03$ cm.	(cylinder liquid wavelength)
$a = 50\lambda_1 = 1.5$ cm.	(source radius)
$b = 2a = 3.0$ cm.	(liquid cylinder radius)
$k_1 a = \frac{2\pi a}{\lambda_1} = 100\pi$	
$\rho_2/\rho_1 = \rho_3/\rho_1 = 7$	(density ratio)
$k_1/k_2 = k_1/k_3 = k_1/k_C = 4$	(wave number ratio)
$\nu = 0.325$	(Poisson's ratio)
$T = 1.0$ cm.	(tube wall thickness)

TABLE 2
 The Roots X_{Lm} and Orthogonality Checks
 for Reference Parameters of Table 1 except
 $k_1 a = 20\pi$ or $\lambda_1 = 0.15$ cm.

m	X_{Lm}	Orth. Check
1	2.2716377	-
2	5.2211344	-1.269465×10^{-7}
3	8.2022980	+1.501627
4	11.2055952	-1.632731
5	14.2292985	+1.697591
6	17.2712781	-1.720454
7	20.3289243	+1.718015
8	23.3996145	-1.701534
9	26.4809976	+1.677856
10	29.5710924	-2.038622
11	32.6682830	+1.624821
12	35.7712728	-1.599700
13	38.8790273	+1.576982
14	41.9907212	-1.557219
15	45.1056940	+1.540742
16	48.2234141	-1.527754
17	51.3434505	+1.518400
18	54.4654514	-1.512808
19	57.5891272	+1.511116
20	60.7142374	-1.513498
21	63.8405807	$+1.520180 \times 10^{-7}$
22	66.9679868	-1.531461
23	70.0963105	+1.547735
24	73.2254264	-1.569518
25	76.3552248	+1.597487
26	79.4856088	-1.632527
27	82.6164906	+1.678582
28	85.7477895	-1.728905
29	88.8794289	+1.793230
30	92.0113338	-1.873832
31	95.1434277	+1.972802
32	98.2756279	-2.097020
33	101.4078399	+2.256007
34	104.5399468	-2.465297
35	107.6717908	+2.752281
36	110.8031348	-3.170842
37	113.9335679	+3.846300
38	117.0622018	-5.170171
39	120.1859282	+9.726968

functions are almost orthogonal. Continuing further, Table 3 compares the expansion coefficients obtained by the correct procedure and the orthogonality assumption and again indicates near-agreement even for this poorer case. But Tables 4 and 5 which compare $\langle P \rangle_{rel}$ and $\langle \theta \rangle_{rel}$ calculated by both procedures demonstrates conclusively the degree of validity of the orthogonality assumption for this selection of operating parameters. Since the results for the parameter used herein, which amount to a frequency five times larger than utilized in the previous example, are in even better agreement, the orthogonality assumption will be used henceforth. It should be noted also that in (17) plots of R vs X , where the impedance is $Z_0 = R + iX$, were also indistinguishable for $k_1 a = 20\pi$ and identical for $k_1 a = 100\pi$ when actual and orthogonal assumption coefficient calculations were compared. It should also be noted that the almost orthogonal Characteristic Functions could have been replaced by an orthogonal set obtained by an orthogonalization procedure such as the Gram-Schmidt, but as demonstrated, this is unnecessary.

IX.2 Selection of Parameters to Render Source Boundary Condition Choice Indifferent

Another point of interest is that the relatively large $k_1 a$ employed herein has resulted in calculations for both $\langle P \rangle_{rel}$ and $\langle \theta \rangle_{rel}$ being in very close agreement irrespective of whether a uniform velocity piston or uniform pressure piston is assumed. This is shown for LI boundary conditions in Table 6. The agreement is best understood by recalling that we are obtaining average values over a receiver of the same dimensions as the source, which condition closely matches the real experiment.

IX.3 Satisfaction of Source Boundary Condition With Propagating Modes Only

A point to be checked now concerns the concept of finality for the limiting condition modes with orthogonal characteristic functions. Another way, the question is whether a summation over only the propagating modes is sufficient to describe the source boundary condition which is most realistically a uniform velocity piston of $r = a$ set in a rigid baffle. That is

$$\left. \frac{\partial \phi}{\partial z} \right|_{z=0} = U_0 \quad \text{for } 0 \leq r \leq a$$

$$= 0 \quad \text{for } r > a$$

For the limiting boundary conditions R_m and F_m , orthogonality-derived expansion coefficients are appropriate and the equation for particle velocity at the source as a function of r is simply

TABLE 3
 Comparison of Coefficients K_{Lm} Obtained by
 Orthogonality Assumption and by Correct Matrix
 Inversion for Reference Parameters of Table 1
 except $k_1 a = 20\pi$ or $\lambda_1 = 0.15$ cm.

m	K_{Lm} (Orth. Assump.)	K_{Lm} (Actual)	Relative Error (re Actual)
1	+0.7016619	+0.7016466	+0.0000217
2	+0.6946078	+0.6945457	+0.0000895
3	-0.1551839	-0.1551602	+0.0001531
4	-0.5036120	-0.5034236	+0.0003741
5	+0.0447238	+0.0446840	+0.0008928
6	+0.4150456	+0.4148227	+0.0005374
7	+0.0034498	+0.0034203	+0.0086066
8	-0.3591414	-0.3588310	+0.0008650
9	-0.0281100	-0.0281205	-0.0003730
10	+0.3195555	+0.3193022	+0.0007933
11	+0.0416518	+0.0415708	+0.0019474
12	-0.2897809	-0.2894400	+0.0011606
13	-0.0493929	-0.0493879	+0.0001014
14	+0.2664664	+0.2662270	+0.0008993
15	+0.0539082	+0.0537956	+0.0020930
16	-0.2476499	-0.2473100	+0.0013743
17	-0.0565419	-0.0565328	+0.0001600
18	+0.2320947	+0.2318738	+0.0009525
19	+0.0580382	+0.0579030	+0.0023354
20	-0.2189810	-0.2186361	+0.0015772
21	-0.0588300	-0.0588218	+0.0001397
22	+0.2077433	+0.2075363	+0.0009976
23	+0.0591800	+0.0590240	+0.0026427
24	-0.1979790	-0.1976210	+0.0018116
25	-0.0592541	-0.0592484	+0.0000965
26	+0.1893926	+0.1891914	+0.0010635
27	+0.0591619	+0.0589820	+0.0030515
28	-0.1817621	-0.1813764	+0.0021267
29	-0.0589801	-0.0589763	+0.0000631
30	+0.1749157	+0.1747074	+0.0011924
31	+0.0587673	+0.0585530	+0.0036590
32	-0.1687168	-0.1682744	+0.0026290
33	-0.0585770	-0.0585709	+0.0001037
34	+0.1630505	+0.1628042	+0.0015130
35	+0.0584744	+0.0581954	+0.0047953
36	-0.1578094	-0.1572207	+0.0037444
37	-0.0585826	-0.0585447	+0.0006466
38	+0.1528488	+0.1523702	+0.0031411
39	+0.0594298	+0.0587811	+0.0110368

TABLE 4

Comparison of Average Relative Pressure Values Obtained by Using
Orthogonal Assumption K_{Lm} and Actual K_{Lm} from Table 3.

$z \frac{\lambda}{a^2}$ (Dimensionless)	$(\langle p \rangle_{rel})_L$ (Orth. Assump.)	$(\langle p \rangle_{rel})_L$ (Actual)	Relative Error (re Actual)
0.0	0.9895775	0.9894456	+0.0001334
0.1	0.9306396	0.9305719	+0.0000728
0.2	0.9018492	0.9018035	+0.0000508
0.3	0.8832659	0.8832215	+0.0000503
0.4	0.8747904	0.8747423	+0.0000550
0.5	0.8601329	0.8600888	+0.0000513
0.6	0.8296854	0.8296640	+0.0000258
0.7	0.8454234	0.8453774	+0.0000545
0.8	0.8156356	0.8156078	+0.0000340
0.9	0.8024712	0.8024510	+0.0000251
1.0	0.8094636	0.8094384	+0.0000311
2.0	0.7535671	0.7535548	+0.0000162
3.0	0.7475792	0.7475292	+0.0000668
4.0	0.5320858	0.5321009	-0.0000285
5.0	0.5033542	0.5033521	+0.0000043
6.0	0.3703530	0.3703732	-0.0000546
7.0	0.2964656	0.2964915	-0.0000873
8.0	0.4134798	0.4134609	+0.0000458
9.0	0.3812747	0.3813003	-0.0000671
10.0	0.5912150	0.5912050	+0.0000171

TABLE 5

Comparison of Average Relative Phase-Difference Values Obtained by
Using Orthogonal Assumption K_{Lm} and Actual K_{Lm} from Table 3.

$z \frac{\lambda}{a^2}$ (Dimensionless)	$(\langle \theta \rangle_{rel})_L$ (Orth. Assump.)	$(\langle \theta \rangle_{rel})_L$ (Actual)	Relative Error (re Actual)
0.0	0.0000006	0.0000006	0
0.1	0.0770784	0.0770483	+0.0003907
0.2	0.1104181	0.1103926	+0.0002308
0.3	0.1358862	0.1358591	+0.0001993
0.4	0.1639416	0.1639192	+0.0001367
0.5	0.1836409	0.1836184	+0.0001226
0.6	0.2061965	0.2061710	+0.0001238
0.7	0.2209007	0.2208823	+0.0000832
0.8	0.2617586	0.2617183	+0.0001541
0.9	0.2418164	0.2418140	+0.0000100
1.0	0.2425141	0.2425331	-0.0000786
2.0	0.3661808	0.3661959	-0.0000412
3.0	0.7017445	0.7016980	+0.0000663
4.0	0.7916116	0.7916051	+0.0000082
5.0	0.7776839	0.7777139	-0.0000386
6.0	1.0905651	1.0904750	+0.0000826
7.0	0.6155605	0.6156242	-0.0001034
8.0	0.6405180	0.6405112	+0.0000106
9.0	0.4942622	0.4943238	-0.0001246
10.0	0.5903329	0.5903391	-0.0000104

TABLE 6
 Comparison of Results with Uniform Velocity
 Piston Assumption Versus Uniform Pressure
 Piston Assumption for Pertinent Parameters of
 Table 1 for LI Boundary Conditions.

$z \frac{\lambda}{a^2}$	$\langle p \rangle_{rel}^{U_0}$	$\langle p \rangle_{rel}^{P_0}$	$\langle \theta \rangle_{rel}^{U_0}$	$\langle \theta \rangle_{rel}^{P_0}$
0.00	0.999503	0.997917	0.000000	0.000000
0.05	0.950692	0.950767	0.052472	0.052588
0.10	0.930707	0.930667	0.076451	0.076394
0.15	0.915531	0.915802	0.093686	0.093624
0.20	0.907251	0.907193	0.110055	0.109990
0.25	0.896877	0.896674	0.123808	0.123863
0.30	0.884174	0.884425	0.144242	0.144449
0.35	0.879778	0.879708	0.156224	0.156289
0.40	0.872737	0.872976	0.156974	0.157149
0.45	0.856739	0.856513	0.175648	0.175467
0.50	0.859623	0.859423	0.177288	0.177297
0.55	0.849449	0.849361	0.207341	0.207482
0.60	0.827450	0.827619	0.203258	0.203205
0.65	0.839162	0.839305	0.206781	0.206644
0.70	0.843402	0.843294	0.234454	0.234032
0.75	0.827145	0.827165	0.251471	0.251600
0.80	0.806176	0.806094	0.249257	0.249315
0.85	0.797646	0.797701	0.250928	0.251142
0.90	0.802938	0.803033	0.231199	0.231246
0.95	0.809582	0.809520	0.254687	0.254496
1.00	0.815821	0.815692	0.265994	0.265971

$$\left. \left(\frac{\partial \phi}{\partial z} \right)_{rel}^{U_0} \right|_{z=0} = \frac{2a}{b} \sum_m \frac{J_1 \left(X_{0m} \frac{a}{b} \right) J_0 \left(r \frac{X_{0m}}{b} \right)}{X_{0m} [J_0^2(X_{0m}) + J_1^2(X_{0m})]}$$

and calculations using X_{Rm} are shown in Table 7a. Obviously the source condition is beautifully represented by the propagating modes alone.

An even better fit is obtained at $z = 0$ if evanescent modes are considered in addition to the propagating ones. Table 7b shows the improvement when an equal number of such modes (201) are also included. However, a Gibbs'-type phenomenon is appearing at $r = 0$ and $r = a$ as shown in Table 7c which covers the first interval of Table 7b in finer detail. This phenomenon would appear to contraindicate the inclusion of additional modes short of an infinite number.

That the evanescent modes are unimportant in the field is shown in Table 7d which compares both $\langle p \rangle_{rel}$ and $\langle \theta \rangle_{rel}$ calculated first using only the propagating modes and then including an equal number of evanescent modes.

TABLE 7A

Relative Particle Velocity at Source Calculated Using Only Propagated Modes X_{Rm} for Pertinent Parameters of Table 1 for $0 \leq r \leq b$ with Uniform Velocity Piston Assumption

r/b	$\left(\frac{\partial\phi}{\partial z}\right)_{rel}^{U_0} @ z=0$	r/b	$\left(\frac{\partial\phi}{\partial z}\right)_{rel}^{U_0} @ z=0$
0.00	0.980870	0.55	0.010202
0.05	0.997761	0.60	0.005186
0.10	0.998123	0.65	0.003532
0.15	0.998158	0.70	0.002721
0.20	0.998044	0.75	0.002250
0.25	0.997793	0.80	0.001949
0.30	0.997352	0.85	0.001748
0.35	0.996560	0.90	0.001613
0.40	0.994918	0.95	0.001523
0.45	0.989908	1.00	0.001470
0.50	0.500056		

TABLE 7B

Relative Particle Velocity at Source Calculated Using an Equal Number of Evanescent Modes in Addition to the 201 Propagated Modes X_{Rm} for Pertinent Parameters of Table 1 for $0 \leq r \leq b$ with Uniform Velocity Piston Assumption

r/b	$\left(\frac{\partial\phi}{\partial z}\right)_{rel}^{U_0} @ z=0$	r/b	$\left(\frac{\partial\phi}{\partial z}\right)_{rel}^{U_0} @ z=0$
0.00	1.032718	0.55	0.004422
0.05	1.001755	0.60	0.001803
0.10	1.000779	0.65	0.000889
0.15	1.000203	0.70	0.000414
0.20	0.999741	0.75	0.000124
0.25	0.999302	0.80	-0.000063
0.30	0.998824	0.85	-0.000186
0.35	0.998210	0.90	-0.000262
0.40	0.997200	0.95	-0.000300
0.45	0.994525	1.00	-0.000307
0.50	0.499464		

TABLE 7C

Same as Table 7b Except Finer Detail in First Internal to Show Gibb's-type Phenomenon about $r/b = 0$. The Same Effect is Noted at $r/b = 0.50$ (or $r = a$). Even Finer Detail Indicates No Smaller Period.

r/b	$\left(\frac{\partial\phi}{\partial z}\right)_{rel}^{U_0} @ z = 0$	r/b	$\left(\frac{\partial\phi}{\partial z}\right)_{rel}^{U_0} @ z = 0$
0.0000	1.032718	0.0275	0.997278
0.0025	0.990153	0.0300	1.002569
0.0050	1.007047	0.0325	0.997567
0.0075	0.994272	0.0350	1.002310
0.0100	1.004918	0.0375	0.997302
0.0125	0.995646	0.0400	1.002096
0.0150	1.003930	0.0425	0.997999
0.0175	0.996405	0.0450	1.001913
0.0200	1.003321	0.0475	0.998168
0.0225	0.996909	0.0500	1.001755
0.0250	1.002894		

TABLE 7D

Comparison of Field Results With and Without an Equal Number of Evanescent Modes for Pertinent Parameters of Table 1 for R_m Boundary Conditions

$(z \lambda/a^2)$	$[\langle p \rangle_{rel}]_{prop. modes}$	$[\langle p \rangle_{rel}]_{prop. + evanescent modes}$	$[\langle \theta \rangle_{rel}]_{prop. modes}$	$[\langle \theta \rangle_{rel}]_{prop. + evanescent modes}$
0.00	0.997975	0.998983	0.000000	0.000000
0.05	0.950753	0.950753	0.052676	0.052676
0.10	0.930879	0.930879	0.076601	0.076601
0.15	0.915571	0.915571	0.094493	0.094493
0.20	0.905772	0.905772	0.109019	0.109019
0.25	0.894796	0.894796	0.123246	0.123246
0.30	0.887153	0.887153	0.142057	0.142057
0.35	0.879781	0.879781	0.150887	0.150887
0.40	0.866130	0.866130	0.157411	0.157411
0.45	0.858369	0.858369	0.177639	0.177639
0.50	0.851132	0.851132	0.179308	0.179308
0.55	0.854024	0.854024	0.198167	0.198167
0.60	0.837945	0.837945	0.216605	0.216605
0.65	0.833067	0.833067	0.208948	0.208948
0.70	0.839845	0.839845	0.214782	0.214782
0.75	0.834864	0.834864	0.237585	0.237585
0.80	0.818207	0.818207	0.262335	0.262335
0.85	0.811075	0.811075	0.264782	0.264782
0.90	0.790786	0.790786	0.267581	0.267581
0.95	0.801277	0.801277	0.256635	0.256635
1.00	0.796728	0.796728	0.259642	0.259642

IX.4 Satisfaction of Source Boundary Condition With Existing Finite Number of Modes

But another question arises with the finite impedance of infinite extent boundary conditions where a finite number of modes, all propagating, was found. Namely, can this smaller number of modes still adequately describe the source boundary condition? The modes X_{Lm} were used and the result shown in Table 8a. Again we note the very nice representation of the source boundary condition for $0 \leq r \leq b$, demonstrating that the existing modes can in fact be used to describe our actual source. Undoubtedly an even better fit could be obtained, but not in the manner utilized in the previous section, because here there are no evanescent modes. However, the orthogonality assumption expansion coefficients were utilized, and although as seen they do not effect field calculations, they could be expected to have a slight effect on the plane $z = 0$. Thus, if actual coefficients obtained from the complete matrix were used instead, the fit should improve. Such a procedure is lamentably beyond the capabilities of the CDC computer at the Naval Research Laboratory and so the fit in Table 8 is the best that can be presented now. However, the fit at $z = 0$ has little bearing on the nicety of calculation in the field and the cases of infinite extent surrounding media are not much more realistic than the infinite and zero impedance cases.

TABLE 8a
Relative Particle Velocity at Source Calculated
Using All Modes X_{Em} for Pertinent Parameters of
Table 1 for $0 \leq r \leq b$ With Uniform Velocity
Piston Assumption

r/b	$\left(\frac{\partial\phi}{\partial z}\right)_{rel}^{U_0} @ z = 0$	r/b	$\left(\frac{\partial\phi}{\partial z}\right)_{rel}^{U_0} @ z = 0$
0.00	1.019618	0.55	-0.006035
0.05	0.999963	0.60	-0.001615
0.10	0.998383	0.65	-0.003446
0.15	0.997948	0.70	-0.002308
0.20	0.998698	0.75	-0.000054
0.25	1.000450	0.80	-0.001600
0.30	1.002425	0.85	-0.001723
0.35	1.003299	0.90	-0.000534
0.40	1.001459	0.95	-0.000910
0.45	0.993976	1.00	-0.001510
0.50	0.500057		

IX.5 Satisfaction of " ρC " Loading of Source

If we turn to the impedance formulation appropriate to the interferometer situation we discover from calculations that the large $k_1 a$ utilized results in fact in " ρc " loading and that Z_0 is real, or for $Z_0 = R + iX$ we find

$$R \sim 28.$$

$$X \sim 0.0000$$

from a summation of the propagated modes for R_m and F_m and all the finite number of modes for L_m and E_m . Thus even without arguing that we are concerned only with the change in source impedance associated with moving the reflector and that the source impedance is tuned to pure R we find that its impedance alone is in fact pure real.

IX.6 No Untoward Implication for $r > b$ Because of Limiting Integration Limit to $r = b$

Returning to particle velocity, we note that if the calculations for Table 8 are continued for $r > b$, we obtain the result that the particle velocity remains zero there. But this raises yet another question. In the first place the Bessel function with the argument r is not J_0 for this surrounding medium, but instead $H_0^{(1)}$ or K_0 was used for the scalar displacement potential there. And besides, the expansion coefficients utilized for the potential inside the liquid cylinder were obtained by integrating only inside the liquid cylinder or from $r = 0$ to $r = b$. While it follows that these same coefficients must be used outside the liquid cylinder, possible untoward implication on the source ($z = 0$) boundary condition for $r > b$ must be investigated. That is, even though the region of interest is the liquid cylinder, the possibility of implied sources in the wall material at $z = 0$ must be checked.

We reformulate the expansion coefficient calculation for those cases where acoustic energy penetrates the surrounding medium, selecting the LI boundary condition for relative simplicity, as follows.

The potential inside the liquid cylinder ($0 \leq r \leq b$) was expressed in a mode summation as

$$\phi^I = \sum_m K_{Lm}^I J_0(r \sqrt{k_1^2 - q_{Lm}^2}) e^{iq_{Lm} z}$$

and the potential in the radially surrounding medium of infinite extent as

$$\phi^{II} = \sum_m K_{Lm}^{II} H_0^{(1)}(r \sqrt{k_2^2 - q_{Lm}^2}) e^{iq_{Lm} z}$$

where the q_{Lm} were obtained from a characteristic (frequency) equation derived from matching impedances at the boundary between the two media.

If we restrict ourselves to the liquid cylinder we may determine the expansion coefficients by the Fourier method which yields the smallest least square error (zero for actual convergence, i.e., if all the members of the set are used), as

$$\int_0^b \phi^I(r, 0) J_0(r\sqrt{k_1^2 - q_{L\ell}^2}) r dr = \int_0^b \sum_m K_{Lm}^I J_0(r\sqrt{k_1^2 - q_{Lm}^2}) J_0(r\sqrt{k_1^2 - q_{L\ell}^2}) r dr$$

and, assuming a uniform velocity piston of radius a , obtain

$$\int_0^a \frac{\partial \phi^I(r, 0)}{\partial z} J_0(r\sqrt{k_1^2 - q_{L\ell}^2}) r dr = i \int_0^b \sum_m K_{Lm}^I q_{Lm} J_0(r\sqrt{k_1^2 - q_{Lm}^2}) J_0(r\sqrt{k_1^2 - q_{L\ell}^2}) r dr.$$

The left hand side becomes

$$U_0 \int_0^a J_0(r\sqrt{k_1^2 - q_{0\ell}^2}) r dr = \frac{U_0 a}{\sqrt{k_1^2 - q_{0\ell}^2}} J_1(a\sqrt{k_1^2 - q_{0\ell}^2}).$$

where we note we have previously defined

$$\sqrt{k_1^2 - q_{L\ell}^2} = X_{L\ell}/b.$$

Instead of using the complete matrix formulation for evaluating the coefficients, we may, as was shown acceptable, employ the orthogonality assumption

$$\int_0^b J_0\left(X_{L\ell} \frac{r}{b}\right) J_0\left(X_{Lm} \frac{r}{b}\right) r dr = 0, \ell \neq m$$

and

$$\int_0^b J_0^2\left(X_{Lm} \frac{r}{b}\right) r dr = \frac{b^2}{2} [J_0^2(X_{Lm}) + J_1^2(X_{Lm})]$$

and calculate the K_{Lm}^I by the resulting separate equations.

If we instead restrict ourselves to the surrounding liquid we would have for $r \geq b$

$$\left. \frac{\partial \phi^{II}}{\partial z} \right|_{z=0} = i \sum_m q_{Lm} K_{Lm}^{II} H_0^{(1)}(r\sqrt{k_2^2 - q_{Lm}^2})$$

and if we demand

$$\left. \frac{\partial \phi^{II}}{\partial z} \right|_{\substack{z=0 \\ r \geq b}} = 0$$

we would obtain only the trivial result all $K_{Lm}^{II} = 0$. But actually, we must have

$$W_m K_{Lm}^I = K_{Lm}^{II}$$

since the total potential must be expressible as

$$\sum_m \phi_{Lm} = \sum_m (\phi_{Lm}^I + \phi_{Lm}^{II}) = \sum_m K_{Lm} [J_0(r\sqrt{k_1^2 - q_{Lm}^2}) + W_m H_0^{(1)}(r\sqrt{k_2^2 - q_{Lm}^2})] e^{iq_{Lm}z}.$$

We have already indicated the satisfaction of the source boundary condition at $z = 0$ for $0 \leq r \leq b$ obtained by using expansion coefficients calculated only for the liquid cylinder. Using these same expansion coefficients for the outer medium we write

$$\begin{aligned} \left. \left(\frac{\partial \phi^{II}}{\partial z} \right)_{r \leq b} \right|_{\substack{z=0 \\ r \geq b}} &= \frac{2a}{b} \sum_m \frac{J_1\left(X_{Lm} \frac{a}{b}\right) H_0^{(1)}\left(r \frac{\sqrt{X_{Lm}^2 - Y^2}}{b}\right)}{X_{Lm} [J_0^2(X_{Lm}) + J_1^2(X_{Lm})]} W_m \\ &= \frac{4a}{\pi i b} \sum_m \frac{J_1\left(X_{Lm} \frac{a}{b}\right) K_0\left(r \frac{\sqrt{Y^2 - X_{Lm}^2}}{b}\right)}{X_{Lm} [J_0^2(X_{Lm}) + J_1^2(X_{Lm})]} W_m. \end{aligned}$$

The individual W_m are determined by equating *either* the pressure or the radial particle velocity at the boundary $r = b$. The former yields

$$\rho_1 \sum_m K_{Lm}^I J_0(b\sqrt{k_1^2 - q_{Lm}^2}) = \rho_2 \sum_m W_m K_{Lm}^I H_0^{(1)}(b\sqrt{k_2^2 - q_{Lm}^2})$$

and the latter gives

$$\sum_m K_{Lm}^I \sqrt{k_1^2 - q_{Lm}^2} J_1(b\sqrt{k_1^2 - q_{Lm}^2}) = \sum_m W_m K_{Lm}^I \sqrt{k_2^2 - q_{Lm}^2} H_1^{(1)}(b\sqrt{k_2^2 - q_{Lm}^2}).$$

So that individual equations are obtained

$$W_m = \frac{\rho_1}{\rho_2} \frac{J_0(b\sqrt{k_1^2 - q_{Lm}^2})}{H_0^{(1)}(b\sqrt{k_2^2 - q_{Lm}^2})}$$

and also

$$W_m = \frac{\sqrt{k_1^2 - q_{Lm}^2}}{\sqrt{k_2^2 - q_{Lm}^2}} \frac{J_1(b\sqrt{k_1^2 - q_{Lm}^2})}{H_1^{(1)}(b\sqrt{k_2^2 - q_{Lm}^2})}$$

which are consistent since elimination of W_m between them yields the Lm characteristic equation. We note W_m is also expressible as

$$\begin{aligned} W_m &= \frac{\rho_1}{\rho_2} \frac{J_0(X_{Lm})}{H_0^{(1)}(\sqrt{X_{Lm}^2 - Y^2})} = \frac{\pi i}{2} \frac{\rho_1}{\rho_2} \frac{J_0(X_{Lm})}{K_0(\sqrt{Y^2 - X_{Lm}^2})} \\ &= \frac{X_{Lm}}{\sqrt{X_{Lm}^2 - Y^2}} \frac{J_1(X_{Lm})}{H_1^{(1)}(\sqrt{X_{Lm}^2 - Y^2})} = \frac{\pi i}{2\sqrt{Y^2 - X_{Lm}^2}} \frac{J_1(X_{Lm})}{K_1(\sqrt{Y^2 - X_{Lm}^2})} \end{aligned}$$

So that the calculated particle velocity at the source in the z direction is real and given by

$$\left. \left(\frac{\partial \phi_{II}}{\partial z} \right)_{rel}^{U_0} \right|_{z=0} \Big|_{r \geq b} = \sum_m \frac{J_0(X_{Lm}) J_1(X_{Lm}/2) \rho_1 K_0\left(\frac{r}{b} \sqrt{Y^2 - X_{Lm}^2}\right)}{X_{Lm} [J_0^2(X_{Lm}) + J_1^2(X_{Lm})] \rho_2 K_0(\sqrt{Y^2 - X_{Lm}^2})}$$

We note that the largest term occurs when X_{Lm} is nearest Y for which the argument of v_0 is approximately

$$\sqrt{(608)^2 - (607)^2} \sim 40$$

and

$$K_0(X) \sim \frac{1.2533}{\sqrt{X}} e^{-X} \sim 10^{-17}$$

Thus utilization in the surrounding medium of the K_{Lm} calculated as appropriate for the liquid cylinder is expected to result in near zero values of particle velocity for $r \geq b$. Actually, as seen in Table 8b, the largest value found for the sum is $+10^{-54}$ with the smallest value -10^{-156} , which is considered sufficiently close to zero.

This above could be demonstrated in another way. If we write the coefficient evaluation equation in terms of the potential in all space (not only for $0 \leq r \leq b$) we would have an additional term on the right hand side as

TABLE 8B
 Relative Particle Velocity at Source Calculated
 Using All Modes X_{Lm} for Pertinent Parameters
 of Table 1 for $r \geq b$ With Uniform Velocity
 Piston Assumption

r/b	$\left. \frac{\partial \phi}{\partial z} \right _{rel} \Big _{z=0}^{U_0}$	r/b	$\left. \frac{\partial \phi}{\partial z} \right _{rel} \Big _{z=0}^{U_0}$
1.00	0.000000	1.60	$3.196116 \times 10^{-118}$
1.10	0.000000	1.70	$2.050313 \times 10^{-130}$
1.20	7.028863×10^{-54}	1.80	$5.054501 \times 10^{-139}$
1.30	2.624787×10^{-73}	1.90	$3.565257 \times 10^{-148}$
1.40	2.684155×10^{-90}	2.00	$-2.210963 \times 10^{-156}$
1.50	$-3.820700 \times 10^{-105}$		

$$\frac{2}{\pi} \sum_m q_{Lm} K_{Lm} \int_b^\infty K_0 \left(\frac{r \sqrt{Y^2 - X_{Lm}^2}}{b} \right) J_0 \left(r \frac{X_{Lm}}{b} \right) r dr$$

which becomes, using asymptotic expressions

$$\sqrt{2} b \sum_m \frac{q_{Lm} K_{Lm}}{\sqrt{Y^2 - X_{Lm}^2} \sqrt{X_{Lm}}} \int_b^\infty e^{-\frac{r \sqrt{Y^2 - X_{Lm}^2}}{b}} \begin{bmatrix} \cos \frac{r X_{Lm}}{b} \\ + \sin \frac{r X_{Lm}}{b} \end{bmatrix} dr$$

which evaluates to

$$\frac{-\sqrt{2} b^2}{Y^2} \sum_m \frac{q_{Lm} K_{Lm} e^{-\sqrt{Y^2 - X_{Lm}^2}}}{\sqrt{Y^2 - X_{Lm}^2} \sqrt{X_{Lm}}} \begin{bmatrix} (X_{Lm} - \sqrt{Y^2 - X_{Lm}^2}) \sin X_{Lm} \\ -(X_{Lm} + \sqrt{Y^2 - X_{Lm}^2}) \cos X_{Lm} \end{bmatrix}$$

We note that $b q_{Lm} = \sqrt{(k_1 b)^2 - X_{Lm}^2}$ and for the selected parameters we have

$$Y \approx 608$$

and the smallest X_{Lm} is

$$X_{L1} \sim \sqrt{2}$$

and the largest X_{Lm} is

$$X_{L173} \sim 607.$$

The smallest total term here corresponds to the smallest root and is approximately

$$e^{-608}$$

while the largest total term corresponding to the largest root is approximately

$$e^{-40}$$

so that the contribution of the second integral on the right hand side of the expansion coefficient determination equation written for the potential everywhere may be safely neglected, as we have already seen another way.

IX.7 No Untoward Implication for $r > b$ Because of Constant Reflector Impedance Assumption

In the same manner that no untoward implication for $r > b$ because of invoked assumptions at $z = 0$ was demonstrated, we now investigate the effect at $z = l$ for $r > b$ of the assumption that the reflector impedance is independent of r and l and may be denoted $\rho_3 c_3$. As before, in medium I, the liquid cylinder of interest, we have

$$\phi^I = \sum_m J_0 \left(r \frac{X_{0m}}{b} \right) [K_{0m} e^{iq_{0m}z} + L_{0m} e^{-iq_{0m}z}]$$

and in medium II, the radially surrounding material

$$\phi^{II} = \sum_m H_0^{(1)} \left(r \frac{\sqrt{X_{0m}^2 - Y^2}}{b} \right) [K_{0m} e^{iq_{0m}z} + L_{0m} e^{-iq_{0m}z}] W_m$$

and we recall that the reflector material, medium III is chosen to be identical with medium II.

As before, we simplify the formulation slightly by considering medium II a liquid with the density and sound speed of a metal, whereby W_m is given as

$$W_m = \frac{\rho_1}{\rho_2} \frac{J_0(X_{Lm})}{H_0^{(1)}(\sqrt{X_{Lm}^2 - Y^2})}$$

The impedance in medium I is then given by

$$[Z(r, z)]_{0 \leq r < b}^{U_0} = [\rho_1 c_1] \frac{\sum_m J_0\left(r \frac{X_{Lm}}{b}\right) [K_{Lm} e^{iq_{Lm}z} + L_{Lm} e^{-iq_{Lm}z}]}{\sum_m \left(\frac{q_{Lm}}{k_1}\right) J_0\left(r \frac{X_{Lm}}{b_1}\right) [K_{Lm} e^{iq_{Lm}z} - L_{Lm} e^{-iq_{Lm}z}]}$$

and the impedance in medium II as

$$[Z(r, z)]_{r \geq b}^{U_0} = [\rho_3 c_3] \frac{\sum_m H_0^{(1)}\left(\frac{r \sqrt{X_{Lm}^2 - Y^2}}{b}\right) [K_{Lm} e^{iq_{Lm}z} + L_{Lm} e^{-iq_{Lm}z}] W_m}{\sum_m \left(\frac{q_{Lm}}{k_3}\right) H_0^{(1)}\left(\frac{r \sqrt{X_{Lm}^2 - Y^2}}{b}\right) [K_{Lm} e^{iq_{Lm}z} - L_{Lm} e^{-iq_{Lm}z}] W_m}$$

The two simultaneous equations in K_{Lm} and L_{Lm} are

$$K_{Lm} - L_{Lm} = -\frac{2ia}{b} \frac{U_0}{q_{Lm}} \frac{J_1\left(X_{Lm} \frac{a}{b}\right)}{X_{Lm} [J_0^2(X_{Lm}) + J_1^2(X_{Lm})]}$$

and

$$K_{Lm} \left(1 + \frac{\rho_3}{\rho_1} \frac{q_{Lm}}{k_3}\right) e^{iq_{Lm}\ell} + L_{Lm} \left(1 - \frac{\rho_3}{\rho_1} \frac{q_{Lm}}{k_3}\right) e^{-iq_{Lm}\ell} = 0$$

where $z \equiv \ell$. These yield

$$L_{Lm} = \frac{-i \frac{2a}{b} \frac{U_0}{q_{Lm}} \frac{J_1\left(X_{Lm} \frac{a}{b}\right)}{X_{Lm} [J_0^2(X_{Lm}) + J_1^2(X_{Lm})]}}{\frac{\left(\frac{\rho_3}{\rho_1} \frac{q_{Lm}}{k_3} - 1\right) e^{-iq_{Lm}\ell}}{\left(\frac{\rho_3}{\rho_1} \frac{q_{Lm}}{k_3} - 1\right) e^{iq_{Lm}\ell}} - 1}$$

and

$$K_{Lm} = L_{Lm} - i \frac{2a}{b} \frac{U_0}{q_{Lm}} \frac{J_1\left(X_{Lm} \frac{a}{b}\right)}{X_{Lm} [J_0^2(X_{Lm}) + J_1^2(X_{Lm})]}$$

The impedance calculated in this manner at $z = \ell = 50$ cm. is given in Table 9a for medium I or $0 \leq r/b \leq 1$ and in Table 9b for medium II or $1 \leq r/b \leq 2$. Obviously, not only is the impedance constraint that

$$[Z(r, z)]_{0 \leq r \leq b}^{U_0} = \rho_3 c_3 = 28 \rho_1 c_1$$

beautifully indicated by the calculations, but they also demonstrate that

$$[Z(r, z)]_{r \geq b}^{U_0} = \rho_3 c_3$$

and no outward result occurs in the outer medium because of the constant reflector impedance assumption.

TABLE 9A
Impedance Within Liquid Cylinder at $z = \ell$ With Constant Reflector Impedance Assumption and for LIM Radial Boundary Conditions

r/b	$[Z(r, z)]_{0 \leq r \leq b}^{U_0} / [\rho_1 c_1]$	r/b	$[Z(r, z)]_{0 \leq r \leq b}^{U_0} / [\rho_1 c_1]$
0.00	28.000056	0.55	28.000113
0.05	28.000054	0.60	28.000091
0.10	28.000098	0.65	27.999848
0.15	27.999906	0.70	28.000097
0.20	27.999905	0.75	28.000089
0.25	27.999923	0.80	28.000140
0.30	28.000013	0.85	27.999958
0.35	27.999948	0.90	27.999954
0.40	27.999943	0.95	27.999952
0.45	27.999957	1.00	27.999999
0.50	28.000021		

TABLE 9B
Impedance in Surrounding Liquid Medium II at $z = \ell$ With Constant Reflector Impedance Assumption and for LIM Radial Boundary Conditions

r/b	$[Z(r, z)]_{r \geq b}^{U_0} / [\rho_3 c_3]$	r/b	$[Z(r, z)]_{r \geq b}^{U_0} / [\rho_3 c_3]$
1.00	1.000000	1.55	1.000000
1.05	1.000000	1.60	1.000000
1.10	1.000000	1.65	1.000000
1.15	1.000000	1.70	1.000000
1.20	1.000002	1.75	1.000000
1.25	0.999999	1.80	1.000000
1.30	0.999998	1.85	1.000000
1.35	1.000000	1.90	1.000000
1.40	1.000000	1.95	1.000000
1.45	1.000000	2.00	1.000000
1.50	1.000000		

IX.8 Mode Sound Speed Dispersion Plots

We return now to the main substance of this report, but before summing the modes for our selected parameters $k_1 a = 100\pi$ and $k_1 b = 200\pi$, we first indicate the nature of the mode sound speed dispersion plots versus $k_1 b$ for much smaller values of the abscissa extending down to zero frequency. Figure 2 shows these dispersion plots for **R**, **F**, **LI**, and **EI** radial boundary conditions. It is seen that there is an **RO** mode whose speed coincides with the intrinsic sound speed of the liquid constituting the liquid cylinder, and which exists at all frequencies. There is no comparable **FO** mode and all the higher order **Rm** and **Fm** modes display minimum cutoff frequencies at which the apparent phase velocity for the mode goes to infinity. There is an **LI** mode which has been numbered **LI0** simply by analogy with the **RO** mode since the higher **LIm** modes track fairly well just above the **Rm** mode with corresponding m . These **LIm** modes all display minimum cutoff frequencies also, **LI0** existing almost down to $k_1 b = 0$, but their apparent phase velocity never exceeds the sound speed of the surrounding liquid medium. Thus, each **LIm** mode terminates at $C_{0m}/C_1 = C_2/C_1$. It should be noted that the surrounding liquid has been given a density and sound speed equivalent to the density and compressional sound speed of an elastic solid comparable to a nickel-steel and this fact explains the close tracking between the **Rm** curves and the **LIm** curves. The **Elm** modes are especially interesting since they correspond to the closest approximation to experimental conditions yet discussed. The single imaginary root to the **EI** equation falls just below the **RO** curve, the closeness resulting from the large impedance mismatch since $\rho_2/\rho_1 = 7$ and $k_1/k_c = 4$. But the density does not affect the apparent sound speed of this **EI0** mode as much as might be expected. For example, the first computed value for the relative sound speed of this mode was made for $k_1 b = 0.20944$ and resulted in a ratio of 0.98348 for $\rho_2/\rho_1 = 7$. But dropping the density ratio down to $\rho_2/\rho_1 = 2$ dropped this speed ratio at the same frequency only down to 0.94561. The higher order **Elm** modes also display minimum cutoff frequencies terminating at a ratio $C_{0m}/C_1 = C_s/C_1$. They apparently all cross the **Fm** mode of corresponding m (except **EI1** does not exist below **F1**), tracking just below the **Rm** mode of corresponding m at higher frequencies and aiming for an intersection with the **Rm** mode of one lower m at lower frequencies.

IX.9 Zero Mode Controversy Settled

We arrive now at the most realistic boundary condition, the finite impedance elastic solid finite thickness tube. Figure 3 shows the relative sound speed dispersion plots for the first few modes at low frequency for this case.

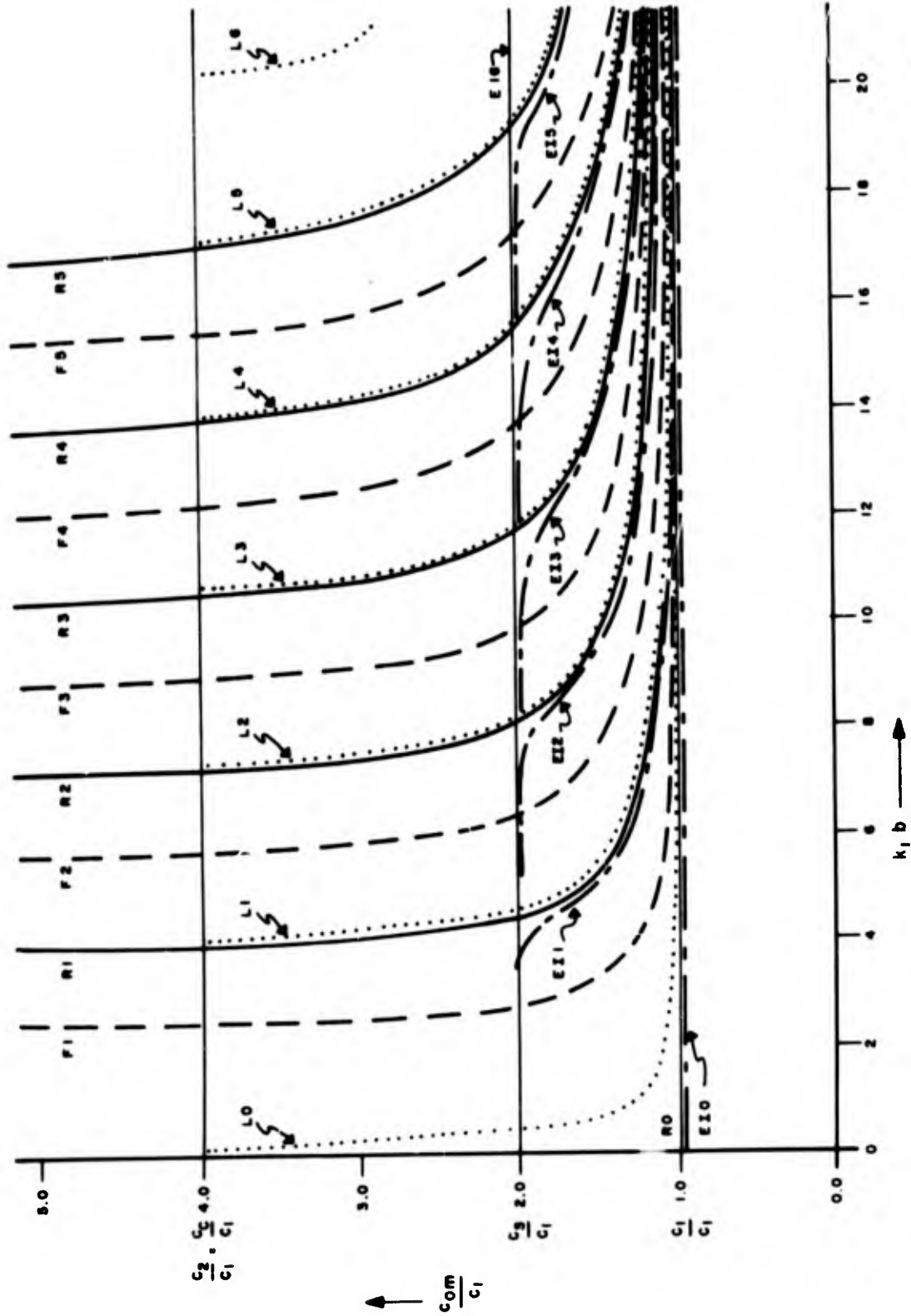


Fig. 2—Sound Speed Dispersion Plots C_{0m}/C_1 vs $k_1 b$ for liquid cylinder modes of order m for rigid radial boundary condition R_m , free radial boundary condition F_m , infinite liquid radial boundary condition L_m , and infinite elastic solid radial boundary condition E_m with appropriate reference conditions in Table 1

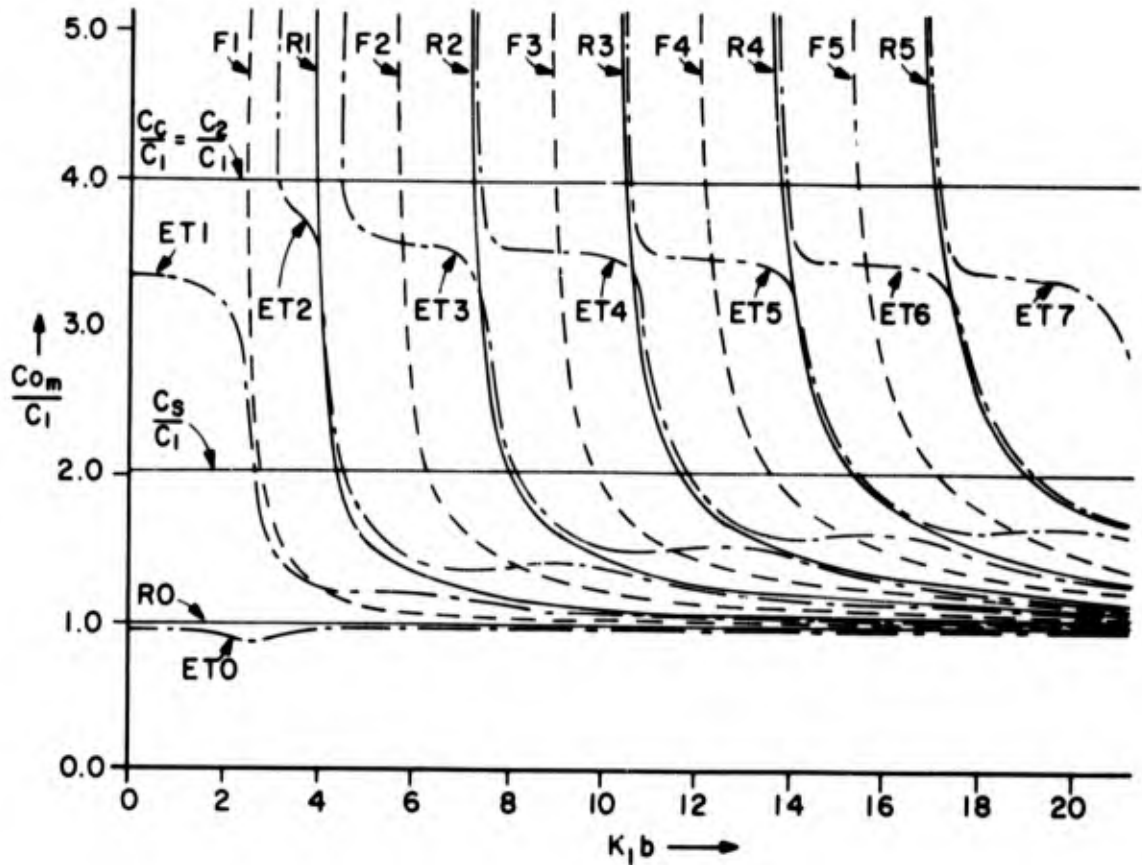


Fig. 3—Sound Speed Dispersion Plots C_{0m}/C_1 vs $k_1 b$ for liquid cylinder modes of order m for finite elastic solid tube radial boundary condition ET_m with appropriate reference conditions in Table 1

Obviously the latest work by Kumar (1) is in error, undoubtedly because of the simplifying approximations he used which apparently changed the physics of the situation drastically. The zero mode labelled ET0 does in fact exist at all frequencies as stated by Lin and Morgan (3) based on their approximate theory and also by Thomson (2) based on his approximate theory. Although the physical significance of Kumar's approximations are not at all clear to this writer they must involve the neglect of flexural or shear forces in the wall since Kumar's curve is obtained for this mode if the term relating to shear is omitted from Fay, Brown, and Fortier's approximate equation (5) as has been pointed out by Jacobi (4). Of course, with the significance of Kumar's approximation unclear, the possibility of a computational error can not be ruled out, but appears unlikely since his higher order modes do track nicely with those of Lin and Morgan. Indeed, the behavior of Kumar's zero mode is similar to the first mode in the wall of a cylindrical shell if the membrane theory is erroneously utilized, as has been indicated by Junger and Rosato (19). They show that the membrane theory predicts a "dead-zone" of frequency where no propagation occurs, but point out that the assumptions or basic requirements of the membrane theory are not met at the "dead-zone" frequency. That is, the requirement that the shell be "thin" is not fulfilled there because the sound speed and hence the wavelength become increasingly smaller as that frequency is approached. Another point they make is that as the wavelength decreases, the curvature changes and so the flexural stresses increase to become comparable to the membrane stresses and thus invalidate the membrane theory requirements. From the foregoing, it is not surprising that the behavior predicted for the zero mode by Kumar's approximations is not indicated by the exact equations utilized here. The first mode missed by Thomson but indicated both by Lin and Morgan and by Kumar does not have a lower cutoff frequency as do all the higher order modes. The plateaus for the higher order modes (which do then go to infinity with decreasing frequency unlike the EIm modes which terminate on their corresponding plateaus) occur somewhat below the C_c/C_1 value indicated by (1) and (3). For their parameters the minimum in ET0 is lower and the lower "plateaus" are absent.

IX.10 Relative Pressure and Phase Plots for Non-Terminated Cylinder

The expansions detailed in Section 5 leading to $\langle P \rangle_{rel}$ and $\langle \theta \rangle_{rel}$ were carried out and plots of these quantities vs $z(\lambda/a^2)$ are shown along with the free field diffraction results calculated as detailed in Section 3 for the radial boundary conditions R, F, LI, EI and ET in Figs. 4a. and b. thru 8a. and b. respectively. From these plots it is noted that the curves do not deviate appreciably from the free field diffraction results but

rather oscillate about them. It is readily seen without belaboring the point that failure to apply appropriate corrections to guided mode propagation results or, alternatively, failure to select optimum configurations so as to preclude the necessity for corrections can lead to appreciable errors in sound speed and sound absorption.

While the sound speed corrections are self explanatory, consisting of the indicated phase shift or timing excess over the experimental distance, a word is desirable concerning the absorption correction. The intrinsic absorption coefficient α is obtained most readily from

$$\alpha = \frac{1}{(z_2 - z_1)} \ln \frac{A_1}{A_2}$$

where $z_2 - z_1 = \Delta z$ represents a sufficiently small distance interval and the A_1/A_2 ratio is obtained from the measured amplitudes N and the diffraction amplitude D at the respective z as

$$\frac{A_2}{A_1} = \frac{N_2 D_1}{N_1 D_2}$$

where no interaction was assumed or

$$\alpha = \nu - \delta$$

where

$$N_2 = N_1 \exp[-\nu(z_2 - z_1)]$$

$$D_2 = D_1 \exp[-\delta(z_2 - z_1)].$$

An interesting observation regarding the imaginary modes found for the infinite elastic EI and elastic tube ET equations and labelled EI0 and ET0 respectively is that, unlike the rigid case where R0 contributes significantly to the sums, the imaginary modes, while leading to real propagation constants, do not affect the sums as much as 10^{-8} . The nature of these imaginary modes is that of a surface wave as observed earlier. The potential form $J_0(rX_{00}/b)$ becomes $J_0(ri\bar{X}_{00}/b) = I_0(rX_{00}/b)$ and $I_0(0) = 1$ so that the potential does not disappear on the axis but rather decreases to unity.

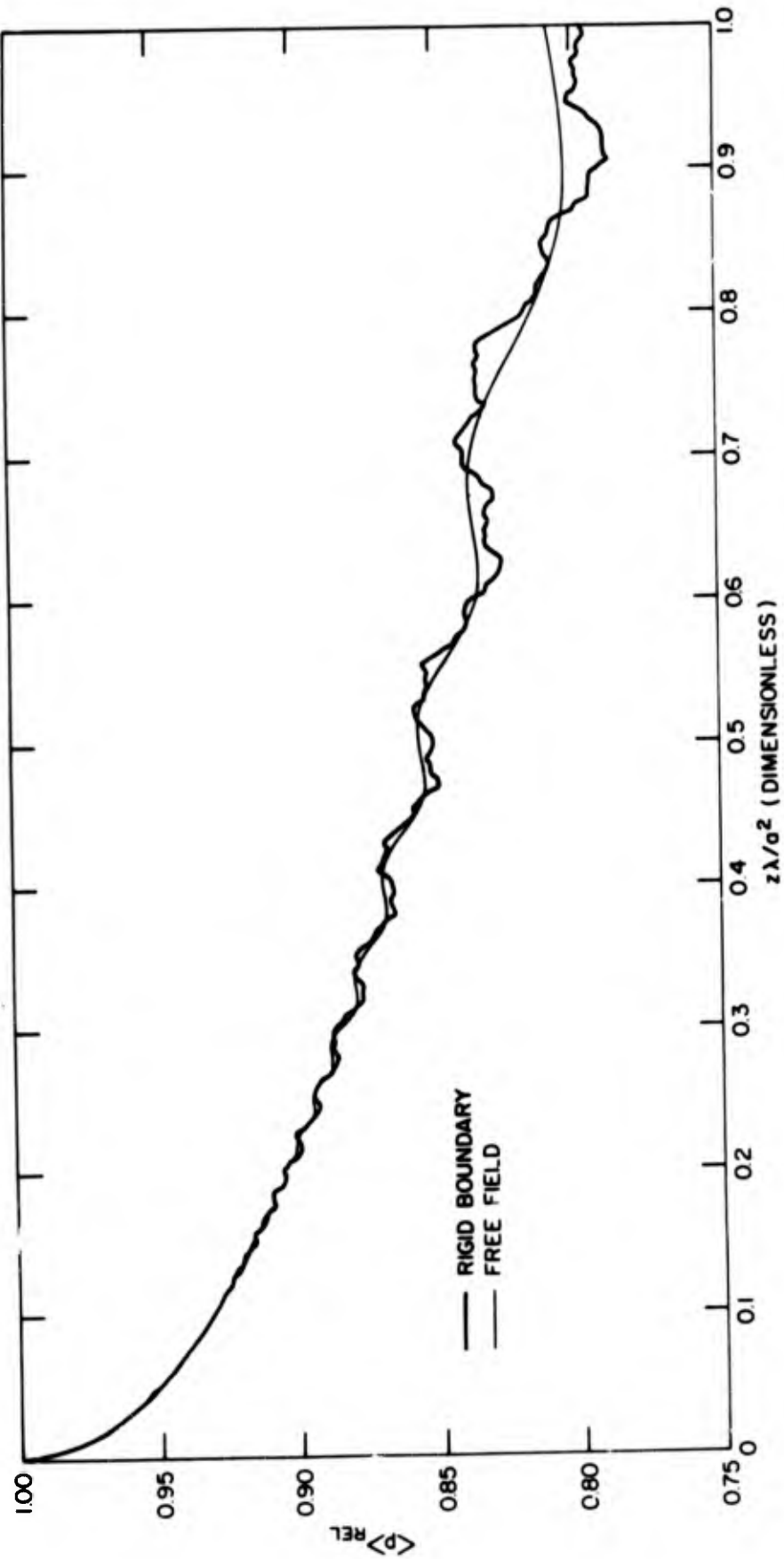


Fig. 4a— $\langle P \rangle_{REL}$ vs $0 \leq z(\lambda/a^2) \leq 1$ for liquid cylinder with rigid radial boundary condition R_m and uniform velocity source assumption and including all propagated modes for appropriate reference conditions in Table 1. Free Field Diffraction curves are plotted for comparison

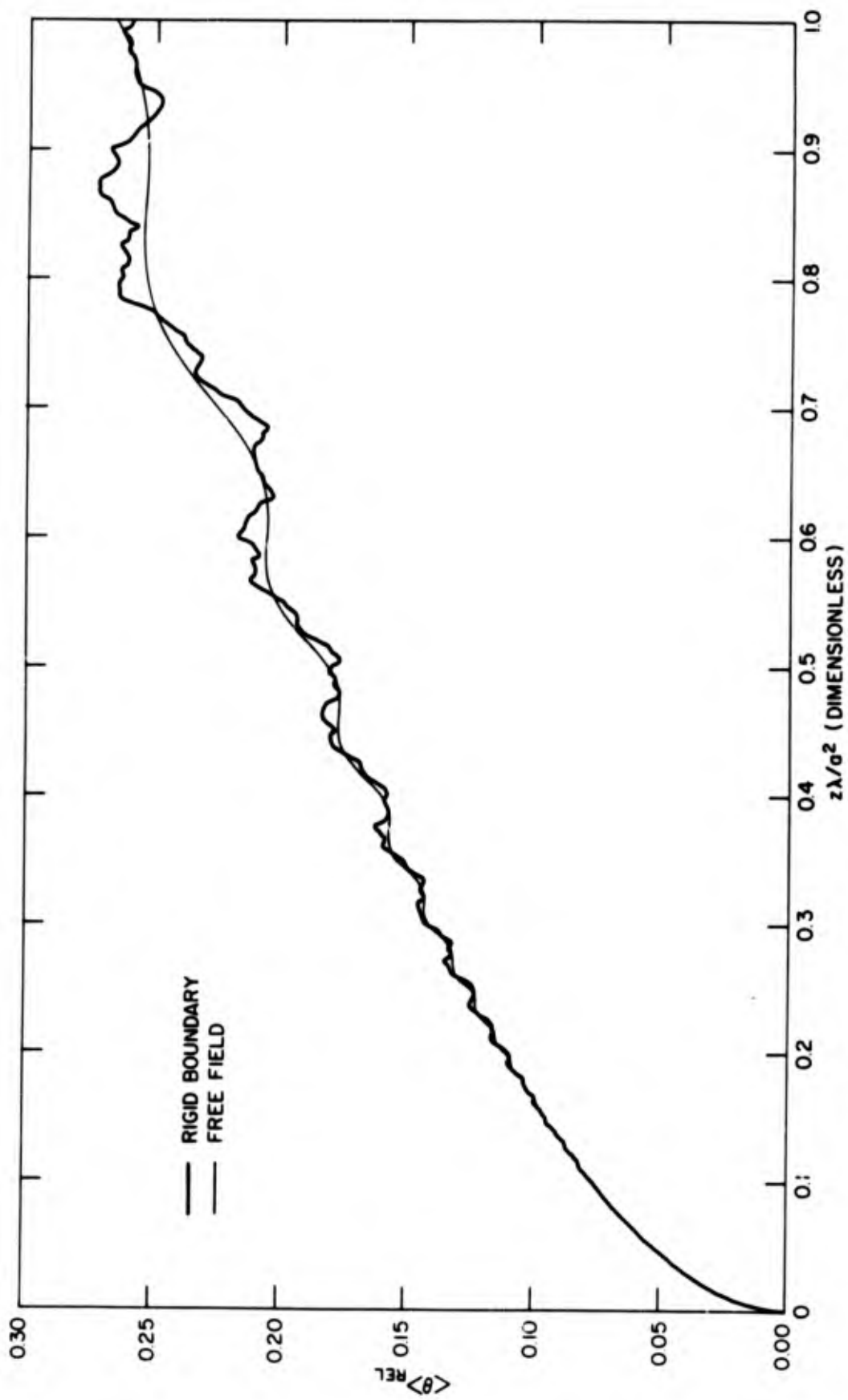


Fig. 4b - $\langle \theta \rangle_{REL}$ vs $0 \leq z(\lambda/a^2) \leq 1$ for liquid cylinder with rigid radial boundary condition R_m and uniform velocity source assumption and including all propagated modes for appropriate reference conditions in Table 1. Free Field Diffraction curves are plotted for comparison

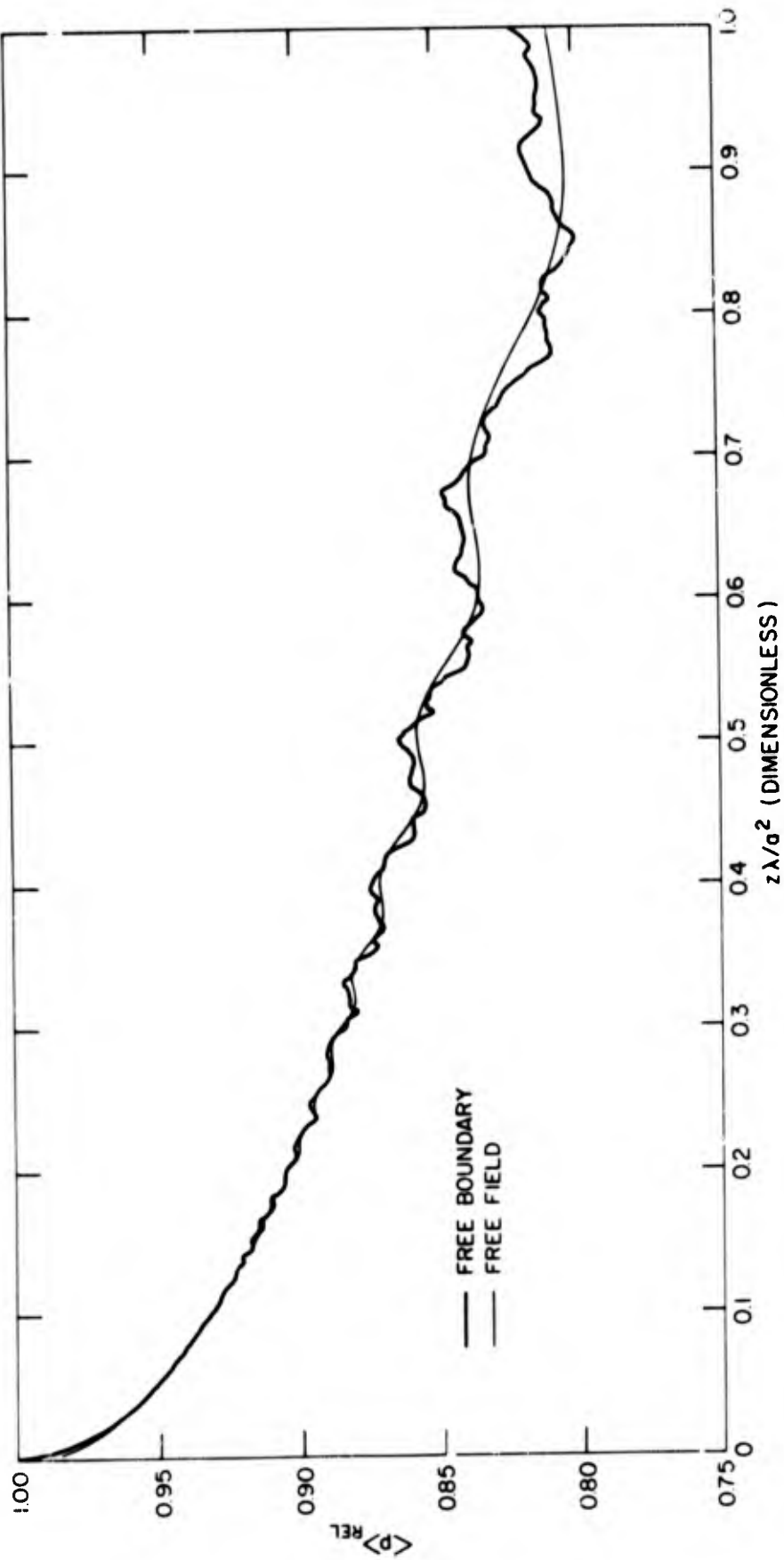


Fig. 5a - $\langle P \rangle_{REL}$ vs $0 \leq z(\lambda/a^2) \leq 1$ for liquid cylinder with free radial boundary condition F_{∞} and uniform velocity source assumption and including all propagated modes for appropriate reference conditions in Table 1

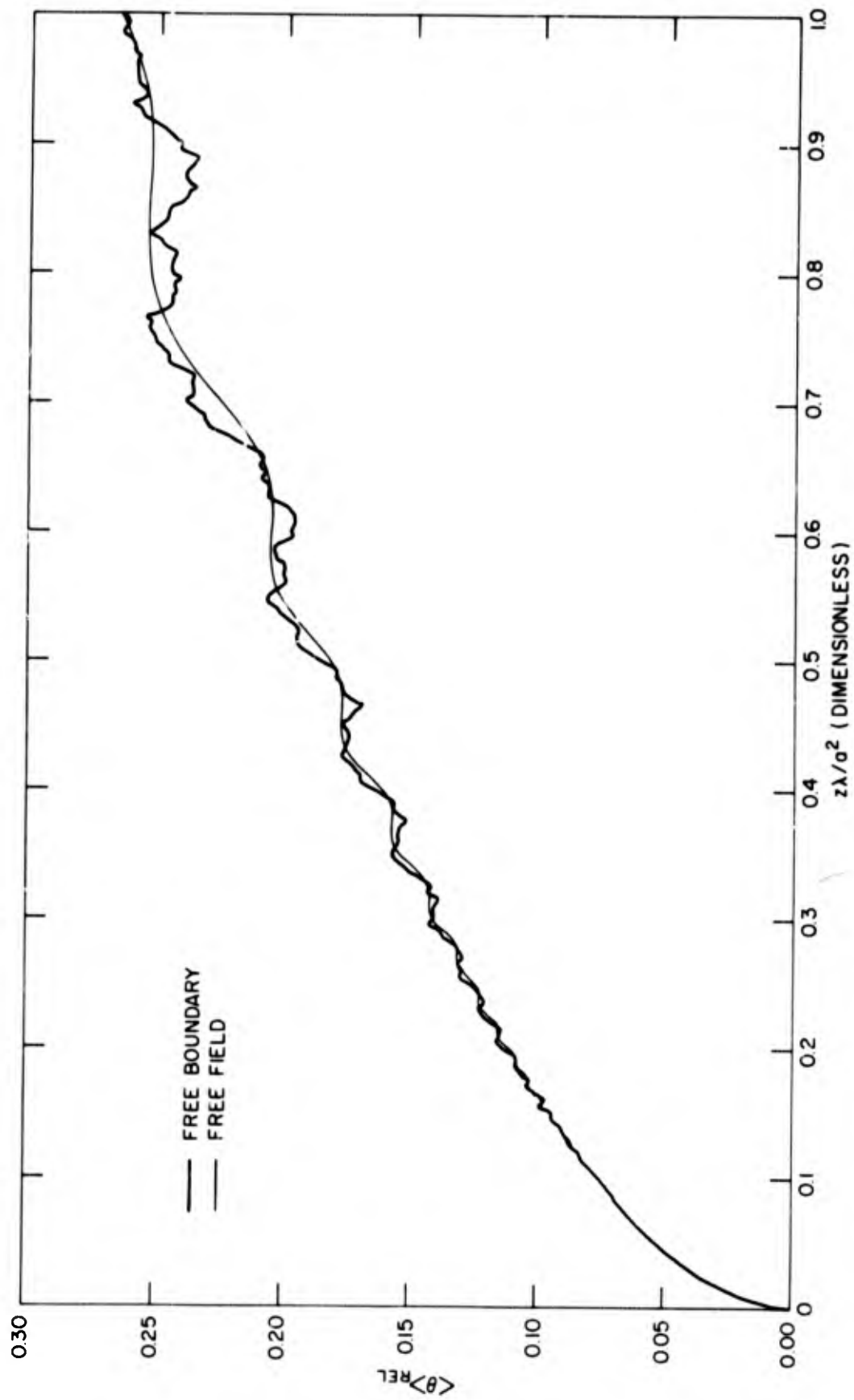


Fig. 5b - $\langle \theta \rangle_{REL}$ vs $0 \leq z(\lambda/a^2) \leq 1$ for liquid cylinder with free radial boundary condition F_{∞} and uniform velocity source assumption and including all propagated modes for appropriate reference conditions in Table 1. Free Field Diffraction curves are plotted for comparison

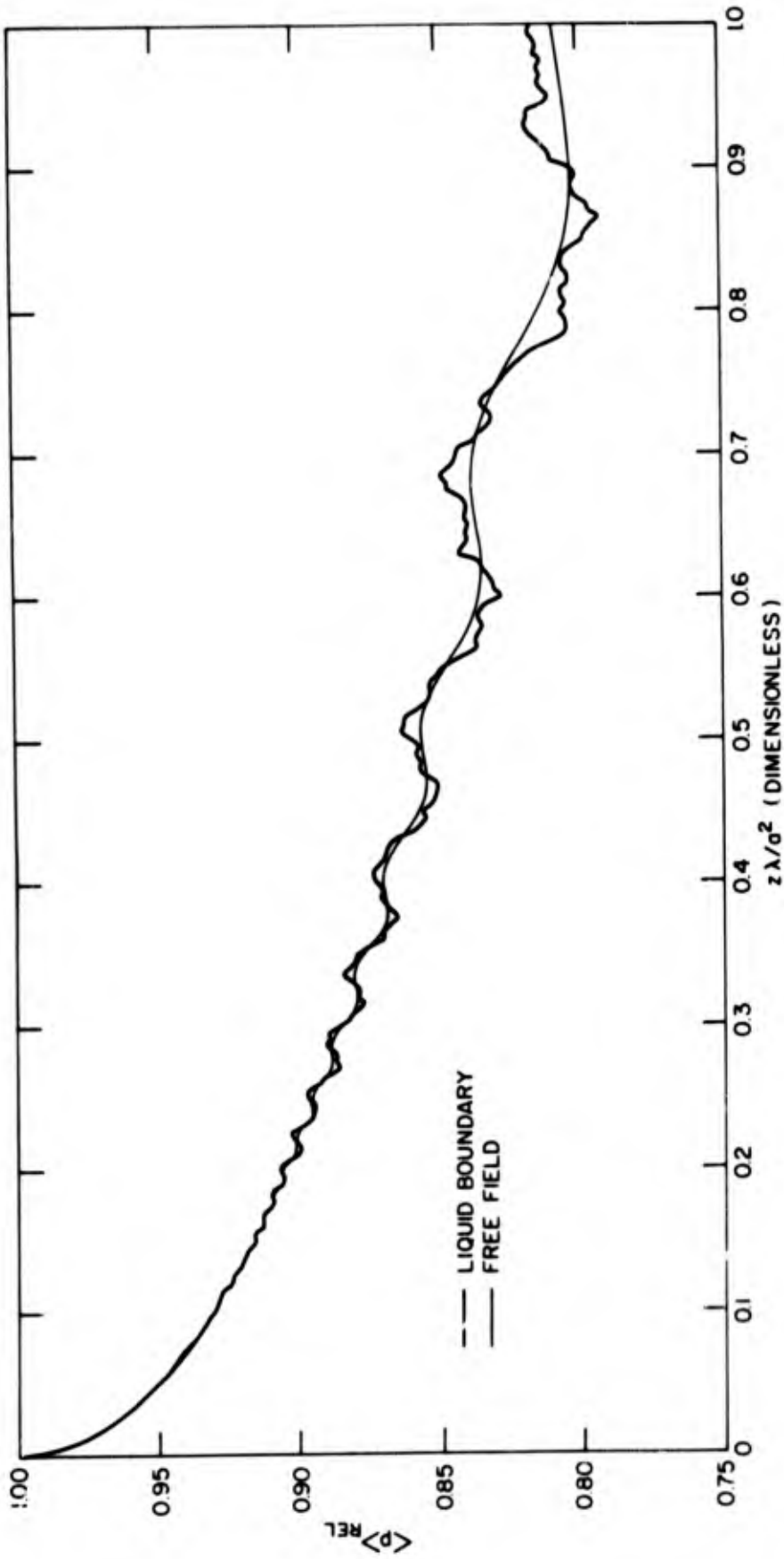


Fig. 6a - $\langle P \rangle_{REL}$ vs $0 \leq z(\lambda/a^2) \leq 1$ for liquid cylinder with infinite liquid radial boundary condition L_{Im} and uniform velocity source assumption using orthogonal Characteristic Function assumption and including all propagated modes for appropriate reference conditions in Table 1. Free Field Diffraction curves are plotted for comparison

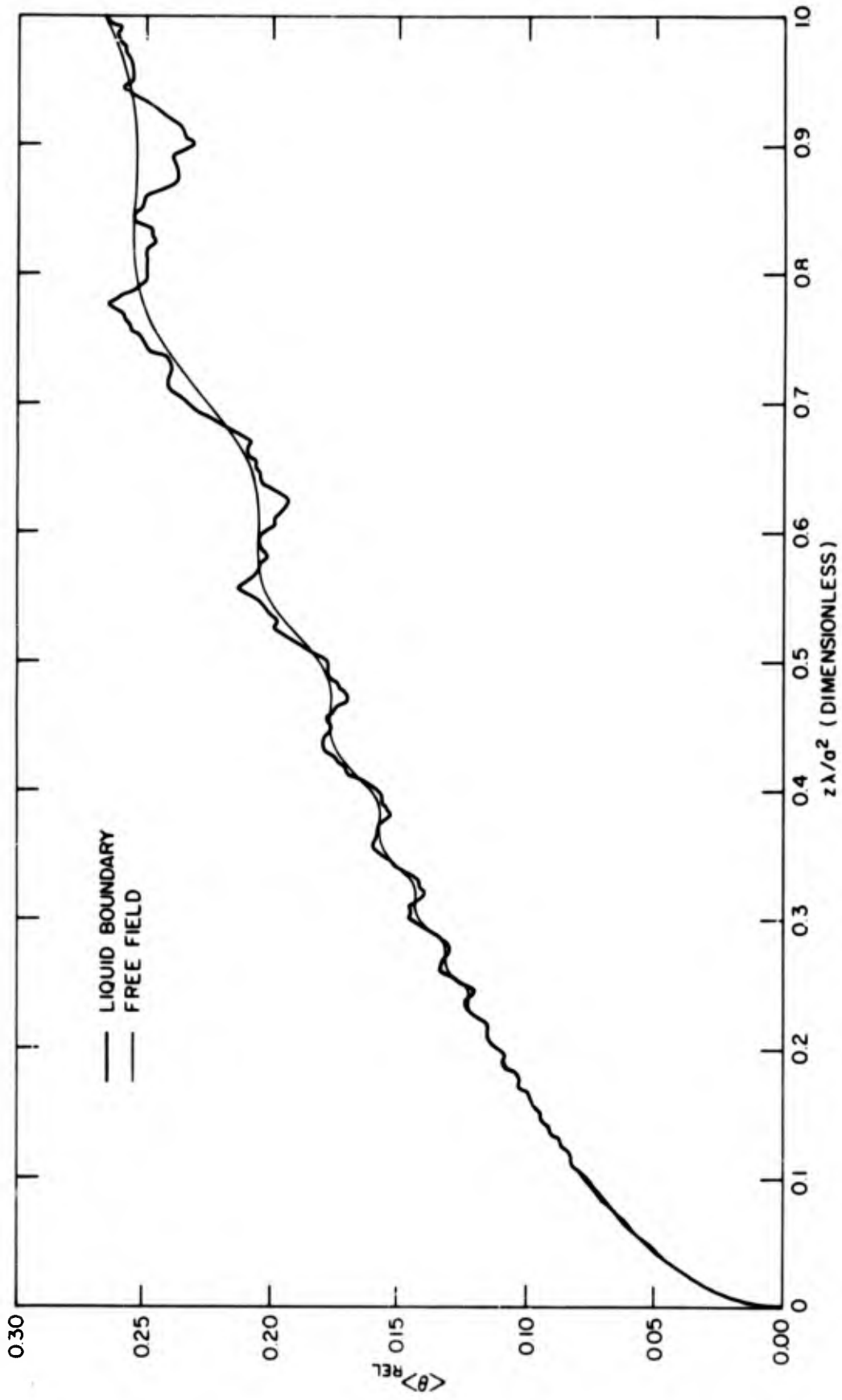


Fig. 6b - $\langle \theta \rangle_{REL}$ vs $0 \leq z(\lambda/a^2) \leq 1$ for liquid cylinder with infinite liquid radial boundary condition L_{lm} and uniform velocity source assumption using orthogonal Characteristic Function assumption and including all propagated modes for appropriate reference conditions in Table 1. Free Field Diffraction curves are plotted for comparison

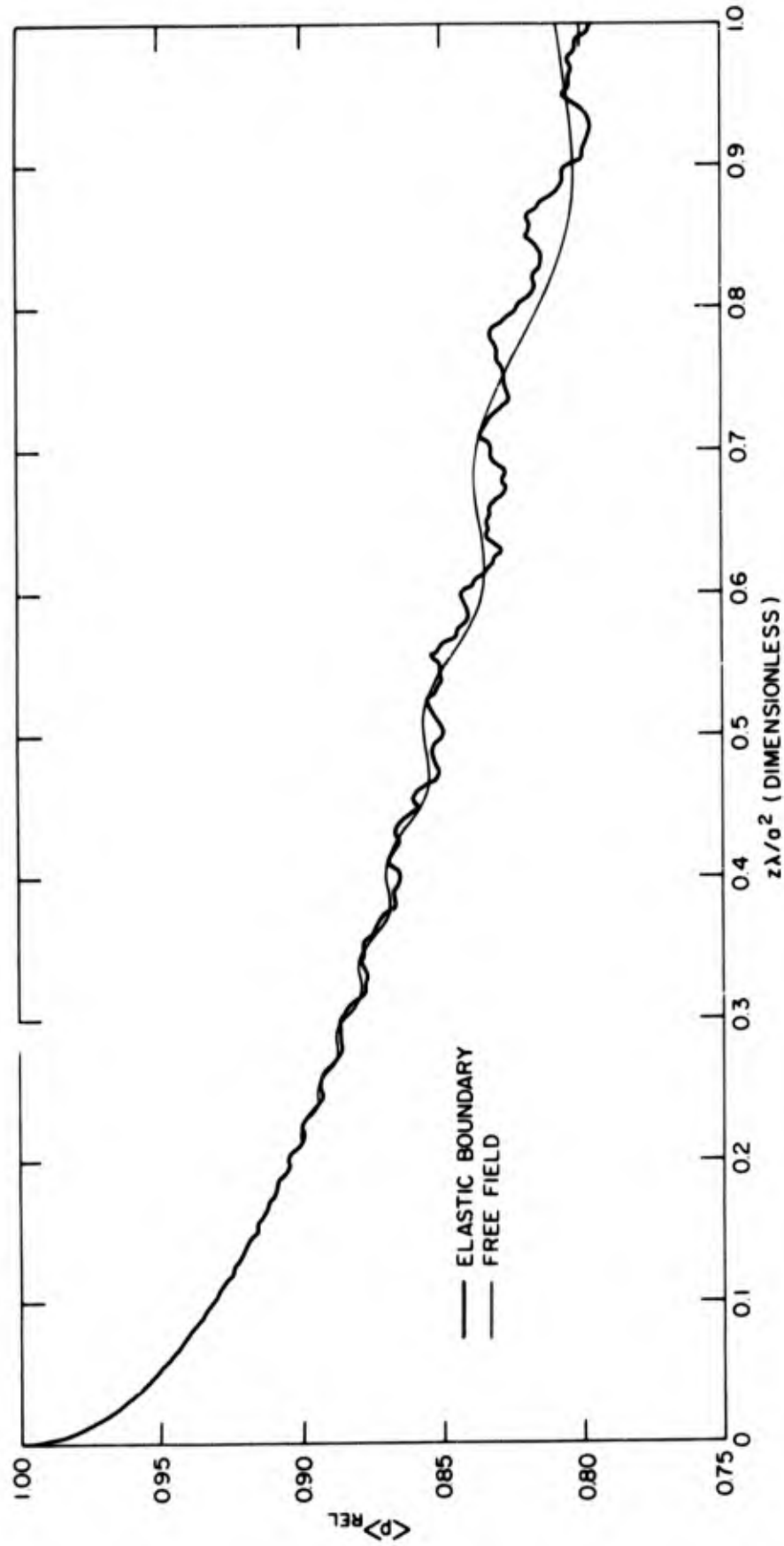


Fig. 7a - $\langle P \rangle_{REL}$ vs $0 \leq z(\lambda/a^2) \leq 1$ for liquid cylinder with infinite elastic solid radial boundary condition E_{lm} and uniform velocity source assumption using orthogonal Characteristic Function assumption and including all propagated modes for appropriate reference conditions in Table 1. Free Field Diffraction curves are plotted for comparison

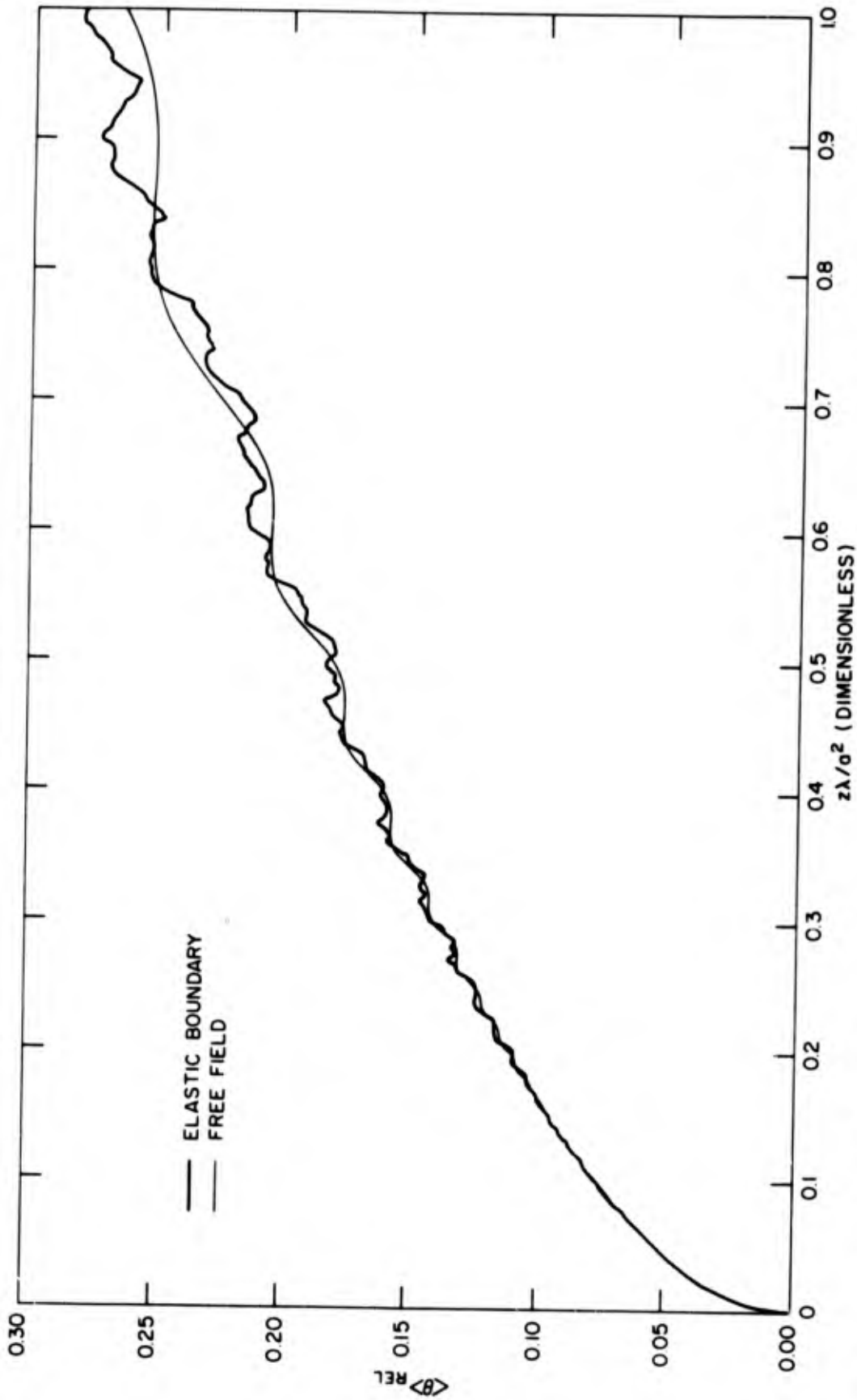


Fig. 7b - $\langle \theta \rangle_{REL}$ vs $0 \leq z(\lambda/a^2) \leq 1$ for liquid cylinder with infinite elastic solid radial boundary condition E_{∞} and uniform velocity source assumption using orthogonal Characteristic Function assumption and including all propagated modes for appropriate reference conditions in Table 1. Free Field Diffraction curves are plotted for comparison

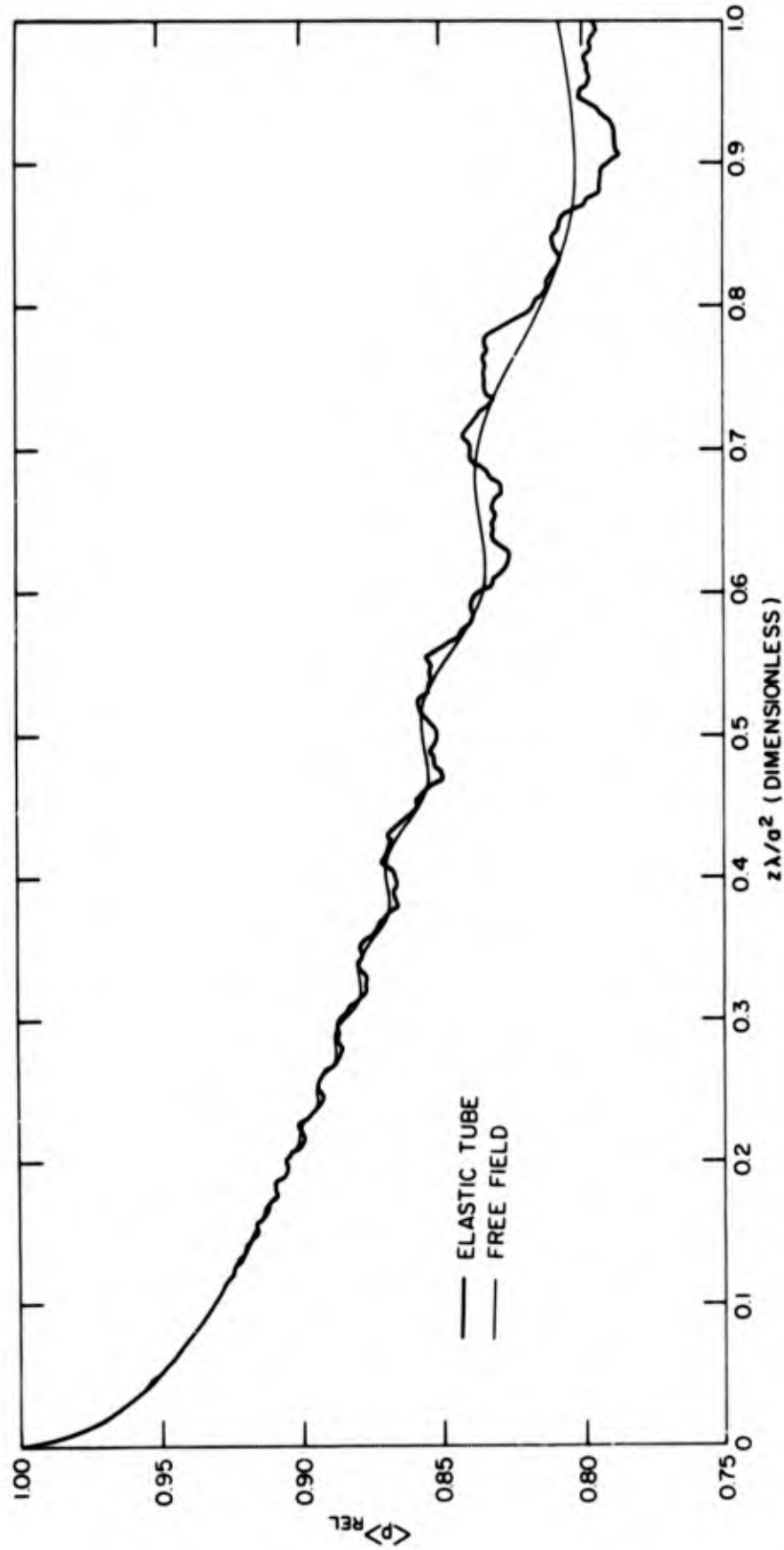


Fig. 8a - $\langle P \rangle_{REL}$ vs $0 \leq z(\lambda/a^2) \leq 1$ for liquid cylinder with finite elastic solid tube radial boundary condition E_{Tm} and uniform velocity source assumption using orthogonal Characteristic Function assumption and including all propagated modes for appropriate reference conditions in Table 1. Free Field Diffraction curves are plotted for comparison

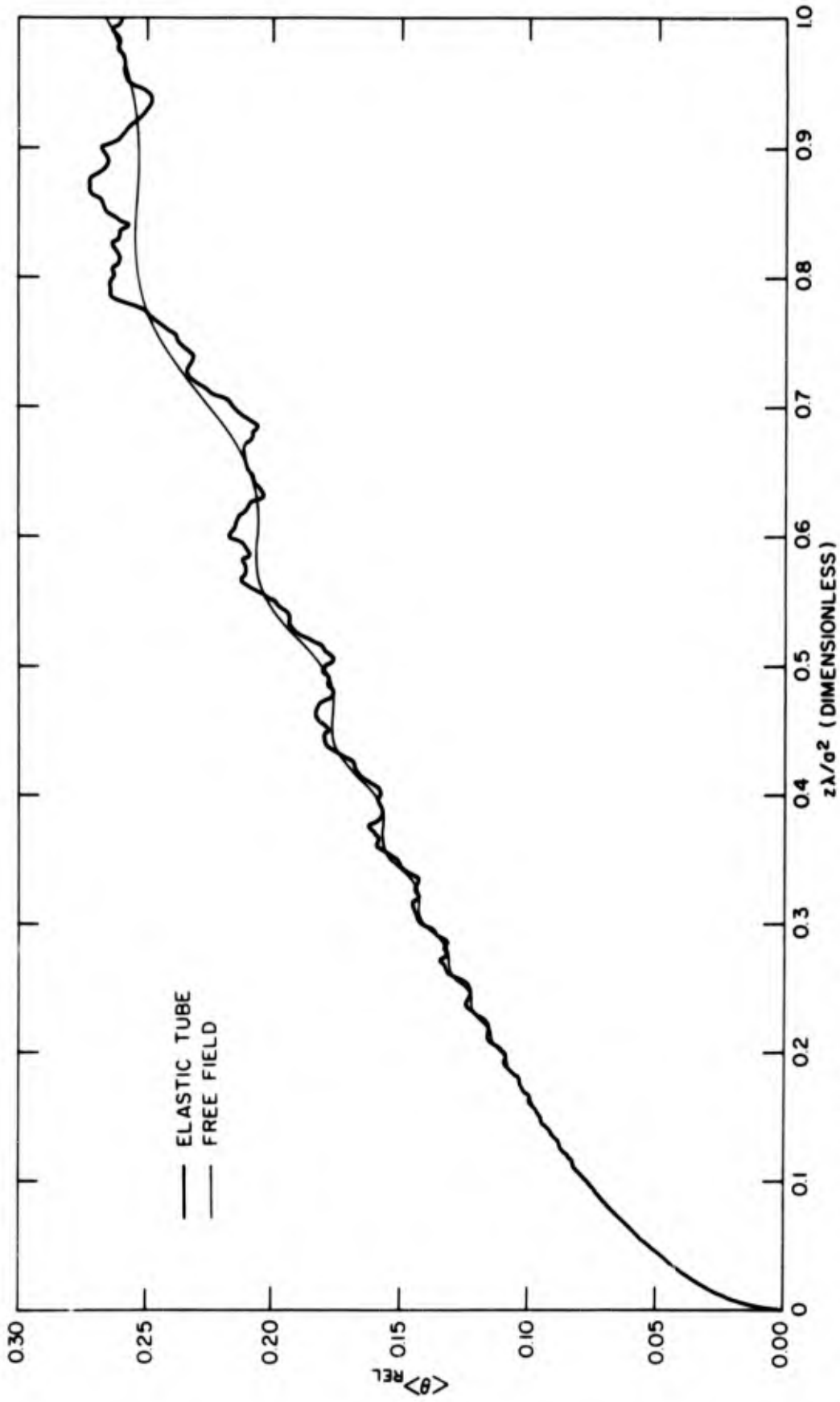


Fig. 8b — $\langle \theta \rangle_{REL}$ vs $0 \leq z(\lambda/a^2) \leq 1$ for liquid cylinder with finite elastic solid tube radial boundary condition ET_m and uniform velocity source assumption using orthogonal Characteristic Function assumption and including all propagated modes for appropriate reference conditions in Table 1. Free Field Diffraction curves are plotted for comparison

IX.11 Source Impedance Variation Plots for Terminated Cylinder

The interferometer situation has been used by the author for sound speed determinations (17) and so more attention is devoted here to the summations detailed in Section 6 and leading to the source ($z = 0$) impedance variation with reflector location $z = \ell$. Figures 9 through 13 indicate source impedance circle plots R vs X where $Z_0 = R + iX$ for the radial boundary conditions R , F , LI , EI , and ET . These plots are based on calculations employing the pertinent parameters of Table 1. The small numbered circles refer to the value of n where $\ell = n \lambda_1/2$, that is they indicate the impedance presented at those indicated integer half-wavelengths calculated from the intrinsic sound speed of the liquid constituting the liquid cylinder. The smaller un-numbered circles indicate impedances for successive ℓ changes of 0.2 micrometers.

The previous statement that Z_0 at $\ell = 0$ is real is demonstrated by the first such point on these graphs which is the one furthest to the right and occurs at $X = 0$ and $R \sim 28$ for all the graphs. The graph of impedance (R vs X) moves clockwise with increasing ℓ approximately in a spiral converging on the point $(1, 0)$ even without the inclusion of absorption in the liquid constituting the liquid cylinder.

If not corrected for, then, an error occurs in sound speed determinations by interferometry if the imposed characteristic selected to experimentally determine those ℓ values corresponding to integer changes in number of half wavelengths does not coincide with the $n(\lambda_1/2)$ points or does not result in constant $\Delta\ell$ deviations from those points. That this does not occur is obvious from a perusal of the R vs X plots. These plots were originally drawn to 30 inch by 30 inch size and ℓ values were interpolated at imposed characteristics of zero phase, maximum resistance ($\text{Max } R$), and maximum impedance ($\text{Max } Z$) respectively for the loops of indicated n on the figures. Apparent sound speeds were then calculated for the intervals between successive loops and are given in Tables 10 thru 14 along with the resultant error in parts per million from the intrinsic sound speed used of 1500 meters per second. These tables, like the corresponding figures, are respectively for R , F , FI , EI , and ET radial boundary conditions with the pertinent parameters from Table 1. Apparently $\text{Max } Z$ is the preferred imposed characteristic and the error, if uncorrected for, can be kept to 6 ppm.

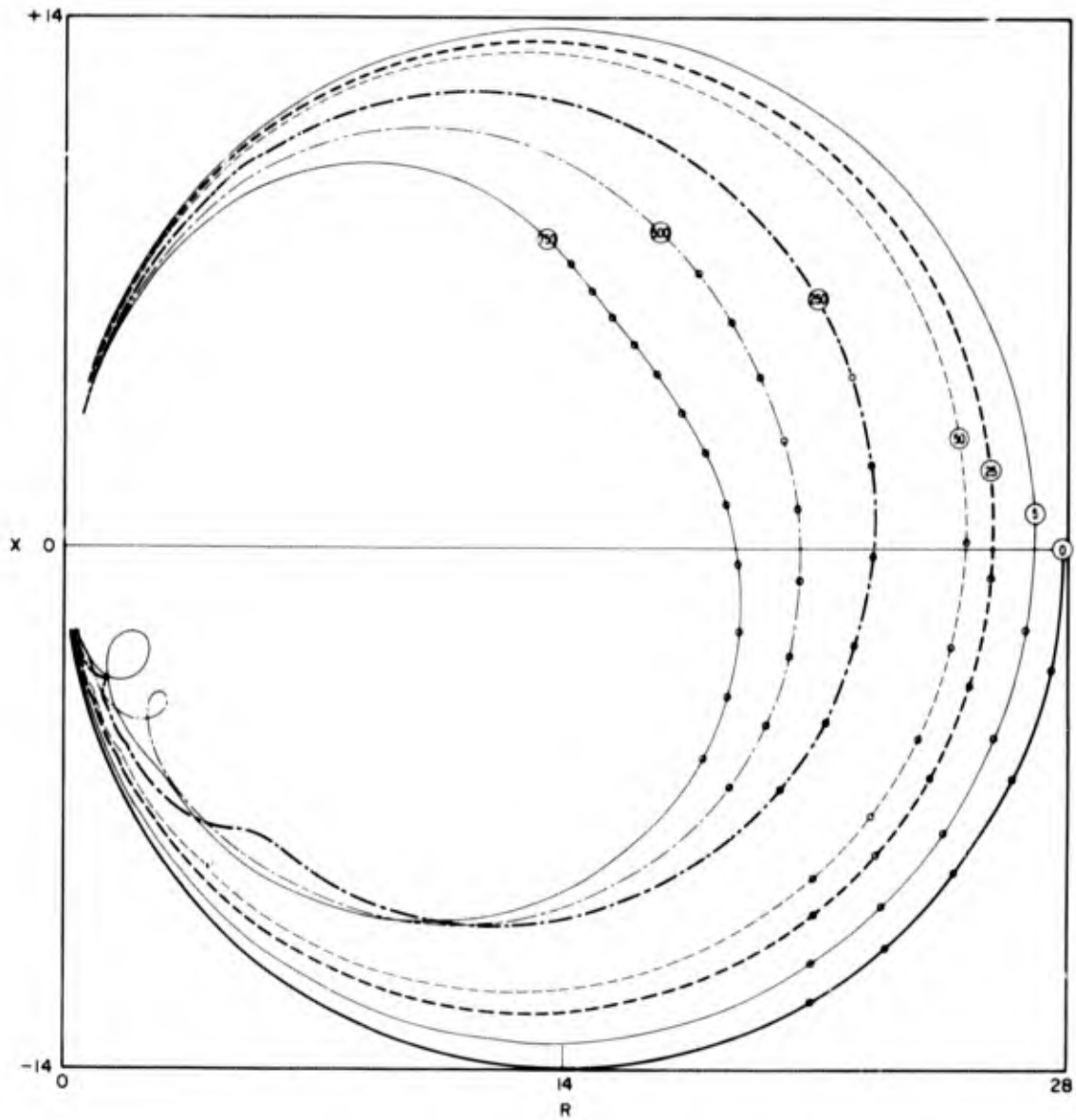


Fig. 9—R vs X Circle Diagram for terminated liquid cylinder with rigid radial boundary condition R_m and uniform velocity source assumption and including all propagated modes for appropriate reference conditions in Table 1. The points are separated by $\Delta l = 0.2$ micrometers and the circled numerals refer to the value of n where $l = n(\lambda_1/2)$

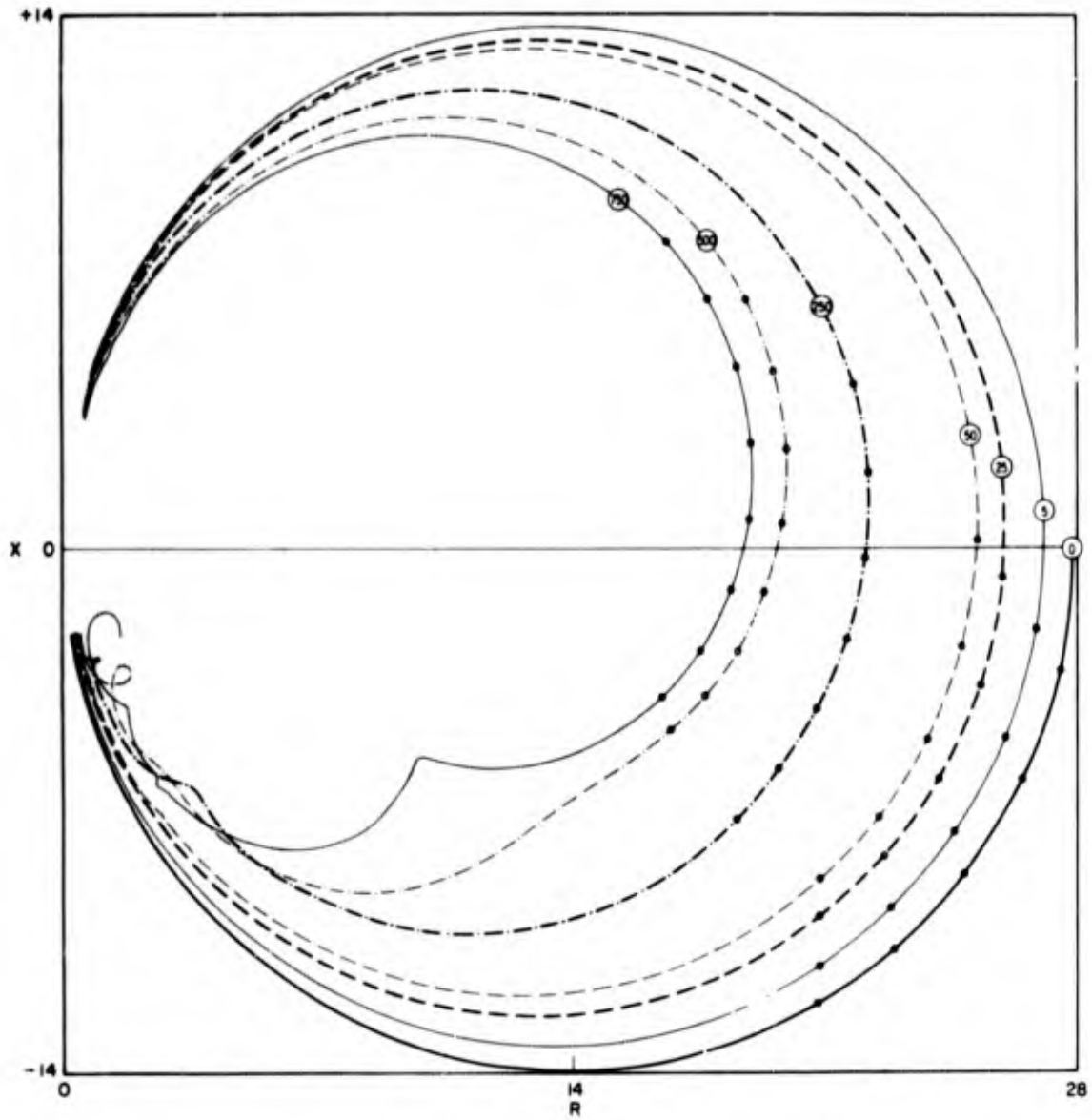


Fig. 10—R vs X Circle diagram for terminated liquid cylinder with free radial boundary condition F_m and uniform velocity source assumption and including all propagated modes for appropriate reference conditions in Table i. The points are separated by $\Delta \ell = 0.2$ micrometers and the circled numerals refer to the value of n where $\ell = n(\lambda_1/2)$

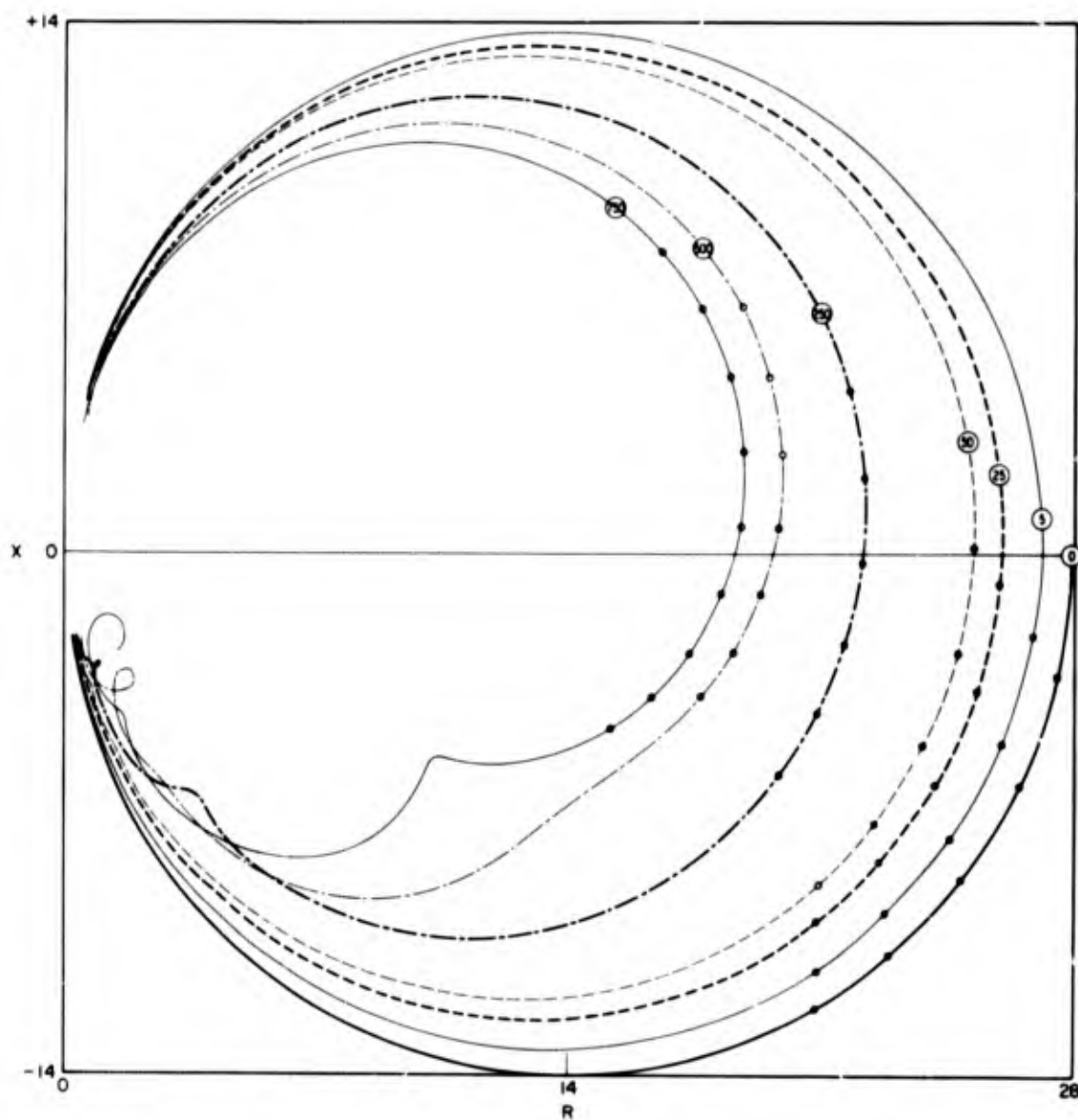


Fig. 11 - R vs X Circle diagram for terminated liquid cylinder with infinite liquid radial boundary condition Llm and uniform velocity source assumption using orthogonal Characteristic Function assumption and including all propagated modes for appropriate reference conditions in Table 1. The points are separated by $\Delta \ell = 0.2$ micrometers and the circled numerals refer to the value of n where $\ell = n(\lambda_1/2)$

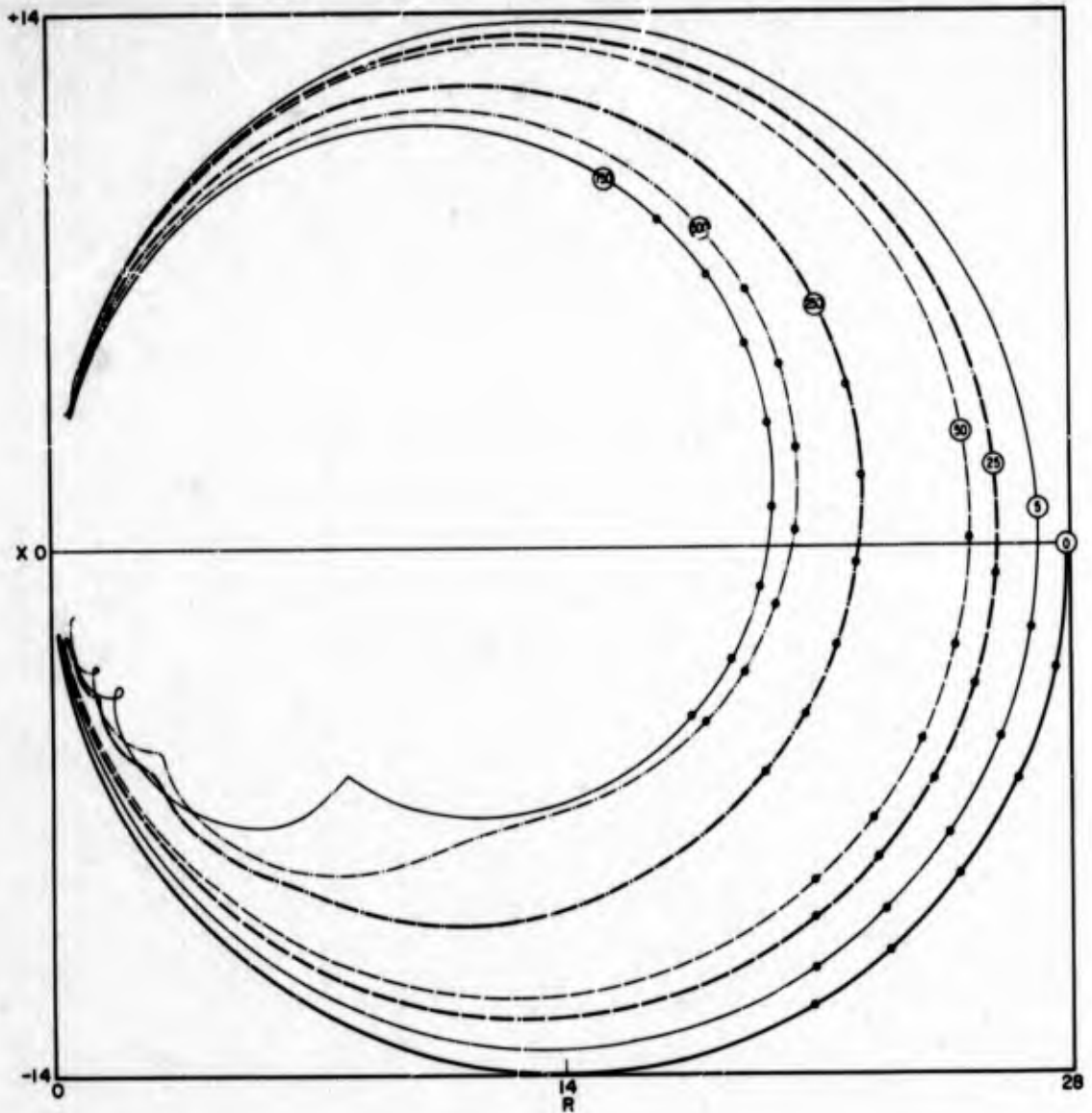


Fig. 12—R vs X Circle diagram for terminated liquid cylinder with infinite elastic solid radial boundary condition Elm and uniform velocity source assumption using orthogonal Characteristic Function assumption and including all propagated modes for appropriate reference conditions in Table 1. The points are separated by $\Delta \ell = 0.2$ micrometers and the circled numerals refer to the value of n where $\ell = n(\lambda_1/2)$

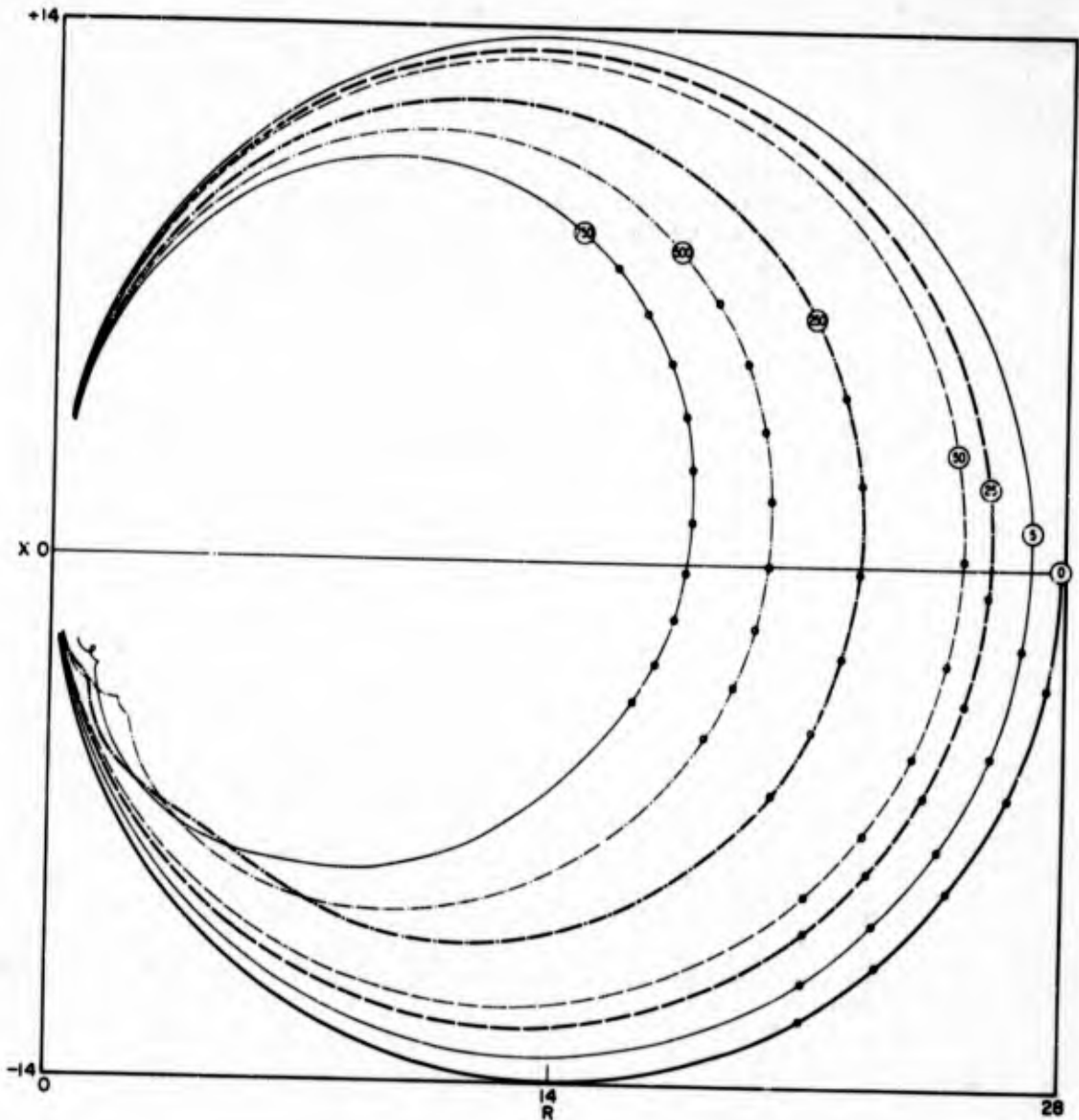


Fig. 13—R vs X Circle diagram for terminated liquid cylinder with finite elastic solid tube boundary condition ETm and uniform velocity source assumption using orthogonal Characteristic Function assumption and including all propagated modes for appropriate reference conditions in Table 1. The points are separated by $\Delta l = 0.2$ micrometers and the circled numbers refer to the value of n where $l = n(\lambda_1/2)$

TABLE 10
Apparent Sound Speeds C for Successive Intervals Between Indicated
Source-to-Reflector Separations l Corresponding to
Half Wavelengths n for the Imposed Characteristics of Zero Phase,
Maximum R, and Maximum Z for the Standard Reference
Parameters of Table 1 with Absolutely Rigid Boundary Conditions R_m

Imposed Characteristic	n	l (cm)	C (m/s)	Error (ppm)
Zero phase	5	0.075006	1500.120	80
	25	0.375015	1500.045	30
	50	0.750021	1500.024	16
	250	3.750058	1500.019	12
	500	7.500111	1500.021	14
	750	11.250175	1500.026	17
Max R	5	0.075002	1500.040	27
	25	0.375011	1500.045	30
	50	0.750020	1500.036	24
	250	3.750051	1500.016	10
	500	7.500112	1500.024	16
	750	11.250192	1500.032	21
Max Z	5	0.075001	1500.020	13
	25	0.375002	1500.005	3
	50	0.750017	1500.060	40
	250	3.750047	1500.015	10
	500	7.500121	1500.030	20
	750	11.250210	1500.036	24

TABLE 11
Apparent Sound Speeds C for Successive Intervals Between Indicated
Source-to-Reflector Separations l Corresponding to
Half Wavelengths n for the Imposed Characteristics of Zero Phase,
Maximum R, and Maximum Z for the Standard Reference
Parameters of Table 1 with Free Boundary Conditions F_m

Imposed Characteristic	n	l (cm)	C (m/s)	Error (ppm)
Zero phase	5	0.075006	1500.120	80
	25	0.375015	1500.045	30
	50	0.750021	1500.024	16
	250	3.750058	1500.019	12
	500	7.500087	1500.012	7
	750	11.250108	1500.008	6
Max R	5	0.075002	1500.040	27
	25	0.375011	1500.045	30
	50	0.750016	1500.020	13
	250	3.750056	1500.020	13
	500	7.500065	1500.004	2
	750	11.250088	1500.009	6
Max Z	5	0.075001	1500.020	13
	25	0.375002	1500.005	3
	50	0.750011	1500.036	24
	250	3.750036	1500.013	8
	500	7.500046	1500.004	2
	750	11.250076	1500.012	7

TABLE 12
Apparent Sound Speeds C for Successive Intervals Between Indicated
Source-to-Reflector Separations l Corresponding to
Half Wavelengths n for the Imposed Characteristics of Zero Phase,
Maximum R, and Maximum Z for the Standard Reference
Parameters of Table 1 with Infinite Liquid Boundary Conditions LIm

Imposed Characteristic	n	l (cm)	C (m/s)	Error (ppm)
Zero phase	5	0.075006	1500.120	80
	25	0.375015	1500.045	30
	50	0.750021	1500.024	16
	250	3.750058	1500.019	12
	500	7.500086	1500.011	8
	750	11.250108	1500.009	6
Max R	5	0.075005	1500.100	67
	25	0.375010	1500.025	16
	50	0.750018	1500.032	22
	250	3.750048	1500.015	10
	500	7.500065	1500.007	5
	750	11.250086	1500.008	6
Max Z	5	0.075002	1500.040	27
	25	0.375007	1500.025	16
	50	0.750011	1500.016	10
	250	3.750040	1500.015	10
	500	7.500055	1500.006	4
	750	11.250071	1500.006	4

TABLE 13
Apparent Sound Speeds C for Successive Intervals Between Indicated
Source-to-Reflector Separations l Corresponding to
Half Wavelengths n for the Imposed Characteristics of Zero Phase,
Maximum R, and Maximum Z for the Standard Reference Parameters of
Table 1 with Infinite Elastic Solid Boundary Conditions Elm

Imposed Characteristic	n	l (cm)	C (m/s)	Error (ppm)
Zero phase	5	0.075006	1500.120	80
	25	0.375015	1500.045	30
	50	0.750021	1500.024	16
	250	3.750056	1500.018	12
	500	7.500084	1500.011	7
	750	11.250110	1500.010	/
	Max R	5	0.075003	1500.060
25		0.375011	1500.040	27
50		0.750018	1500.028	19
250		3.750043	1500.013	8
500		7.500069	1500.010	7
750		11.250094	1500.010	7
Max Z		5	0.075001	1500.020
	25	0.375006	1500.025	17
	50	0.750017	1500.044	29
	250	3.750034	1500.009	6
	500	7.500058	1500.010	6
	750	11.250082	1500.010	6

TABLE 14
Apparent Sound Speeds C for Successive Intervals Between Indicated
Source-to-Reflector Separations l Corresponding to
Half Wavelengths n for the Imposed Characteristics of Zero Phase,
Maximum R, and Maximum Z for the Standard Reference Parameters of
Table 1 with finite elastic solid tube boundary conditions ET_m

Imposed Characteristic	n	l (cm)	C (m/s)	Error (ppm)
Zero phase	5	0.075006	1500.120	80
	25	0.375015	1500.045	30
	50	0.750021	1500.024	16
	250	3.750058	1500.019	12
	500	7.500099	1500.016	10
	750	11.250136	1500.015	10
Max R	5	0.075003	1500.600	397
	25	0.375010	1500.035	23
	50	0.750018	1500.032	21
	250	3.750050	1500.016	10
	500	7.500083	1500.013	8
	750	11.250110	1500.011	7
Max Z	5	0.075001	1500.020	13
	25	0.375006	1500.025	17
	50	0.750015	1500.036	24
	250	3.750043	1500.014	9
	500	7.500069	1500.010	7
	750	11.250080	1500.004	3

IX.12 Other Sources of Error in Measurement of Propagation Parameters

Although this work is concerned solely with the effect of diffraction or the dispersion of sound speed due to a finite source and a container of finite cylindrical geometry and finite wall impedance, it is instructive to briefly consider other factors affecting the accuracy of acoustic propagation parameter determinations. Of course, a claim of accuracy beyond that warranted by the specification of the attendant physical parameters such as pressure, temperature, purity or chemical composition is wholly unjustified. And the accuracy of distance measurement and frequency or time determination is hopefully an upper limit. But apart from its impedance, other effects could be attributed to the wall of the container. Specifically these would include viscous drag and thermal conduction. The correct handling of an intrinsic viscosity attributed to the contained liquid is difficult. The author has derived such formulations and is attempting programming for numerical solution as a sequel to this work. However, an approximate treatment can be given. In (7) Richardson (20) was quoted on viscous damping as a wall effect on the indicated speed of sound in tubes. The observed speed to true speed ratio is given as

$$\frac{C'}{C} = 1 - \frac{1}{b} \sqrt{\frac{\eta}{2\omega}}$$

for the lowest mode only where b is tube radius, η the kinematic viscosity and ω the angular frequency. For water in our 3 cm tube at 5 MHz this predicts a reduction of sound speed of about 3 parts per million.

The effect of thermal conductivity was first recognized by Kirchhoff and, as shown by Rayleigh (quoted in (21)) results in a new value η_e for the kinematic viscosity or

$$\frac{C'}{C} = 1 - \frac{1}{b} \sqrt{\frac{\eta_e}{2\omega}}$$

where

$$\sqrt{\eta_e} = \sqrt{\eta} \left[1 + (\gamma - 1) \left(\frac{K}{\rho c_p} \right)^{1/2} \right],$$

γ is the ratio of specific heats, C_p is the specific heat at constant pressure and K is the coefficient of thermal conductivity of the fluid. The modification is generally negligible for liquids.

The effect of attenuation in the liquid, not necessarily due to viscosity was also treated approximately in (7). At 5 MHz the attenuation coefficient for water is about $3 \times 10^{-3} \text{ cm}^{-1}$. In the above quoted report, plane wave results were unmodified until an

unrealistic absorption coefficient of 1 cm^{-1} was used. In the same report, interferometer calculations including attenuation were limited to 1 MHz by the computer (NAREC). However, the apparent sound speed errors were changed by the inclusion of absorption from their zero absorption values by only +1 part per million for $\alpha_1 = 10^{-3} \text{ cm}^{-1}$ and -2 parts per million for $\alpha_1 = 10^{-2} \text{ cm}^{-1}$. Thus, for a medium such as water, other effects seem to be negligible in comparison to diffraction. However, as stated previously, the effect of viscous absorption in particular will be considered in more adequate detail in another report. In particular, the simple discussion above did not consider the effect of viscosity on the boundary conditions where the tangential components of both displacement and stress must then be continuous.

The existence of a piston source is yet an unproved assumption, but the fortuitous result that the mathematical selection of the source boundary condition as either a uniform pressure piston or a uniform velocity piston still yields nearly identical field results indicates that the piston assumption itself may not be critical to the results. In any event an experiment is being designed to test the validity of this assumption.

Section X

CONCLUSIONS

The sound propagation results of various researchers (22) including the author, are affected by systematic errors of their instrumentation, so that their apparent values differ from the intrinsic values. It is demonstrated here that predicted results of more exact theoretical formulations than previously employed indicate that the effects of diffraction and guided modes, in particular, can be kept to within a very few parts per million, even if the decision to not apply easily obtained corrections is made, simply by designing the experimental configuration as guided by the theoretical predictions.

In this report, for the first time, mode summations have been carried out for realistic radial boundary conditions appropriate to a finite thickness elastic solid tube radially enclosing the liquid cylinder of interest. Characteristic equations for the modes have been obtained not only for the above, but also for the condition of a radially surrounding elastic solid of infinite extent outwards. In this latter case, the equation has been shown to degenerate properly to the case of a radially surrounding (different) liquid as well as to the trivial cases of absolutely rigid and free radial boundaries.

The characteristic equations have been solved for the modes, found to be finite in number and all propagating for both the radially surrounding elastic solid of infinite extent outwards and the radially surrounding liquid of infinite extent outwards. The finite number of modes in both these cases was found to be sufficient to describe a piston source of uniform velocity in an expansion for the potential in an otherwise unterminated liquid cylinder, as well as being sufficient to describe the source impedance when the liquid cylinder is terminated also at the other end. In both these cases the use of a source of sufficiently large ka has rendered indifferent the mathematical selection of either a uniform pressure piston source or a uniform velocity piston source in the expansion for the potential. This large source also results in " ρc " loading whereby the source impedance for zero reflector-source separation becomes pure real.

In the limiting cases of absolutely rigid or free radial boundaries, as well as the most realistic case of a finite wall thickness surrounding tube, the family of modes consists of a finite number of propagating ones and an infinite number of evanescent

modes, but here too a summation over only the propagating modes was found to be more than adequate to describe the source.

The deliberately large radial impedance mismatch has resulted in the characteristic functions for the realistic cases being sufficiently orthogonal to cause no significant difference if either the proper matrix evaluation of the expansion coefficients is applied or a simplifying orthogonality assumption is utilized.

The evaluation of the expansion coefficients was accomplished by integrating only over the liquid cylinder of interest, but this is shown to not only imply no untoward source assumption in the radially surrounding medium but to be actually proper.

An incidental result of this investigation is the mode sound speed dispersion plot for the case of a finite wall thickness elastic solid surrounding tube which in this exact formulation indicates that the most recently published work (1) on these modes is in error. Specifically, the single imaginary root or ETO mode does exist at all frequencies and does not as concluded by (1) exhibit an upper cutoff frequency.

REFERENCES

1. Kumar, Ram, *Axially Symmetric Vibrations of a Thin Cylindrical Elastic Shell Filled with Nonviscous Compressible Fluid*, *Acustica* 17, No. 4, 218-222 (1966).
2. Thomson, W. T., *Transmission of Pressure Waves in Liquid Filled Tubes*, Proc. 1st U. S. Nat. Congr. Appl. Mech. 927 (1951).
3. Lin, T. C.; Morgan, G. W., *Wave Propagation Through Fluid Contained in a Cylindrical, Elastic Shell*, *Journal of the Acoustical Society of America*, 28, 1165 (1956).
4. Jacobi, W. G., *Propagation of Sound Waves Along Liquid Cylinders*, *Journal of the Acoustical Society of America*, 21, 120 (1949).
5. Fay, R. D.; Brown, R. L.; Fortier, D. V., *Measurement of Acoustic Impedances of Surfaces in Water*, *Journal of the Acoustical Society of America*, 19, 850 (1947).
6. Del Grosso, V. A., *The Velocity of Sound in Sea Water at Zero Depth*, NRL Report 4002, June 11, 1952, Naval Research Laboratory, Washington, D. C.
7. Del Grosso, V. A., Smura, E. J., Fougere, P. R., *Accuracy of Ultrasonic Interferometer Velocity Determinations*, NRL Report 4439, December 1954, Naval Research Laboratory, Washington, D. C.
8. King, L. V., *On the Acoustic Radiation Field of the Piezo-Electric Oscillator and the Effect of Viscosity on Transmission*, *Can. J. Research* 11, 135 (1934).
9. Williams, A. O., Jr., *The Piston Source at High Frequencies*, *Journal of the Acoustical Society of America* 23, 1 (1951).
10. Seki, H., Granata, A., Truell, R., *Diffraction Effects in the Ultrasonic Field of a Piston Source . . .*, *Journal of the Acoustical Society of America* 28, 230 (1956).
11. Bass, R., *Diffraction Effects in the Ultrasonic Field of a Piston Source*, *Journal of the Acoustical Society of America* 30, 602 (1958).
12. Del Grosso, V. A., *Systematic Errors in Ultrasonic Propagation Parameter Measurements - Part I - Effect of Free-Field Diffraction*, NRL Report 6026, January 29, 1964, Naval Research Laboratory, Washington, D. C.

13. Del Grosso, V. A., *Systematic Errors in Ultrasonic Propagation Parameter Measurements - Part II - Effects of Guided Cylindrical Modes*, NRL Report 6133, January 29, 1965, Naval Research Laboratory, Washington, D. C.
14. Morse, P. M., Feshbach, H., *Methods of Theoretical Physics*, McGraw Hill, N. Y., 1953, Part 1, eq. 7.2.7.
15. Mangulis, V., *Radiation of Sound From a Circular Disk With a Uniform Pressure Distribution*, *Acustica* 15, No. 2, 98-103 (1965).
16. Spence, R. J., *J. Acous. Soc. Amer.* 20, 380 (1948).
17. Del Grosso, V. A., *Systematic Errors in Ultrasonic Propagation Parameter Measurements - Part III - Iterative Reflection Interferometry*, NRL Report 6409, August 9, 1966, Naval Research Laboratory, Washington, D. C.
18. Biot, M. A., *Propagation of Elastic Waves in a Cylindrical Bore Containing a Fluid*. *J. Appl. Phys.* 23, 997 (1952).
19. Junger, M. C.; and Rosato, F. J.; *The Propagation of Elastic Waves in Thin-Walled Cylindrical Shells*. *Jour. Acous. Soc. Am.* 26, 709 (1954).
20. Richardson, E. G., *Ultrasonic Physics*, Elsevier Pub. Co., New York (1952).
21. Stephens, R. W. B., Bate, A. E., *Acoustics and Vibrational Physics*, St. Martin's Press, New York (1966).
22. Del Grosso, V. A., Walker, W. F., La Lumiere, L. P., *Results of Sound Speed Measurements in Water*, NRL Rept. Progress, Oct. 1967, p. 44-48.

DOCUMENT CONTROL DATA - R & D

(Security classification of title, body of abstract and indexing annotation must be entered when the overall report is classified)

1. ORIGINATING ACTIVITY (Corporate author) Naval Research Laboratory Washington, D.C. 20390		2a. REPORT SECURITY CLASSIFICATION Unclassified	
		2b. GROUP	
3. REPORT TITLE SYSTEMATIC ERRORS IN ULTRASONIC PROPAGATION PARAMETER MEASUREMENTS, PART 4 - EFFECT OF FINITE THICKNESS ELASTIC SOLID TUBES ENCLOSING THE LIQUID CYLINDER OF INTEREST			
4. DESCRIPTIVE NOTES (Type of report and inclusive dates) A Doctor of Philosophy dissertation issued as an interim report on a continuing problem.			
5. AUTHOR(S) (First name, middle initial, last name) Vincent A. Del Grosso			
6. REPORT DATE November 15, 1968	7a. TOTAL NO. OF PAGES 141	7b. NO. OF REFS 22	
8a. CONTRACT OR GRANT NO. NRL Problem S01-02	8b. ORIGINATOR'S REPORT NUMBER(S) NRL Report 6852		
b. PROJECT NO. RF 05-511-401-5251	8c. OTHER REPORT NO(S) (Any other numbers that may be assigned this report) Ph.D. dissertation; the Catholic University of America		
10. DISTRIBUTION STATEMENT This document has been approved for public release and sale; its distribution is unlimited.			
11. SUPPLEMENTARY NOTES Dissertation title: "Axial Acoustic Propagation Within Inviscid Liquid Cylinders in Elastic Solid Tubes - Mode Summa- tions for Propagation Parameter Measurements"		12. SPONSORING MILITARY ACTIVITY Department of the Navy (Office of Naval Research), Washington, D.C. 20360	
13. ABSTRACT The exact formulation of the characteristic or frequency equation for an inviscid liquid cylinder radially enclosed within a finite impedance elastic solid of finite wall thickness is solved for the permissible modes, including degenerations to the surrounding medium being of infinite extent and either an elastic solid or another liquid, as well as to the limiting cases of infinite impedance (rigid boundary) and zero impedance (free boundary). These modes are utilized to expand both the potential within the otherwise unterminated cylinder and the source impedance variation with position of an opposing termination. A piston source of appreciable ka ($= 100$) is found to render further source specification indifferent as to uniform pressure or uniform velocity, and a large radial impedance mismatch ($= 28$) is found to permit a simplifying orthogonality assumption. With the inviscid assumption, the formulation indicates that a judicious selection of experimental configuration can limit diffraction propagation uncertainties to a few parts per million. An incidental result is the demonstration that the zero elastic tube mode exists at all frequencies rather than displaying an upper cutoff frequency as was recently reported.			

14 KEY WORDS	LINK A		LINK B		LINK C	
	ROLE	WT	ROLE	WT	ROLE	WT
Underwater acoustics						
Sound transmission						
Underwater sound transmission						
Ultrasonic tests						
Wave propagation						
Acoustic velocity						
Analysis (mathematics)						
Potential theory						
Wave equations						
Boundary value problems						
Bessel functions						
Vectors (mathematics)						